AD-A159 920 ANNUAL GASEOUS ELECTRONICS CONFERENCE (37TH) HELD AT BOULDER COLORADO ON 9-12 OCTOBER 1984 PROGRAM AND ABSTRACTS(U) COLORADO UNIV AT BOULDER 12 OCT 84 1/2

UNCLASSIFIED N00014-84-F-0137 F/G 9/5 NL

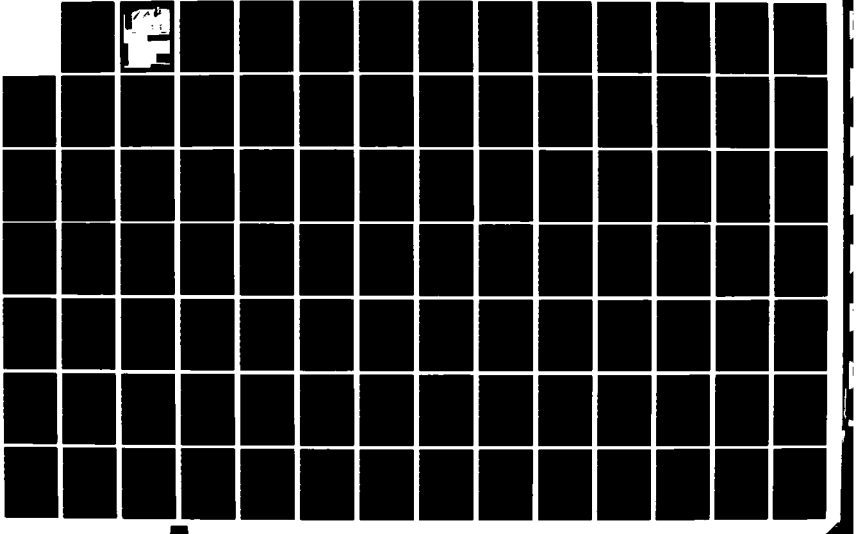

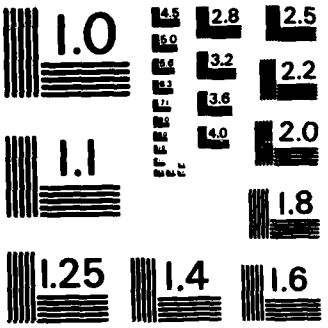

[redacted]

October 9-12, 1984

University of Colorado
Boulder

Thirty-seventh Annual

Gaseous Electronics Conference

October 9-12, 1984

Program and Abstracts

A Topical Conference of the American Physical Society

Hosted By:
National Bureau of Standards
University of Colorado
Joint Institute for Laboratory Astrophysics

Assisted By:
Office of Naval Research
Air Force Office of Scientific Research
National Science Foundation

ACKNOWLEDGEMENTS

On behalf of the Membership, the GEC Executive Committee gratefully acknowledges the support of many participating institutions. The National Bureau of Standards, the University of Colorado, and the Joint Institute for Laboratory Astrophysics are serving as hosts for this year's conference. These organizations provided staff and facilities without which the conference could not be held. Financial assistance has been provided by the National Science Foundation, the Air Force Office of Scientific Research, and the Office of Naval Research. The Gaseous Electronics Conference is a Topical Conference of the American Physical Society with sponsorship by the Division of Electron and Atomic Physics.

Contract N00014-84-F-0137

CONTENTS

TECHNICAL PROGRAM

TUESDAY MORNING, 9 OCTOBER

A: ION TRANSPORT
Chairperson: W.P. Allis, MIT
08:30 UMC Center Ballroom

A-1 NEGATIVE-ION DENSITY FROM NATURAL SOURCES IN SF_6: J.P. Novak and G. Ellena, IREQ, Varennes, Quebec, Canada

A-2 MOBILITY OF POSITIVE IONS IN SF_6 GAS: F. Li Avavena and M. Saporoschenko, Southern Illinois U. in Carbondale

A-3 NEGATIVE DIFFERENTIAL CONDUCTIVITY (NDC) RE-VISITED: W.F. Bailey and A. Garscadden, Air Force Inst. of Technology and Air Force Wright Aeronautical Labs

A-4 MEASUREMENT OF OSCILLATION IN GASES WITH NEGATIVE DIFFERENTIAL CONDUCTIVITY: P. Bletzinger, Air Force Wright Aeronautical Labs

A-5 MEASUREMENT OF THE DIFFUSION COEFFICIENT OF SODIUM IN NEON AT 530 K: H.J. Cornelissen, Philips Research Labs, Eindhoven

A-6 AMBIPOLAR DIFFUSION COEFFICIENTS FOR DISCHARGES IN ATTACHING GASES: G.L. Rogoff, GTE Labs, Inc.

B: ELECTRON COLLISIONS
Chairperson: N. Padial, U. of New Mexico
10:15 UMC Center Ballroom

B-1 PHOTOENHANCED ELECTRON ATTACHMENT IN VINYLCHLORIDE AND TRIFLUORETHYLENE: M.J. Rossi, H. Helm, and D.C. Lorents, SRI International

B-2 MEASUREMENTS OF ELECTRON TRANSPORT, ATTACHMENT, AND IONIZATION IN HUMID AIR: D.K. Davies, Westinghouse R&D Center

B-3 EFFECT OF TEMPERATURE ON DISSOCIATIVE ATTACHMENT TO CCl_2F_3 AND C_2F_6:: S.M. Spyrou and L.G. Christophorou, ORNL and U. of Tennessee

B-4 EFFECTIVE 3-BODY ATTACHMENT RATE AND ELECTRON DRIFT VELOCITY IN HEXAFLUOROPROPYLEN: T. Aschwanden, Swiss Fed. Inst. of Technology, ETH, Zurich, Switzerland

B-5 DISSOCIATIVE ATTACHMENT IN LOW-ENERGY e + Li_2 COLLISIONS: H.H. Michels and J.M. Wadehra, AFWAL/APL, Wright-Patterson AFB

B-6 DEVELOPMENT OF A NEW TECHNIQUE FOR MEASUREMENT OF ELECTRON ATTACHMENT COEFFICIENT: T.H. Harding and Y.W. Kim, Lehigh U.

B-7 COLLISIONAL-RADIATIVE COUPLING COEFFICIENTS FOR MODELING OF HIGH PRESSURE DISCHARGES: P.A. Vicharelli and A.V. Phelps, JILA, U. of Colorado and NBS

B-8 RF-PROBE MEASUREMENTS OF ELECTRON AND ION DENSITY DECAYS IN ATMOSPERIC-DENSITY He-H_2 and He-SF_6 AFTERGLOWS: R. Johnsen, U. of Pittsburgh

TUESDAY AFTERNOON, 9 OCTOBER

CA: LASERS
Chairperson: Gerald Hays, Sandia National Lab
13:15 UMC Center Ballroom

CA-1 LOW THRESHOLD LONG GAIN LENGTH SOLAR-PUMPED C_3F_7I LASER: R.J. De Young, NASA Langley Research Center

CA-2 TRANSIENT ABSORPTION SPECTRA OF RARE GAS DIMER MOLECULES: K.P. Killeen and J.G. Eden, U. of Illinois at Urbana-Champaign

CA-3 PHOTODISSOCIATION OF Xe_2 EXICMER: OBSERVATION OF ELECTRONIC EXCITED STATES: M.N. Ediger and J.G. Eden, U. of Illinois at Urbana-Champaign

CA-4 VIBRATIONAL RELAXATION IN THE B STATE OF XeF: G. Black, L.E. Jusinski, D.C. Lorents, and D.L. Huestis, SRI International

CA-5 FLUORESCENCE CROSS SECTIONS OF $HgBr_2$: C.L. Chen and P.J. Chantry, Westinghouse R&D Center

CA-6 ELECTRON-BEAM EXCITATION OF IONIZED AND NEUTRAL ATOMIC LINE LASERS: K. Ono, T. Oomori, S. Fujita, and Y. Ueda, Mitsubishi Electric Corp., Amagasaki, Japan, and T. Narikawa, MFC, Japan

CA-7 COMPUTER MODEL OF CW ION LASERS EXCITED BY ELECTRON BEAMS: G. Feltzer, J.J. Rocca, G.J. Collins, and R. Jacobs, Colorado State U.

CA-8 NOVEL THERMIONICALLY-COOLED PLASMA RECOMBINATION LASER: J.L. Lawless, Carnegie-Mellon U.; E.J. Britt, and J.B. McVey, Rasor Associates

CA-9 LASER EMISSION FROM AN EMBEDDED-PINCH SHEATH: J.F. Asmus, R.H. Lovberg, J.D. Keeler, P.E. Hudson, and K. Boyer, U. of California, San Diego

CB: GLOWS AND SWITCHING
Chairperson: Erich Kunhardt, Polytechnic Inst. of New York
13:15 UMC East Ballroom

CB-1 X-RAY INITIATED UNIFORM GLOW DISCHARGES: K. Jayaram, and A.J. Alcock, National Research Council of Canada, Ottawa

CB-2 RADIATION FROM TRANSIENT DISCHARGES: W.W. Byszewski and H. Kullmann, GTE Labs, Inc.

CB-3 OPTICAL CONTROL OF THE BREAKDOWN OF A DIFFUSE DISCHARGE USING PHOTO-DETACHMENT: G.Z. Hutcheson, L.E. Thurmond, G. Schaefer, K.H. Schoenbach, and P.F. Williams, Texas Tech U.

CB-4 MAGNETIC CONTROL OF LOW PRESSURE GLOW DISCHARGES: J.R. Cooper, K.H. Schoenbach, G. Schaefer, Texas Tech U.; J.M. Proud, W.W. Byszewski, GTE Labs

CB-5 PRODUCTION RATES OF OXYGENATED SPECIES IN SF_6/O_2 and SF_6/N_2 CORONA DISCHARGES: R. J. Van Brunt and M.C. Siddagangappa, National Bureau of Standards

CB-6 THE FREE RECOVERY OF A SHORT DURATION, HIGH CURRENT DISCHARGE: R. Piejak, GTE Labs, Inc.

CB-7 EXPERIMENTAL INVESTIGATIONS OF A RADIAL OPENING SWITCH: C.M. Young, J.W. Benze, J. M. Elizondo, W.M. Moeny, J.G. Small, Tetra Corp.

CB-8 SOME ASPECTS OF SURFACE FLASHOVER: E.W. Gray, Sandia National Labs

D: WORKSHOP ON ION-MOLECULE REACTIONS
Chairperson: R. Johnsen, U. of Pittsburgh
15:15 UMC Center Ballroom

D-1 VIBRATIONAL RELAXATION OF MOLECULAR IONS IN COLLISIONS WITH MOLECULES: E.E. Ferguson, NOAA

D-2 THE FORMATION AND REACTIVITY OF HOC^+: M.T. Bowers, U. of California

D-3 ION MOLECULE REACTIONS AT VERY LOW TEMPERATURES AND DENSITIES: G. Dunn, JILA

D-4 ION-MOLECULE REACTIONS AT VERY LOW TEMPERATURES USING THE CRESU TECHNIQUE (SUPERSONIC JETS): B.R. Rowe, Laboratoire de Aerothermique

WEDNESDAY MORNING, 10 OCTOBER

E: ION-MOLECULE REACTONS
Chairperson: Michael Henchman, Air Force Geophysics Lab
08:15 UMC Center Ballroom

E-1 ENERGY DEPENDENCE OF REACTIONS OF ATOMIC IONS WITH H_2, HD, AND D_2: K. Ervin, J.L. Elkind, and P.B. Armentrout, U. C. Berkeley

E-2 LASER-INDUCED FLUORESCENCE MEASUREMENT OF NASCENT VIBRATIONAL AND ROTATIONAL PRODUCT STATE DISTRIBUTIONS IN THE CHARGE TRANSFER OF $Ar^+ + CO \rightarrow Ar + CO^+$ AT THERMAL ENERGY: G.H. Lin, J. Maier, and S.R. Leone, JILA, U. of Colorado and NBS

E-3 COMPARATIVE EFFECTS OF TEMPERATURE AND KINETIC ENERGY CHANGE ON THE REACTION OF O_2^+ WITH CH_4: N.G. Adams and D. Smith, U. of Birmingham, U.K.; and E.E. Ferguson, NOAA

E-4 PRODUCT STATES OF D_3^+, D_2^+ AND O_2^+ DISSOCIATIVE CHARGE TRANSFER IN Cs: J.R. Peterson and K.Y. Bae, SRI International

E-5 FOURIER TRANSFORM MASS SPECTROMETRY OF SILANE: P. Haaland, Air Force Aero Propulsion Lab, and A. Rahbee, Air Force Geophysics Lab

E-6 THE ASSOCIATION OF AMMONIA WITH HALIDE IONS IN THE GAS PHASE: R.G. Keesee, D.H. Evans, and A.W. Castleman, Jr., Pennsylvania State U.

E-7 NEGATIVE ION MOLECULE REACTIONS OF WF_6: EVIDENCE FOR A PRESSURE DEPENDENT BRANCHING RATIO: A.A. Viggiano and J.F. Paulson, AFGL

E-8 FLOWING AFTERGLOW MEASUREMENTS OF NEGATIVE ION ASSOCIATION REACTIONS: H. Böhringer, D.W. Fahey, F.C. Fehsenfeld, and E.E. Ferguson, NOAA

E-9 HYDRATED-ION MOLECULE REACTIONS: TEMPERATURE DEPENDENCE AS A FUNCTION OF HYDRATION NUMBER: P.M. Hierl, A.F. Ahrens, A.A. Viggiano, M.J. Henchman, and J.F. Paulson, Air Force Geophysics Lab

F: ARGON AND SF_6 ARCS
Chairperson: H-P Stormberg, Philips Research Labs, Aachen
10:55 UMC Center Ballroom

F-1 FREE-BURNING ARCS IN ARGON: G.N. Haddad, CSIRO, Sydney, Australia

F-2 IMPACT OF ANODE EVAPORATION ON THE ANODE REGION OF A HIGH INTENSITY ARGON ARC: K. Etemadi and E. Pfender, State U. of New York at Buffalo and U. of Minnesota

F-3 COMPOSITON AND THERMODYNAMIC PROPERTIES OF NON-LTE ARGON PLASMA: A. Sedghinasab, and T.L. Eddy, Georgia Inst. of Technology

F-4 INFLUENCE OF ADDITIVES ON ATMOSPHERIC PRESSURE RF DISCHARGE IN ARGON: V.M. Goldfarb, Avco Everett Research Lab

F-5 TRANSIENT 2-D SIMULATIONS OF FORCED CONVECTION-STABILIZED ARCS IN N_2 AND SF_6: R.R. Mitchell, D.T. Tuma, and J.F. Osterle, Carnegie-Mellon U.

WEDNESDAY AFTERNOON, 10 OCTOBER

G: POSTERS. MOSTLY DISCHARGES
Chairperson: Harald Tischer, JILA
13:30 UMC West Ballroom

GA: SWARMS

GA-1 ELECTRON ENERGY AND $N_2(X)$ VIBRATIONAL DISTRIBUTIONS IN STATIONARY DISCHARGES: J. Loureiro and C.M. Ferreira, U. Tec. Lisboa

GA-2 STRONGLY COUPLED NON-NEUTRAL ION PLASMA: J.J. Bollinger, D.J. Wineland, and J.D. Prestage, National Bureau of Standards

GA-3 A 2 1/2 TERM SPHERICAL HARMONIC SOLUTION TO THE BOLTZMANN EQUATION: A.V. Phelps, JILA, NBS, and U. of Colorado; and L.C. Pitchford, GTE Labs

GA-4 A NEW DETERMINATION OF CROSS SECTIONS IN METHANE AND SILANE BY USING AN EXACT METHOD OF SOLUTION OF THE BOLTZMANN EQUATION: P. Segur, J.P. Balaguer, Centre de Physique Atomique, Toulouse

GA-5 SPACE AND TIME DEPENDENT BOLTZMANN CALCULATION IN THE FORWARD/BACKWARD SCATTERING APPROXIMATION: J.P. Boeuf and E. Marode, Ecole Superieure d'Electricité (CNRS) Gif/Yvette; and P. Segur, Centre de Physique Atomique (CNRS), Toulouse

GA-6 THE EINSTEIN RELATION FOR ELECTRONS IN HIGH DENSITY ARGON: T.F. O'Malley, GE

GB: ARCS

GB-1 COLLECTIVE ARC SPOT MOTION IN A MAGNETIC FIELD: H.P. Mercure, R.J. Rajotte, and M.G. Drouet. IREQ, Varennes, Canada

GB-2 EFFECT OF WALL REFLECTIONS ON THE HIGH-PRESSURE SODIUM ARC: J.T. Dakin and T.H. Rautenberg, Jr., GE Corporate Research and Development

GB-3 EROSION OF SILICON CARBIDE ARC ELECTRODES: V. Goldfarb, AVCO Everett Research Lab

GB-4 THEORETICAL APPROACH TO THE INTERACTION OF ARC AND GAS FLOW: Zhong-Jie, Li, 7th Designing Inst., Ministry of Machine Building, Xian, P.R. China

GB-5 PHYSICALLY BASED ARC-CIRCUIT INTERACTION: Zhong-Jie, Li, 7th Designing Inst., Ministry of Machine Building, Xian, P.R. China

GB-6 THE INFLUENCE OF ARC TUBE DIAMETER ON THE PROPERTIES OF A HIGH PRESSURE SODIUM DISCHARGE: P.L. Denbigh, B.F. Jones, and D.A.J. Mottram, Thorn EMI Lighting Ltd. UK

GB-7 SPECTROSCOPIC TEMPERATURE MEASUREMENTS FOR SF_6 DOUBLE-NOZZLE ARCS: W. Tiemann, Siemens R & D Center, FRG

GC: LASERS

GC-1 SURFACE-WAVE PHENOMENA IN MICROWAVE EXCITED RARE-GAS HALIDE LASERS: R.W. Waynant, W.M. Bollen, and C.P. Christensen, Naval Research Lab

GC-2 XeCL QUANTUM YIELDS AND FORMATION RATES FROM Xe^+, CL_2, FCl and HCl: D.C. Lorents, R.L. Sharpless, and D.L. Huestis, SRI International

GC-3 TRIGGERING OF AIR BREAKDOWN WITH AN EXCIMER AND A PULSED CO_2 LASER: S. Yoshida, J. Sasaki, Y. Arai, K. Tateishi, M.P. Lei, and T. Uchiyama, Keio U., Japan

GC-4 THEORETICAL INVESTIGATION OF NUCLEAR-EXCITED Kr2* EXCIMER FLUORESCENCE: A. Chung and M. Prelas, U. of Missouri-Columbia

GC-5 SENSITIVITY ANALYSIS OF ELECTRON-BEAM EXCITED Xe_2 FLUORESENCE: A. Chung and M. Prelas, U. of Missouri-Columbia

GC-6 ELECTRON BEAM EXCITED CW IONIC AND ATOMIC LASERS: J. Meyer, J. Rocca, B. Pihlstrom, and G. Collins, Colorado State U.

GC-7 STIMULATED EMISSION FROM LASER PRODUCED MAGNESIUM PLASMAS: P.D. Klieber, A.M. Lyyra, S.P. Heneghan, and W.C. Stwalley, U. of Iowa

GC-8 PRODUCTION OF SPUTTERED VAPOR IN A PULSED COPPER HOLLOW CATHODE: W. Winiarczyk and L. Krause, U. of Windsor, Canada

GC-9 INTERACTION OF CO_2 LASER RADIATION WITH A SHOCK-HEATED HYDROGEN PLASMA: N.W. Jalufka and B.J. Kloc, NASA, Langley Research Center

GD: LOW PRESSURE DISCHARGES

GD-1 EXCITATION PROCESSES IN MICROWAVE ARGON/HELIUM DISCHARGES: J. Marec, S. Saada, E. Bloyet, E. Dervisevic, C. Laporte, P. LePrince, and M. Pouey, Lab Phys. Gaz et Plasmas, Orsay, France

GD-2 INFLUENCE OF EXCITATION FREQUENCY ON MICROWAVE DISCHARGE CHARACTERISTICS: J. Marec, C. Laporte, E. Bloyet, E. Dervisevic, A. Granier, P. LePrince, and S. Saada, Lab Phys. Gaz et Plasmas, Orsay, France

GD-3 ELECTRON DENSITY AND ELECTRON TEMPERATURE MEASUREMENT IN A LOW-PRESSURE SODIUM DISCHARGE USING LASER ABSORPTION: H.J. Cornelissen and H.J.H. Merks-Eppingbroek, Philips Research Labs, Eindhoven

GD-4 OPTICAL PUMPING IN A LOW-PRESSURE MERCURY DISCHARGE: P. van de Weijer and R.M.M. Cremers, Philips Research Labs, Eindhoven

GD-5 THREE REGIMES OF CAPACITVE RF DISCHARGE: V.A. Godyak, Moscow State U., Moscow, USSR

GD-6 ELECTRON OSCILLATION VELOCITY IN COLLISIONLESS RADIO-FREQUENCY DISCHARGE PLASMAS: O.A. Popov and V.A. Godyak, Moscow State U., Moscow, USSR

GD-7 TIME AVERAGED MEASUREMENTS OF THE SHEATH STRUCTURE IN A PARALLEL PLATE RF DISCHARGE AT 13.56 MHz: C.A. DeJoseph, Jr., and P. Bletzinger, Air Force Wright Aeronautical Labs

GD-8 SPECTROSCOPIC DETECTION OF GAS PHASE SiH_x SPECIES: J.C. Wormhoudt and A.C. Stanton, Aerodyne Research, Inc.

GD-9 LARGE VOLUME PLASMAS SUSTAINED BY SURFACE WAVES AT RADIO AND MICROWAVE FREQUENCIES: M. Chaker, M. Moisan, and G. Sauve, U. of Montreal

GD-10 A He-Ne LASER USING A SURFACE WAVE PRODUCED PLASMA: C. Moutoulas, L. Bertrand, J.-L. Lachambre, and M. Moisan, U. of Montreal

GD-11 AN IMPROVED MODEL OF THE LOW PRESSURE Hg-RARE GAS POSITIVE COLUMN DISCHARGE: R. Lagushenko and J. Maya, GTE Lighting Products

GD-12 THEORETICAL INVESTIGATION OF A RADIAL OPENING SWITCH: M. vonDadelszen and W.M. Moeny, Tetra Corp.; and P. J. Roache, Ecodynamics, Inc.

GD-13 EFFECTS OF TURBULENCE ON THE CHARACTERISTICS OF A GLOW DISCHARGE AS DERIVED FROM CONTINUITY AND ENERGY CONSIDERATIONS: O. Biblarz, W.R. Oker, and R.J. Wallace, Naval Postgraduate School

GE: BREAKDOWN

GE-1 ELECTRON-DENSITY GROWTH IN RAPIDLY-VARYING FIELDS: G.N. Hays and J.B. Gerardo, Sandia National Labs; L.C. Pitchford, GTE Labs, Inc., and J.T. Verdeyen, U. of Illinois

GE-2 AIR CORONA DISCHARGE CHEMICAL KINETICS: L.E. Kline and I.E. Kanter, Westinghouse R&D

GE-3 SURFACE FLASHOVER DISCHARGES AS INTENSE PHOTON SOURCES IN THE EXTREME ULTRAVIOLET: J.R. Woodworth and P.F. McCay, Sandia National Labs

GE-4 A MODEL OF FLASHBOARD BREAKDOWN WITH EMPIRICAL SCALING LAWS: C.M. Young, J.M. Elizondo, W.M. Moeny, and J.G. Small, Tetra Corp.

HA: SILANE DISCHARGES

Chairperson, Vince Donnelly, AT&T Bell Labs
15:30 UMC Center Ballroom

HA-1 NEGATIVE GLOW-DIFFUSION MODEL OF THE RF PLASMA REACTOR: Alan Garscadden and W.B. Bateson, Air Force Wright Aeronautical Labs

HA-2 MEASUREMENT OF ELECTRON DENSITY IN d.c. and r.f. SILANE DISCHARGES USING MICROWAVE TECHNIQUES: C.B. Fleddermann, L.J. Overzet, and J.T. Verdeyen, U. of Illinois at Urbana-Champaign

HA-3 SHEATH MODELS FOR DC SILANE DISCHARGES: H. Chatham, and A. Gallagher, JILA, U. of Colorado and NBS

HA-4 THEORY OF THE PLASMA EDGE: RECYCLING ↔ SHEATHS: J.H. Whealton, R.J. Raridon, W.L. Stirling, M.A. Bell, S.L. Milora, and C.C. Tsai, ORNL

HA-5 INFRARED MEASUREMENTS OF DISILANE PRODUCTION FROM A D.C. DISCHARGE IN SILANE: R. Cheney, R. Schadt, and R. Anderson, U. of Missouri-Rolla; and C.A. DeJoseph, Jr., Air Force Wright Aeronautical Labs

HA-6 DISSOCIATION RATES OF SILANE IN AN R.F. DISCHARGE BY TUNABLE DIODE LASER ABSORPTION: C.A. DeJoseph, Jr., and D.R. Pond, Air Force Wright Aeronautical Labs

HA-7 GLOW DISCHARGE ELECTRON BEAM PROCESSING OF MICROELECTRIC MATERIALS: J.J. Rocca, C.A. Moore, L.R. Thompson, and G.J. Collins, Colorado State U.

HB: METAL HALIDE AND MERCURY ARCS
Chairperson: Harald Witting, General Electric R&D, Schenectady
15:30 UMC East Ballroom

HB-1 CONVECTION AND ADDITIVE SEGREGATION IN HIGH-PRESSURE LAMP ARCS: EARLY RESULTS FROM A SPACE SHUTTLE EXPERIMENT: A.H. Bellows, A.E. Feuersanger, and G.L. Rogoff, GTE Labs, Inc.; and H.L. Rothwell, GTE Lighting Products

HB-2 MEASUREMENT OF CADMIUM VAPOR PRESSURE IN THE METAL HALIDE ARC: R.P. Gilliard and T.D. Russell, General Electric Co.

HB-3 A MULTITHERMAL EQUILIBRIUM (MTE) ARC PLASMA HEAT TRANSFER MODEL: T.L. Eddy and D.W. Pruitt, Georgia Tech and AEDC

HB-4 ANALYTICAL EXPRESSIONS FOR THE POPULATIONS AND IONIZATION FREQUENCIES OF EXCITED ATOMS IN NON-EQUILIBRIUM HYDROGEN PLASMA: J.A. Kunc, U. of Southern California

HB-5 DETERMINATION OF PARTICLE NUMBERS IN HIGH PRESSURE LAMPS: R. Schäfer, Philips GmbH Forschungslaboratorium Aachen, Germany

HB-6 DETERMINATION OF TEMPERATURE PROFILES FROM OPTICALLY THICK LINES: H.-P. Stormberg, Philips GmbH Forschungslaboratorium, Aachen, Germany

HB-7 VOLUMETRIC INSTABILITY IN A HIGH POWER MERCURY DISCHARGE: A. Mandl and M.W. McGeoch, Avco Everett Research Lab

WEDNESDAY EVENING, 10 OCTOBER

I: WORKSHOP ON RF DISCHARGES
Chairperson: J. Verdeyen, U. of Illinois
19:30 UMC Center Ballroom

I-1 THINGS WE DON'T UNDERSTAND ABOUT PLASMA ETCHING: B. Chapman, Tegal Corp.

I-2 PLASMA POTENTIALS OF 13.56 MHz rf ARGON GLOW DISCHARGES IN A PLANAR SYSTEM: J.W. Coburn, IBM Research

I-3 DYNAMICS OF RADIO FREQUENCY GLOW DISCHARGES: R. Gottscho and M.L. Mandich, AT&T Bell Labs

I-4 THEORETICAL MODELLING OF PLANAR RF DISCHARGES: D.W. Ernie, U. of Minnesota

I-5 ENERGY PARTITIONING AND EXCITATION RATES IN RF PARALLEL PLATE DISCHARGES: M.J. Kushner, Math Sciences Northwest

THURSDAY MORNING, 11 OCTOBER

JA: ELECTRON TRANSPORT
Chairperson: Barbara Whitten, Lawrence Livermore Lab
08:15 UMC Center Ballroom

JA-1 ELECTRON SWARM PROPERTIES OF SF_6-CCl_2F_2 MIXTURES: M.F. Frechette and J.P. Novak, IREQ, Varennes, Québec, Canada

JA-2 DENSITY GRADIENT EXPANDED ENERGY DISTRIBUTION FUNCTIONS: B.M. Penetrante and J.N. Bardsley, U. of Pittsburgh

JA-3 MODEL CALCULATIONS OF ELECTRON TRANSPORT IN NON-UNIFORM FIELDS: T.J. Moratz and L.C. Pitchford, Sandia National Labs

JA-4 HYDRODYNAMIC MODELS OF ELECTRON TRANSPORT IN RAPIDLY VARYING FIELDS: L.C. Pitchford, Sandia National Labs, and J. Ingold, General Electric Co.

JA-5 EQUATION OF EVOLUTION FOR ELECTRONS IN A WEAKLY IONIZED GAS AND INFLUENCED BY SPACE-TIME VARYING ELECTRIC FIELDS: E. E. Kunhardt, Polytechnic Inst. of New York

JB: THERMAL ARC SPRAYS
Chairperson: Paul A. Siemers, GE R&D, Schenectady
08:15 UMC East Ballroom

JB-1 PLASMA SPRAYING: E. Pfender, U. of Minnesota

JB-2 PLASMA-PARTICLE INTERACTIONS IN THERMAL PLASMA SPRAYING: M. Boulos, Université de Sherbrooke, Sherbrooke, Quebéc, Canada

JB-3 PROPERTIES OF PLASMA-SPRAYED COATINGS: P. Fauchais, Université de Limoges, France

K: GLOW DIAGNOSTICS
Chairperson: Louis Palumbo, Schaefer Associates
10:00 UMC Center Ballroom

K-1 DETERMINATION OF THE EFFECTIVE RADIATIVE LIFETIMES OF THE $6\,^3P_1$ ATOMIC MERCURY LEVEL IN LOW-PRESSURE MERCURY DISCHARGES: P. van de Weijer and R.M.M. Cremers, Philips Research Labs, Eindhoven

K-2 ISOTOPE EFFECTS IN ATOMIC RESONANCE RADIATION TRANSPORT: M. Grossman, R. Lagushenko, and J. Maya, GTE Lighting Products

K-3 DISSOCIATION AND PRODUCT FORMATION KINETICS OF NF_3 ETCHANT GAS DISCHARGES: K. Greenberg and J.T. Verdeyen, U. of Illinois at Urbana-Champaign

K-4 NEUTRAL PARTICLE DENSITY TRANSIENTS IN GASEOUS DISCHARGES: A. Metze, D.W. Ernie, H.J. Oskam, and L.M. Chanin, U. of Minnesota

K-5 OPTOGALVANIC SPECTROSCOPIC MEASUREMENT OF SINGLET HELIUM RYDBERG SERIES: B.N. Ganguly and Alan Garscadden, AFWAL, Wright Patterson Air Force Base

K-6 ELECTRIC FIELD MEASUREMENTS IN GLOW DISCHARGES USING OPTOGALVANIC DETECTION OF RYDBERG ATOMS: J.E. Lawler, D.K. Doughty, and S. Salih, U. of Wisconsin-Madision

K-7 ENERGY DISTRIBUTION OF IONS ARRIVING AT THE ELECTRODES OF A RF DISCHARGE: A. Metze, D.W. Ernie, and H.J. Oskam, U. of Minnesota

THURSDAY AFTERNOON, 11 OCTOBER

L: POSTERS. MOSTLY ATOMIC AND MOLECULAR
Chairperson: Pablo Vicharelli, NCAR
11:30 UMC West Ballroom

LA: ATOMIC AND MOLECULAR PROPERTIES

LA-1 ATOMIC TRANSITION PROBABILITIES IN REFRACTORY METALS: S. Salih, D.W. Duquette, and J.E. Lawler, U. of Wisconsin-Madison

LA-2 KINETIC MODELING IN NEON-LIKE IONS: B.L. Whitten and A.U. Hazi, Lawrence Livermore National Lab

LA-3 PHOTO-ECHO EXPERIMENTS ON COHERENCE MULTIPOLE DECAYS: M.R. Woodworth and I.D. Abella, U. of Chicago

LA-4 EMISSION AND ABSORPTION CHARACTERISTICS OF LONG-PULSED, ELECTRON-BEAM EXCITED, PURE HELIUM PLASMAS: L.W. Downes, S.D. Marcum, and W.E. Wells, Miami U.

LA-5 EMISSION AND ABSORPTION CHARACTERISTICS OF A THERMICALLY GENERATED HEAT PIPE SODIUM PLASMA: V. Petricevic, L.W. Downes, D.G. Hild, S.D. Marcus, M. Mihailidi, D.A. Stetser, and W.E. Wells, Miami U.

LA-6 ELECTRON STRUCTURE OF THE LITHIUM MOLECULAR ANION, LI_2^-: H.H. Michels and R.H. Hobbs, UTRC; and L.A. Wright, MRC

LB: PHOTON ABSORPTION AND EMISSION

LB-1 VIRTUAL STATE RESONANCE EFFECT ON THE PHOTODETACHMENT THRESHOLD BEHAVIOR OF Li^- LEAVING ^2P Li: Y.K. Bae and J.R. Peterson, Chemical Physics Lab

LB-2 EFFECTS OF FEMTOSECOND LASER PULSES ON ATOMIC COLLISION PROCESSES: J.F. Scipione and Paul L. De Vries, Miami U.

LB-3 PROMPT AND DELAYED PHOTOLYSIS OF Cs_2: F. Davanloo and C.B. Collins, U. of Texas at Dallas; A.S. Inamdar and N.Y. Mehendale, U. of Poona; and A.S. Naqvi, King Saud U. of Riyadh

LB-4 OPTICAL ESCAPE FACTORS FOR SOME NII LINES: IMPLICATIONS ON THE OPACITY OF LIGHTNING: P.A. Vicharelli, NCAR

LC: ELECTRON COLLISIONS

LC-1 ELECTRON-EXCITED HYDROGEN AND HELIUM COLLISIONS: E.J. Mansky and M.R. Flannery, Georgia Inst. of Technology

LC-2 AB INITIO STUDY OF LOW-ENERGY ELECTRONS INTERACTING WITH HCN MOLECULES: A. Jain and D.W. Norcross, JILA, U. of Colorado and NBS

LC-3 RO-VIBRATIONAL EXCITATION OF HCl BY ELECTRONS: N.T. Padial and D.W. Norcross, JILA, U. of Colorado and NBS

LC-4 PRODUCTION OF EXCITED NITROGEN ATOMS AND IONS BY ELECTRON IMPACT ON NITROGEN MOLECULES: D.L.A. Rall, Francis A. Sharpton, C.C. Lin, and L.W. Anderson, U. of Wisconsin-Madison

LC-5 CROSS SECTIONS FOR ELECTRON IMPACT IONIZATION AND DISSOCIATIVE IONIZATION OF THE FREE RADICALS: CF_3, SiF_3, and SiF_2: R.C. Wetzel, F.A. Baiocchi, and R.S. Freund, AT&T Bell Labs

LC-6 ELECTRON IMPACT EXCITATION OF THE $n \geq 3$ STATES OF He: D.F. Register, S. Trajmar, California Inst. of Technology; and D.C. Cartwright and G. Csanak, Los Alamos National Lab

LC-7 DISSOCIATIVE ATTACHMENT IN AMMONIA: P.D. Burrow and K.L. Stricklett, U. of Nebraska

LC-8 ELECTRON TEMPERATURE DEPENDENCE OF THE RECOMBINATION OF ELECTRONS WITH O_4^+ IONS: J.L. Dulaney, M.A. Biondi, and R. Johnsen, U. of Pittsburgh

LC-9 LABORATORY STUDIES OF ELECTRON BEAM GROWTH IN N_2: P. Ip, and W.A.M. Blumberg, AFGL, Hanscom AFB; and B.D. Green, W.J. Marinelli, and G.E. Caledonia, Physical Sciences, Inc.

LC-10 A LIMIT FOR THE QUENCHING OF $H_2(c^3\pi_u)$ METASTABLES: H. Tischer and A.V. Phelps, JILA, U. of Colorado and NBS

LD: ATOMIC AND MOLECULAR COLLISIONS

LD-1 A NEW METHOD FOR THE RAPID AND ACCURATE SOLUTION OF THE SCHRODINGER EQUATION: P.L. De Vries, Miami U.

LD-2 ANALYTICAL AND NUMERICAL SOLUTIONS OF THE TIME DEPENDENT DEBYE-SMOLUCHOWSKI EQUATION: M.R. Flannery and E.J. Mansky, Georgia Inst. of Technology

LD-3 TIME-RESOLVED STUDY OF ION-MOLECULE REACTIONS IN OXYGEN AT HIGH GAS DENSITIES: J. De Urquijo, C. Cisneros, and I. Alvarez, Instituto de Física, UNAM, México

LD-4 REACTIONS OF Zr^+ AND ZrO^+ IONS WITH O_2: S. Dheandhanoo, R. Johnsen, and M.A. Biondi, U. of Pittsburgh

LD-5 ION-MOLECULE ASSOCIATION REACTIONS INVOLVING CYANO-COMPOUNDS: C.V. Speller and M. Meot-Ner (Mautner), NBS-Gaithersburg

LD-6 MASS SPECTROMETRIC STUDY OF $C_{2m}H_{2m}^+ \cdot (N_2)_n$ CLUSTERS: C.V. Speller, NBS-Gaithersburg

LD-7 STRUCTURE AND STABILITY OF $NH_4^+(NH_3)_m(HCN)_n$ CLUSTERS: C.V. Speller, NBS-Gaithersburg; C.A. Deakyne, College of the Holy Cross; and M. Meot-Ner (Mautner), NBS-Gaithersburg

LD-8 MODELING OF ION MOLECULE REACTIONS AT HIGH PRESSURES: C.D. Eberhard and C.B. Collins, U. of Texas at Dallas; and J. Stevefelt, GREMI, U. of Orleans, France

LD-9 STUDY OF TWO-BODY AND THREE-BODY CHANNELS FOR THE REACTION OF METASTABLE HELIUM ATOMS WITH NITROGEN: J.M. Pouvesle and J. Stevefelt, GREMI, U. of Orleans, France; and C.B. Collins, Z. Chen, V. Gylys, and H. Jahani, U. of Texas at Dallas

LD-10 CROSS SECTION FOR ELECTRONIC ENERGY TRANSFER BETWEEN MERCURY ISOTOPES: R. Lagushenko, M.W. Grossman, and J. Maya, GTE Lighting Products

LD-11 AN OODR STUDY OF COLLISION INDUCED ENERGY TRANSFER BETWEEN UNPERTURBED ELECTRONIC STATES: D.H. Katayama, AFGL, Hanscom AFB

LD-12 SYMMETRIC CHARGE-TRANSFER CROSS SECTIONS IN RARE GAS (Rg^+-Rg) SYSTEMS: E.J. Mansky and M.R. Flannery, Georgia Inst. of Technology

LD-13 ASSOCIATION/DISSOCIATION IN DENSE GASES AND ADSORPTION/DESORPTION ON SURFACES: M.R. Flannery, Georgia Inst. of Technology

FRIDAY MORNING, 12 OCTOBER

MA: SPARK DEVELOPMENT
Chairperson: W. Byszewski, GTE Labs, Waltham
8:00 UMC Room 235

MA-1 THE PROBABILITY OF ELECTRICAL BREAKDOWN: EVIDENCE FOR A TRANSITION BETWEEN THE TOWNSEND AND STREAMER MECHANISMS: R.V. Hodges, R.N. Varney, and J.F. Riley, Lockheed Palo Alto Research Lab

MA-2 2-D NUMERICAL SIMULATION OF STREAMERS IN ATMOSPHERIC N_2: S.K. Dhali and P.F. Williams, Texas Tech

MA-3 STREAK PHOTOGRAPHIC STUDIES OF TRIGATRON TRIGGERED BREAKDOWN: M.R. Wages, P.F. Williams, G. Schaefer, and K.H. Schoenbach, Texas Tech

MA-4 KINETIC INVESTIGATION OF STREAMER DEVELOPMENT: E.E. Kunhardt, Polytechnic Inst. of New York, and Y. Tzeng, Auburn U.

MA-5 INTERFEROMETRIC MEASUREMENTS OF LASER PREIONIZATION TRIGGERED SPARK COLUMNS: W.D. Kimura, M.J. Kushner, E.A. Crawford, and S.R. Byron, Mathematical Sciences Northwest

MA-6 A FIRST PRINCIPLES MODEL FOR LASER TRIGGERED SPARK COLUMNS: M.J. Kushner and R.D. Milroy, Mathematical Sciences Northwest

MA-7 A THERMODYNAMIC MODEL FOR LASER TRIGGERED SPARK GAPS: M.J. Kushner, Mathematical Sciences Northwest

MB: IONIZATION PROCESSES
Chairperson: L.W. Anderson, U. of Wisconsin
8:00 UMC Forum Room

MB-1 IONIZING COLLISIONS OF LASER-EXCITED NEON ATOMS: W. Bußert, T. Bregel, M.-W. Ruf, and H. Hotop, Fachbereich Physik der Universitat, FRG

MB-2 PHOTODISSOCIATION DYNAMICS AND ENERGETICS OF SMALL GAS PHASE CLUSTER IONS: M.F. Jarrold, A.J. Illies, and M.T. Bowers, U. of California

MB-3 ELECTRON AND METASTABLE SPATIAL DISTRIBUTIONS FOR POSITIVE COLUMNS WITH IONIZATION FROM A METASTABLE STATE: F.J. Romeriras and C.M. Ferreira, U. Tec Lisboa

MB-4 PHOTOIONIZATION OF Kr and Kr_2 at 193 nm and 248 nm: D.B. Geohegan, A.W. McCown, and J.G. Eden, U. of Illinois at Urbana-Champaign

MB-5 LASER IONIZATION OF LITHIUM VAPOR: J.K. Rice and G.C. Tisone, Sandia National Labs

MB-6 EFFECT OF ELECTRONIC ALIGNMENT UPON THE PROCESS $2Na\ (^2P_{3/2}) \rightarrow Na_2^+ + e^-$: G.P. Reck, E.W. Rothe, R. Theyunni, and C.C. Tung, Wayne State U.

N: INVITED PAPERS
Chairperson: Ronald Waynant, Naval Research Lab
10:00 UMC Center Ballroom

N-1 RF-EXCITED WAVEGUIDE LASERS: L. Newman, United Technology Research Center

N-2 PROGRESS IN THE PURSUIT OF AN X-RAY LASER: W.L Morgan, Lawrence Livermore National Lab

SESSION A

08:30, Tuesday, October 9, 1984

ION TRANSPORT

Chairperson: W.P. Allis
Massachusetts Institute of Technology

A

A-1 Negative-Ion Density from Natural Sources in SF_6, J.P. NOVAK and G. ELLENA, IREQ, Varennes, Québec, Canada--A Gerdien ion counter has been used to measure the natural density of SF_6 negative ions in a Pyrex tube 12 inches in diameter by 50 inches long at atmospheric pressure. The collector and outer electrode of the counter had an outer and inner diameter of 0.25 and 1.5 inches, respectively and a length of 4 inches. The gas flow was varied between 25 and 200 cm^3s^{-1}. The ion mobility evaluated from the current-voltage characteristics was 0.58 $cm^2V^{-1}s^{-1}$, reasonably in agreement with the value 0.55 cm^2V^{-1} s^{-1} obtained by Schmidt et al.[1] The ion densities measured within the span of several days varied between 1400 and 2000 cm^{-3} with an average value of 1700 cm^{-3}.

[1]W.F. Schmidt, H. Jungblut, D. Hansen, and H. Tagashira, in "Gaseous Dielectrics II", ed. L.G. Christophorou (Pergamon, New York, 1980), p. 1.

A-2 Mobility of Positive Ions in SF_6 Gas, F. LI-AVAVENA and M.SAPOROSCHENKO, Southern Illinois University in Carbondale--Following positive ions S^+, SF_2^+, SF_3^+, SF_4^+, SF_5^+, $S_2F_5^+$, $S_2F_6^+$, $S_2F_7^+$, and $S_2F_9^+$ have been mass identified in sulphur hexaflouride gas in the pressure range 0.25 - 0.50 torr using the electron impact ion source. The mobilities of the ions SF_2^+, SF_3^+, SF_4^+, SF_5^+, and $S_2F_7^+$ have been measured for values of E/N between 56 and 250 Td. The zero field reduced mobilities are 0.60, 0.59, o.66, 0.67, and 0.51 cm^2/V-sec, respectively. The processes of formation of some secondary ions will be discussed.

A-3 Negative Differential Conductivity (NDC) Revisited. - W. F. BAILEY and A. GARSCADDEN, Air Force Inst. of Technology and Air Force Wright Aeronautical Laboratories, WPAFB OH 45433 - Recently Petrovic et. al[1] have presented a simple model and critiqued our previous theory[2] of electronic conductivity in gas mixtures. We show that our original expression for the drift velocity is valid and establish new generalized criteria for the occurrence of NDC. These criteria show that the momentum transfer collision frequency must increase with energy and that the fractional energy transfer must change rapidly between channels, which may be momentum transfer, rotational, vibrational, or electronic, as E/N is varied. Also, it is not correct to invoke the effects of higher order terms in the legendre expansion unless significant differences are obtained between this calculation and the two-term expansion.

[1]Petrovic, Z. L., Crompton, R. W., and Haddad, Aust. J. Phys., 37, 23, (1984).

[2]Long, W. H., Bailey, W. F., and Garscadden, A., Phys. Rev. A, 13, 471, (1976).

A-4 Measurement of Oscillations in Gases With Negative Differential Conductivity, P. BLETZINGER, AF Wright Aeronautical Laboratories -- In gases such as methane and mixtures of some rare gases with molecular gases, the drift velocity is a non-monotonic function of the reduced electric field (E/N). In the range where the drift velocity decreases with increasing E/N, the negative characteristic can lead to instabilities. In atmospheric pressure discharges ionized with an electron beam, methane, mixtures of methane with CF_4, C_2F_6, and C_3F_8 and mixtures with argon were investigated at appropriate values of E/N. Instabilities were observed around the expected region of E/N. The instabilities are in the form of moving domains, moving with velocities in the order of the electron drift velocity from cathode to anode. The velocities are a function of E/N, but are also subject to the electrode spacing as a boundary condition. The oscillation frequency is influenced by the electrode spacing, but not in a very reproducible manner. The range over which the instability occurs will have to be avoided when this type of discharge is to be used as a switch for inductive energy storage.

A-5 Measurement of the Diffusion Coefficient of Sodium in Neon at 530 K, H.J. CORNELISSEN, Philips Research Laboratories, Eindhoven - The diffusion coefficient D of sodium in neon has been measured at 530 K. In a cylindrical discharge tube filled with neon at densities N of 10^{23} to 10^{24} m^{-3} a strong radial sodium ground-state density gradient is induced by means of a discharge current. In the afterglow of the discharge the decay rate of the fundamental diffusion mode is measured using dye laser absorption at the sodium D1-line. For D*N the value (143 ± 18) 10^{19} $m^{-1}s^{-1}$ is found. Using additional experimental data in literature a comparison is made with molecular kinetic theory for the temperature region of 300 K to 530 K. The repulsive part of the Na-Ne interaction potential is probed in this temperature range. The potential appears to be less repulsive than a Lennard-Jones (8-6) potential[1].

[1] R.A. Gottscho, R. Ahmad-Bitar, W.P. Lapatovich, I. Renhorn, D.E. Pritchard, J. Chem. Phys. 75 (1981) 2646.

A-6 Ambipolar Diffusion Coefficients for Discharges in Attaching Gases. G.L. ROGOFF, GTE Laboratories Inc.--The process of ambipolar diffusion can be modeled in terms of the ambipolar space-charge field explicitly. To clarify when the use of ambipolar diffusion coefficients is a practical alternative to explicit field calculations we use a general expression for those coefficients in an arbitrary mixture of electrons, positive ions, and negative ions. Since this expression involves charged particle densities and density gradients, it is useful only with assumptions that hold in special cases. Examples of coefficients for three-component discharges and afterglows (electrons, one type of singly-charged negative ion, one type of singly-charged positive ion) will be discussed. In addition, the general expression is used to determine limitations associated with the coefficients for an active three-component plasma published by Thompson.[1] The general expression reduces to Thompson's expressions if $\mu_- = \mu_+$ and $(D_-/\mu_-)(\nabla n_e/n_e) = (D_e/\mu_e)(\nabla n_-/n_-)$, where μ, D, and n are the mobility, diffusion coefficient, and number density, respectively, for the electrons (e), positive ions (+), and negative ions (-). The latter relationship is a special variation of the proportionality condition.

[1] J.B. Thompson, Proc. Phys. Soc. London 73, 818 (1959).

SESSION B

10:15, Tuesday, October 9, 1984

ELECTRON COLLISIONS

Chairperson: N. Padial
University of New Mexico

B

B-1 Photoenhanced Electron Attachment in Vinylchloride and Trifluorethylene.* M. J. ROSSI, H. HELM, AND D. C. LORENTS, Chemical Physics Laboratory, SRI International-- Electron attachment has been measured for ground state and photoexcited vinylchloride, C_2H_3Cl and trifluorethylene, C_2F_3H, in a Grunberg type drift tube apparatus at He pressures between 100 and 500 torr. In their ground state both species were observed to exhibit low attachment coefficients at low E/N, with sharp increases in attachment at E/N values > .8 and 3.2 Td respectively. Following photoexcitation of the gas sample with a 193 nm laser pulse (1 and 10 mJ) enhancements in the attachment rate by 3 to 5 orders of magnitude was observed, the largest enhancement being at low values of E/N. End product analysis of the photolyzed gas leads us to conclude that the enhancement is due to the formation of vibrationally excited HCl and HF in the photodissociation process. The dependence of the photoenhanced attachment rate on E/N, gas pressure, and laser fluence will be presented and discussed.

*Work supported by the Army Research Office.

B-2 Measurements of Electron Transport, Attachment, and Ionization in Humid Air - D.K. DAVIES, Westinghouse R&D Center*--A pulsed drift tube has been used to measure the arrival time spectra of electrons, negative ions, and positive ions in CO_2-free air containing 2% H_2O. Values of electron and ion mobilities together with attachment and ionization rates have been determined from these measurements over the range $0.6 \leq E/N \leq 300 \times 10^{-21}$ Vm^2. The presence of H_2O causes significant changes both in electron and ion kinetics compared with dry air. For values of $E/N \leq 2 \times 10^{-21}$ Vm^2 both the electron mobility and attachment rate are found to be constant having mean values of 0.278 ± 0.006 m^2/Vs and $(1.53 \pm 0.11) \times 10^{-43}$ m^6/s, respectively, and correspond to 300°K thermal values. Values of ion mobility are up to 30% lower than those in dry air presumably due to clustering reactions. At values of $E/N > 100 \times 10^{-21}$ Vm^2, the effective dissociative attachment rate is significantly higher than that in dry air (for which the rate is below that predicted on the basis of O_2 data). The present data are consistent with a lower collisional detachment rate of the heavier negative cluster ions.

*Supported in part by AFWL, Contract F29601-81-C-0044.

B-3 Effect of Temperature on Dissociative Attachment to $CC\ell F_3$ and C_2F_6.* S.M. SPYROU and L.G. CHRISTOPHOROU, ORNL and U. of Tennessee--The total electron attachment rate constant, $k_a(\langle \varepsilon \rangle)$, for C_2F_6 and $CC\ell F_3$ were measured using the electron swarm technique over the mean energy range 0.4 to 5 eV in the range of temperature, T, 300 to 750 K. At each value of T the total electron attachment cross section $\sigma_a(\varepsilon)$ was determined from the measured $k_a(\langle \varepsilon \rangle)$ using the swarm unfolding technique. The $\sigma_a(\varepsilon)$ for C_2F_6 shows a single peak which shifts from 3.9 eV at 300 K to $\sim$3.3 eV at 750 K. For $CC\ell F_3$ the $\sigma_a(\varepsilon)$ shows two peaks at $\sim$1.5 and $\sim$4.5 eV. Especially the $\sim$1.5 eV peak is affected by T. The peak value of $\sigma_a(\varepsilon)$ increased by a factor of $\sim$3, and the peak energy and onset shifted progressively to lower energies when T increased from 300 to 700 K. It was also found that $CC\ell F_3$ dissociates thermally at $T \geq 500$ K. These findings will be presented and discussed by considering the effect of increased internal molecular excitation with increasing T on the rate and energetics of dissociative attachment.

*Research sponsored by the Division of Electric Energy Systems, USDOE, under contract DE-AC05-84OR21400 with Martin Marietta Energy Systems, Inc.

B-4 Effective 3-Body Attachment Rate and Electron Drift Velocity in Hexafluoropropylen. TH. ASCHWANDEN, Swiss Fed. Inst. of Technology, ETH, Zürich, Switzerland -- A time resolved Townsend method was used to study the influence of gas density ($1.6 \cdot 10^{16} cm^{-3} < N < 8.2 \cdot 10^{18} cm^{-3}$) on swarm parameters in n-C_3F_6. Values for v_e and for the effective ionization rate $(k_i - k_a)$, where k_i is the ionization rate and k_a the apparent attachment rate, have been determined over the range $76 < E/N < 1213$ Td. At constant E/N a steady decrease of $(k_i - k_a)$ with increasing N has been observed which is assigned to three-body attachment. This is consistent with the density dependence of $(E/N)_{lim}$ [1,2] $(k_i = k_a)$ in this gas. The effective three body attachment rate k_{a3} was determined using low density swarm data (two body rates) and density dependent $(E/N)_{lim}$ values. At high N (density incl. compressibility), values for $(E/N)_{lim}$ were infered from uniform-field breakdown measurements. For $N > 10^{20}$ cm^{-3} $(E/N)_{lim}$ begins to saturate and k_{a3} is $2 \cdot 10^{-30}$ cm^6/s at 420 Td. Such high values for k_{a3} seem to be compatible with results form buffer gas experiments.[2]

[1]Th. Aschwanden and G. Biasiutti, J. Phys.D: Appl.Phys.14, (1981), L189.
[2]S.R. Hunter et al., J. Phys.D: Appl.Phys. 16,(1983),573.

B-5 Dissociative Attachment in Low-Energy e + Li_2 Collisions, H. H. MICHELS* and J. M. WADEHRA**, AFWAL/APL, Wright-Patterson AFB, OH, 45433--A study of dissociative attachment (DA) in e + Li_2 collisions has been initiated based on ab initio calculations of the pertinent potential energy curves and capture widths. For collision energies less than 1.4 eV, DA occurs only on the lowest $^2\Sigma_g^+$ state of Li_2^-. We find that this state crosses the ground $^1\Sigma_g^+$ state at R_x = 3.45 Å, close to the sixth vibrational level of Li_2. The imaginary part of the $^2\Sigma_g^+$ potential has been calculated by analytic continuation of a discrete representation of e + Li_2 and the autoionizing region of this potential has been treated using the stabilization method. This resonant state of Li_2^- is of the Feshbach type. Our preliminary studies indicate that DA should increase for vibrationally excited Li_2, a result similar to that found for e + H_2.

Permanent addresses: *UTRC, East Hartford, CT, 06108; **Wayne State U., Detroit, MI, 48202. Work supported in part by AFOSR under Contract F49620-83-C-0094.

B-6 Development of a New Technique for Measurement of Electron Attachment Coefficient. T.H. HARDING+ and Y.W. KIM, Lehigh University -- We have developed a new swarm method that allows rapid measurement of electron attachment properties at nearly atmospheric pressures.[1] The apparatus employs a unique cylindrical geometry with a radial electric field between a pair of coaxial electrodes, with the inner one serving as a pulsed photoelectron source. The electron swarm and resulting negative ions are driven radially outward through an attaching gas and buffer gas mixture, and are detected as time-resolved currents by a cylindrical detector contained within the outer electrode as a Faraday cage. The non-uniform radial electric field leads to attachment information as a function of the field strength in a single run. Data collection and analysis are handled by a dedicated minicomputer with two independent digitizers. Measurements have been made for oxygen in helium or nitrogen and for sulphur dioxide in helium in the E/N ratio range of 1.7×10^{-19} to 3.8×10^{-18} Vcm^2. Details of the technique and the results will be presented.

+Present Address: E.I. duPont de Nemours and Company

[1] T.H. Harding, Ph.D. Dissertation (Physics), Lehigh University (1984).

B-7 Collisional-Radiative Coupling Coefficients for Modeling of High Pressure Discharges.* P. A. VICHARELLI† and A. V. PHELPS,‡ JILA, U. of Colo. & NBS.--A simplified model for the behavior of highly excited atomic states in high pressure discharges is presented. The model, based on a reformulation of the collisional-radiative equations of Bates et al.,[1] introduces a coupling coefficient that describes the increase in the population of a state of interest, e.g., a metastable state, caused by recombination into a higher excited state. Thus, dissociative recombination into an excited level m can be easily incorporated into the rate equation of a lower level by adding the recombination rate to level m multiplied by the appropriate coupling coefficient. This leads to a greatly reduced number of rate equations that describe the kinetics of the discharge. Coupling coefficients for a helium discharge are presented.

*Supported in part by AFOSR.

†Present address: National Center for Atmospheric Research, Boulder, CO 80307.

‡Staff Member, Quantum Physics Division, Boulder, CO 80309.

[1]D. R. Bates, A. E. Kingston and R. W. P. McWhirter, Proc. Roy. Soc. A267, 297 (1962).

B-8 RF-Probe Measurements of Electron and Ion Density Decays in Atmospheric-Density He-H_2O and He-SF_6 Afterglows*, R. JOHNSEN, Univ. of Pittsburgh -- A new radio-frequency (f = 15 MHz) conductivity probe method has been developed for studies of de-ionization processes in afterglow plasmas at high neutral gas densities (near atmospheric and above). In a first application of this technique, helium with small additions of H_2O or SF_6 was irradiated by UV pulses from an array of sparks and the decay of the conductivity during the afterglow phase was measured. The results indicate that the rf probe method is capable of following the electron density decay over a range from about 5×10^{10} down to 1×10^6 cm^{-3} and that the sensitivity is sufficient to also detect the presence of (+)/(-) ion plasma in the late afterglow. Details of the technique will be discussed and the observed decay curves will be compared to model calculations involving electron-ion recombination, electron attachment, and ion-ion recombination processes.

*Work supported, in part, by the U. S. Army Research Office.

SESSION CA

13:15, Tuesday, October 9, 1984

LASERS

Chairperson: Gerald Hays
Sandia National Lab

CA-1 Low Threshold Long Gain Length Solar-Pumped C_3F_7I Laser, R. J. De Young, NASA Langley Research Center--The efficient conversion of solar into laser photons could have a significant impact on future space power and propulsion. One successful solar lasant has been C_3F_7I which photodissociates, upon absorption of a 270 nm photon, into $I^*(5^2P_{1/2})$ resulting in lasing at 1.315 μm. A unique laser cavity was constructed which allowed lasing at gain lengths of 40 cm using CW xenon arc solar simulators. The threshold input intensity was 27 w/cm^2 (192 solar constants) which is the lowest threshold solar laser to date. Multimode power was greater than 10 W and intrinsic efficiency was 0.13 percent (max. 0.2 percent). Quenching from I_2 affected lasing pulse length, limiting lasing pulse lengths to a maximum of 120 msec at C_3F_7I pressures of 3 torr. At high pressure (increased energy deposition), the pulse length shortened considerably and at 10 torr lasing ceased. A systematic parameter study was accomplished and the results will be presented. Methods to reduce quenching by I_2 will be discussed.

CA-2 Transient Absorption Spectra of Rare Gas Dimer Molecules, K.P. KILLEEN and J.G. EDEN, University of Illinois at Urbana-Champaign -- The visible and ultraviolet (UV) absorption spectra of the $^{1,3}\Sigma$ excited states of the rare gas dimers (Rg_2) are believed to contribute significantly to the non-saturable optical loss in various excimer lasers. Unfortunately, the existing data for rare gas absorption is fragmentary since previous experiments have relied on a wavelength-by-wavelength acquisition of the data with a tunable dye laser. In the experiments reported here, the visible and near UV absorption spectra of the Rg_2^* excimers produced by e-beam excitation have been studied with a pulsed Xe lamp and an optical multichannel analyzer (OMA). In this way, the entire spectrum is acquired in a single shot. Consequently, the relative absorption at, say, two different wavelengths is fixed and spectra with excellent resolution are obtainable. Examination of the Ar_2^* spectrum in 6000 Torr of Ar reveals several sequences of band heads between 350 and 900 nm. Similar spectra have been observed for Ne_2^*, Kr_2^* and Xe_2^* and the assignment of the terminal levels will be discussed.

CA-3 Photodissociation of Xe_2 Excimer:Observation of Electronic Excited States, M.N. EDIGER and J.G. EDEN, University of Illinois at Urbana-Champaign -- Xenon excimers have been observed in real time by a laser-induced-fluorescence (LIF) technique, in which the moleclues are photodissociated by a dye laser and the subsequent atomic radiation is detected. Spectra have been obtained covering wavelengths from 615 nm to 925 nm, while molecular LIF has been observed for $730 \leq \lambda \leq 920$ nm. A preliminary analysis of the spectra in terms of Mulliken's potential curves [1], indicates that the observed emission results from Xe_2^* ($7d\pi \rightarrow 0_g^+, 0_u^+$) bound $\rightarrow$ free molecular transitions. Also, temporal studies show that the dimer population peaks $\sim$ 350-400 ns after firing the ArF laser. This experimental approach offers a means of studying in detail electronic excited states lying 8-13 eV above ground and hitherto inaccessible.

[1] R.S. Mulliken, J. Chem. Phys. 52, 5170 (1970).

CA-4 Vibrational Relaxation in the B State of XeF,* G. BLACK, L. E. JUSINSKI, D. C. LORENTS, and D. L. HUESTIS, SRI International, Menlo Park, CA 94025 Photodissociation of XeF_2 with a KrF laser has been used to prepare XeF(X). XeF $(B)_{v'=1}$ was then produced by pumping XeF(X) with a dye laser from the v"=0, 1, and 2 levels. Using a monochromator to transmit emission from only $XeF(B)_{v'=0}$, relaxation of the v'=1 to v'=0 level has been observed as a function of added He, Ne, Ar, N_2, Kr and SF_6. Rate coefficients are presently being determined and will be reported.

*Work supported by DARPA ONR Contract No. N00014-84-C-0256.

CA-5 Fluorescence Cross Sections of $HgBr_2$† - C.L. CHEN and P.J. CHANTRY, Westinghouse R&D Center--A previously used method[1] for measuring wavelength resolved emission cross sections has been extended to cover the range of the (B-X), (C-X), and (D-X) emission bands of HgBr* produced by electron impact on $HgBr_2$. In the region of overlap the agreement with our previous data[1] is good. Calculation of total band emission cross sections from the basic data requires appropriate partitioning of the emission spectrum. This is straightforward for the (C-X) and (D-X) bands, but uncertainties are present in separating the (B-X) signal from an overlapping structured band, labelled (B'-X), between 295 and 412 nm. The method now adopted for partitioning the (B-X) and (B'X) emissions, together with more extensive He calibration data, gives a (B-X) band emission cross section 30% lower than previously reported.[1] The total emission cross sections for the B, B', C, and D-X bands rise steeply from thresholds at 6.00, 7.45, 7.40 and 7.65 eV respectively, reaching plateau values of 2.25, 0.72, 0.82, and 0.69 x $10^{-16}cm^2$ respectively above 15 eV.

†Supported in part by ONR, Contract No. N00014-83-C-0240.

[1]C.L. Chen & P.J. Chantry, Bull. Am. Phys. Soc. 28 177 (1983).

CA-6 Electron-Beam Excitation of Ionized and Neutral Atomic Line Lasers, K. Ono, T. Oomori, S. Fujita and Y. Ueda, Mitsubishi Electric Corp., Central Res. Lab., Amagasaki, Japan, and T. Narikawa, MFC, Tokyo, Japan -- Laser action has been observed for neutral atomic lines of rare gases when a 600 kV, 7 kA, 50 ns electron beam is injected into initially-neutral gas. The electron beam is propagated through 0.03 ~ 30 Torr Ne, Ar, Kr or Xe gas in a 175 cm long, 13.4 cm diameter drift tube. No external field is imposed. Visible ~ near-IR laser emissions have been detected in the end-view direction. These emissions have a pulse width of ~ 5 ns, and are amplified in traveling along with the early part of the electron-beam pulse. Similar experiments were performed with a 600 kV, 10 kA, 3 ns electron beam.[1] Laser action was observed for singly-ionized and neutral atomic lines in the UV ~ near-IR region. In the present experiments, laser action is observed for neutral lines only, although the emission spectra consist of ionized and neutral lines similarly to the case of the 3 ns electron beam. Temporal behaviors of side-on emissions have been compared for the 50 ns and 3 ns electron beams.

[1]K. Ono, Jpn. J. Appl. Phys. 19, 1515 (1980).

CA-7 Computer Model of CW Ion Lasers Excited By Electron Beams*, G. FETZER, J.J. ROCCA, G.J. COLLINS, AND R. JACOBS, Colorado State University, Spectra Physics--Direct current electron beam pumping of ion lasers has been recently demonstrated [1]. To determine both the potential and the limitations of this new excitation scheme we have modeled both pure argon and helium-metal vapor electron beam pumped cw ion lasers. The electron energy distribution of the electron beam excited plasmas has been calculated by numerically solving the Boltzmann equation for electrons. This distribution is used to compute excitation and de-excitation rates of the laser levels. Results obtained from the model for an argon-ion laser transversely excited by a 50-110 eV electron beam of current densities between 1 and 30 A/cm^2 show operating efficiencies that are not superior to that obtained with conventional discharge excitation. However, the model shows, helium-metal vapor lasers excited by a kilovolt electron beam offer promise for multiwatt power at efficiencies >0.1% in the visible and ultraviolet.

*Work supported by the National Science Foundation University-Industry Program.

[1]J.J.Rocca, J.D. Meyer and G.J. Collins, "1 W Zn Ion CW Laser," Appl. Phys. Lett., 37, 43, 1983.

CA-8 Novel Thermionically-Cooled Plasma Recombination Laser* - J. L. LAWLESS - *Carnegie-Mellon University*, E. J. BRITT, and J. B. MCVEY - *Rasor Associates*. Finding methods for rapidly cooling a plasma has been a major limitation on the development of plasma recombination lasers. A new mechanism for cooling electrons in an unsteady discharge has been studied theoretically. The cooling occurs in the unsteady two-temperature plasma of a narrow transverse discharge. This mechanism uses thermionic emission of ~1500K electrons to cool ~3000K electrons in the plasma. Cooling can be achieved on the time scale of 1 μs. This is often faster than the gas dynamic cooling more commonly used in experimentally-demonstrated recombination lasers. The plasma dynamics and excited level kinetics of this discharge have been studied theoretically using cesium as the operating gas. The electrons are initially raised to a high temperature by ohmic heating. When the current is shut off, cooling begins. The cooling rate is governed mainly by the Richardson current and the behavior of the plasma sheathes. Plots of electron temperature, electron density, and population inversion versus time show the behavior of the device.

*Supported by NSF grant CPE-8204813.

CA-9 Laser Emission from an Embedded-Pinch Sheath,* J. F. ASMUS, R. H. LOVBERG, J. D. KEELER, P. E. HUDSON+, and K. BOYER+, U. of Cal., San Diego -- Hot plasma pinches emit intense vacuum uv radiation. In the embedded configuration cold surrounding gas damps pinch instabilities and insulates the plasma from vessel walls. When such a pinch is formed within a high-Z gas its copious uv production may induce photolytic processes in the surrounding gas blanket. To explore this process we have investigated laser-initiated high-Z gas-embedded pinches both theoretically and experimentally. Focusing on high-Z and high density media leads to a simplification in the problem because the plasma becomes optically dense and energy is lost principally through black-body radiation. Radiated power densities of 10^7-10^8W/cm^2 have been measured. This flux drives sequential luminous photolytic waves into the enveloping gas at radial velocities in excess of 10^7 cm/sec. XeF (B-X) laser radiation was generated within the photolytic sheath by installing a 350 nm optical resonator and seeding the gas with XeF_2.

*Research supported by the U.S. Air Force Weapons Lab.

+Consultants.

SESSION CB

13:15, Tuesday, October 9, 1984

GLOWS AND SWITCHING

Chairperson: Erich Kunhardt
Polytechnic Institute of New York

CB-1 X-ray Initiated Uniform Glow Discharges, K. JAYARAM** and A.J. ALCOCK, National Research Council of Canada, Ottawa, Ontario--Uniform glow discharges with a volume of ~3 cm x 1 cm x 30 cm have been produced in CO_2 at pressures between 200 and 760 torr or CO_2, He N_2 mixtures at total pressures up to 1200 torr, when breakdown was initiated by X-rays having a mean energy of ~50 keV and pulse duration of~100 nsec.

With a constant voltage applied to the electrodes, the onset of the discharge current occured ~150 nsec from the rise of the X-ray pulse. A reduction in X-ray gun voltage resulted in multiple arcs and then to a localized arc. X-ray dosage was in the range of 1 to 2 mR/pulse for obtaining uniform glows and the glow discharges in CO_2 mixtures yielded 10.6 μm output in an appropriate cavity.

**Visitor, on leave of absence from IEA-CTA., S.J. Campos, Brasil and supported jointly by NSERC (Canada) and CNPq (Brasil).

CB-2 Radiation from Transient Discharges - W.W. Byszewski and H. Kullmann* - GTE Labs, Inc., Waltham, MA. Fast streak photography has been used to investigate the time-dependent, spatial distributions of radiating species produced in nanosecond transient discharges in N_2, He and SF_6. In nitrogen, uniform molecular radiation initially fills the discharge gap and in the later discharge stages the radiation is in the form of filamentary waves which propogate with velocities of about 10^7 cm/sec. The pressure dependence of these effects will be discussed. The filament formation in He has been investigated as a function of pressure and E/N. In low pressure (100 Torr) SF_6 discharges, predominently atomic and ionic flourine emission is observed, but continuum radiation dominates at higher pressures. Conditions for sustaining uniform discharges at high-pressures are the aim of these studies.
This work supported in part by the Naval Surface Weapons Center.
*On leave from the University of Dusseldorf, Germany.

CB-3 Optical Control of the Breakdown of a Diffuse Discharge Using Photodetachment*, G.Z. Hutcheson, L.E. Thurmond, G. Schaefer, K. H. Schoenbach and P. F. Williams, Texas Tech Univ.--Externally controlled diffuse discharges containing attachers are considered as opening switches for inductive energy storage systems. Photodetachment has been proposed as a control mechanism to decrease the transition time from the nonconductive to the conductive stage of the discharge.[1,2] As a test case the breakdown behavior a self-sustained discharge was investigated. Experiments were performed in a buffer gas with admixtures of oxygen. The maximum voltage before breakdown was measured as a function of parameters such as maximum value of the applied voltage pulse, pressure, oxygen concentration, and laser power. A strong influence of impurities was observed.

*Supported by AFOSR and ARO.

[1]G. Schaefer, P. F. Williams, K.H. Schoenbach, and J. Moseley, IEEE Trans. Plasma Sci., PS-11, 263 (1983).

[2]G. Schaefer, K. H. Schoenbach, H. Krompholz, M Kristiansen, and A.H. Guenther, Laser and Particle Beams, to be published (1984).

CB-4 Magnetic Control of Low Pressure Glow Discharges*

J. R. Cooper, K.H. Schoenbach, G. Schaefer, Texas Tech, J.M. Proud, W.W. Byszewski, GTE Laboratories--The energy distribution $f(\varepsilon)$ of electrons in low pressure gases under the influence of an electric field is shifted towards lower energy values if a crossed magnetic field is applied. This change in $f(\varepsilon)$ was studied by means of a Monte Carlo code for gas mixtures containing SF_6, He, and N_2. In gases with a strong increase in the net ionization (ionization minus attachment) coefficient with field strength this effect should lead to a considerable reduction of the electron density and thus the conductivity. The controllability of plasma conductivity by means of magnetic fields was studied experimentally in a low pressure glow discharge in SF_6 plus He. A decrease in conductance of a factor of two was obtained with an applied magnetic field of 1 kGauss.

*Supported by GTE Laboratories and the Center for Energy Research at Texas Tech University.

CB-5 Production Rates of Oxygenated Species in SF_6/O_2 and SF_6/N_2 Corona Discharges,* R. J. VAN BRUNT and M. C. SIDDAGANGAPPA, National Bureau of Standards -- The absolute energy and charge rates of production for gaseous SOF_2, SOF_4, SO_2F_2, SO_2, CO_2, CO, and OCS have been measured for a steady dc, point-plane corona at 40 μA for SF_6 containing 1 to 10% O_2 and 5 to 15% N_2 at a total pressure of 200 kPa. The results suggest that: 1) small quantities of O_2 (but not N_2) modify the electron energy distribution in the discharge so as to reduce the SF_6 dissociation rate; 2) gas phase O_2 is important for SO_2F_2 and SOF_4 (but not SOF_2) formation; and 3) CO_2 results from reactions of O_2 with carbon from the point electrode. It was observed that SO_2, CO, and OCS are minor products compared to the other species, and no detectable stable, gaseous products result from direct reactions of N_2 with SF_6 dissociation products. Mixtures containing more than 3% O_2 also yield observable sulfur deposition on the anode.

*Supported by U. S. Department of Energy

CB-6 The Free Recovery of a Short Duration, High Current Discharge - R. Piejak, GTE Labs, Inc., Waltham, MA. The hold-off voltage between stainless steel electrodes has been measured as a function of time after an initial discharge. The hold-off voltage is the highest voltage that the gap will withstand without appreciable current flow. A high current (600-1200 amp), short duration (170 nsec) discharge was initiated between Rogowski profile electrodes. After a pre-determined time delay, a second pulse was applied to the discharge gap. The hold-off voltage as a function to time was determined up to the Paschen breakdown voltage. Background gas pressure between 30 and 100 torr and electrode separation of 2mm and 4mm were employed. UV preionization was introduced in some tests to create various discharge modes (glow/arc).
The findings indicate significantly higher recovery rates in air than in N_2, presumably due to attachment processes. In addition, the presence of pre-breakdown UV was found to influence the discharge mode, thus affecting the recovery rate of the gap. Hold-off voltage curves for the previously mentioned gases, background pressures and electrode spacing will be presented along with open shutter photographs of the various discharge modes.
This work supported by the Naval Surface Weapons Center.

CB-7 Experimental Investigations of a Radial Opening Switch,* C.M. YOUNG, J.W. BENZE, J.M. ELIZONDO, W.M. MOENY, J.G. SMALL, Tetra Corporation--A UV-sustained, magnetically stabilized, radial opening switch has been constructed. Various combinations of N_2, He, CH_4, and Trimethylamine have been used to study the switch characteristics. Using a 2.5 cm electrode spacing, switching ratios ranging from 1.3 (at high switch voltages) to 22 (at low switch voltages) have been observed. The magnetic field allows an extension of the arc limit by about 15%. Switch voltages range from < 700 V to 16 kV at a gas pressure of 500 torr. Closing times range from 2 to12 μs, while opening times have ranged from 2 μs to 50 μs depending on the gas mixture used. Discharge currents range from 6 A to 100 A. Although an "optimum" mix was not obtained, proof of concept was, thus providing groundwork for future studies.

* Work supported by the Naval Sea Systems Command

CB-8 Some Aspects of Surface Flashover.* EOIN W. GRAY, Sandia National Labs., Albuquerque, New Mexico. Re-examination of surface flashover results of many authors, and some recent work of the author[1], has lead to the conclusion that insulator flashover, from vacuum (10^{-6}torr) to atmospheric pressure, is a local high pressure phenomenon. Voltages ranged from dc to microsecond pulses. Desorption of adsorbed atoms and molecules occurs prior to flashover and these species make up the ambient in which the gaseous breakdown forms. Examination of the insulator surface after flashover shows evidence of the initial electron 'hop' from the triple point(insulator-electrode-gas/vacuum). Field strengths of various insulators appear to lie in a small range from 18-80 kV/cm for various gap spacings from ~$7x10^{-2}$- 1 cm. Velocities of propagation of the ionization wave fronts, whether on an insulator or in gas, range from ~10^5 to 10^7 m/sec.

*This work was supported in part by the U.S. Department of Energy under Contract DE-AC04-76DP00789.

[1]EW Gray & DJ Harrington, J.Appl.Phys.53, 237-264, 1982

SESSION D

15:15, Tuesday, October 9, 1984

WORKSHOP ON ION-MOLECULE REACTIONS

Chairperson: Rainer Johnsen
University of Pittsburgh

D

D-1 Vibrational Relaxation of Molecular Ions in Collisions with Molecules, E.E. FERGUSON, NOAA

D-2 The Formation and Reactivity of HOC^+, M.T. BOWERS, U. of California

D-3 Ion Molecule Reactions at Very Low Temperatures and Densities, G. DUNN, JILA

D-4 Ion-Molecule Reactions at Very Low Temperatures Using the CRESCU Technique (Supersonic Jets), B.R.TOWE, Labatoire de Aerothermique

SESSION E

08:15, Wednesday, October 10, 1984

ION-MOLECULE REACTIONS

Chairperson: Michael Henchman
Air Force Geophysics Lab

E

E-1 Energy Dependence of Reactions of Atomic Ions with H_2, HD, and D_2,* K. ERVIN, J. L. ELKIND, AND P. B. ARMENTROUT, Department of Chemistry, U. C. Berkeley, CA 94720 -- Reactions of several atomic ions with molecular hydrogen have been studied using a new guided ion beam mass spectrometer. This instrument allows the measurement of total reaction cross sections to energies as low as 50 meV (lab) and as high as several hundred eV. This capability has revealed new features in the well studied reactions of Ar^+ and Kr^+. The branching ratios in the HD reactions show surprising non-monotonic behavior in both systems. Reactions of $B^+(^1S)$, $C^+(^2P)$, $A\ell^+(^1S)$ and $Si^+(^2P)$ have also been studied, the latter two for the first time. In contrast to published data,[1] we find the $B^+(^1S) + H_2$ reaction exhibits a substantial activation barrier. $A\ell^+$ does not react at all. The carbon and silicon ion reactions proceed with thresholds at the thermodynamic limit. Results for the reactions of these ions with HD provide insight into the dynamics.

*Work supported in part by the National Science Foundation.

[1]K. C. Lin, H. P. Watkins, R. J. Cotter, and W. S. Koski, J. Chem. Phys., 60, 5134 (1974).

E-2 Laser-Induced Fluorescence Measurement of Nascent Vibrational and Rotational Product State Distributions in the Charge Transfer of $Ar^+ + CO \rightarrow Ar + CO^+$ at Thermal Energy. G. H. LIN, J. MAIER and S. R. LEONE, JILA, U. of Colo. & NBS.—A new experimental technique which utilizes a flowing afterglow ion source and a supersonic nozzle expansion is used to study the charge transfer reaction $Ar^+(^2P_{3/2}) + CO(v=0) \rightarrow CO^+ (v=0-7) + Ar(^1S_0)$ at approximately thermal energy. The reaction is carried out under single collision conditions, and nascent vibrational and rotational distributions are obtained by the method of saturated laser-induced fluorescence. Although the available energy is sufficient to populate the CO^+ vibrational state up to v=7, the major vibrational channels are found to be v=5 and v=6. The preliminary results for the relative populations of the different vibrational states are 0+0.03(v=0), 0.06±0.03(v=1), 0.09±0.03(v=2), 0.06±0.03(v=3), 0.12±0.03(v=4), 0.34±0.03(v=5), 0.23± 0.03(v=6), 0.10±0.03(v=7). The nascent rotational state distributions in both v=5 and v=6 are characterized by Boltzmann distributions with T_{rot} = 800±50 K. It is suggested that the experiment results are best explained in terms of a potential surface crossing at the close approach of the reactants.

E-3 COMPARATIVE EFFECTS OF TEMPERATURE AND KINETIC ENERGY CHANGE ON THE REACTION OF O_2^+ WITH CH_4

N.G. Adams and D. Smith, Department of Space Research, University of Birmingham, Birmingham B15 2TT UK, and Eldon E. Ferguson, Aeronomy Laboratory, NOAA, Boulder Colorado 80303 USA

The rate coefficient k_1 for the reaction $O_2^+ + CH_4 \rightarrow CH_3O_2^+ + H$, where $CH_3O_2^+$ is protonated formic acid, has been measured at several center-of-mass kinetic energies at fixed gas temperatures of 80, 200 and 420K in a variable temperature selected ion flow drift tube. There is a pronounced minimum in k_1 near room temperature for k_1 versus temperature plots. This minimum, and the general shape of the k_1 versus T plots, are closely matched by plots of k_1 versus added mean kinetic energy at the three temperatures measured. There is an approximate equivalence between the temperature increase and the kinetic energy increase required to make equivalent changes in k_1 such that $\Delta\overline{KE}_{cm} \sim 8\Delta kT$. This is interpreted as implying (a) that only kinetic energy, and not rotational energy, in the O_2^+ ions is effective in controlling the reaction rate and, (b) the relative kinetic energy rapidly randomizes into ~ 8 vibrational modes of the long-lived intermediate $[O_2^+ \cdot CH_4]^*$ complex before reaction occurs.

E-4 Product States of D_3^+, D_2^+ and O_2^+ Dissociative Charge Transfer in Cs*, J. R. PETERSON and Y. K. BAE, Chemical Physics Laboratory, SRI International — A new technique has been used to determine the final states and kinetic energies released in dissociative charge transfer of D_3^+, D_2^+, and O_2^+ in Cs. The method exploits the fact that a small fraction of the dissociation product atoms pick up another electron before exiting the Cs vapor. The laboratory energy spectra of these negative ions at 0° lab angle reveal the final state potential energies with quite high precision. D_3^+ yields both D+D+D and D_2+D products, D_2^+ yields D+D from predissociation of $c^3\Pi_u$ and radiative dissociation of $a^3\Sigma_g^+$. The $X^2\Pi_g^+$ and $a^4\Pi_u$ states in the O_2^+ beam yield a surprisingly simple spectrum that is attributable to near-resonant and Franck-Condon type selection rules.

*Work supported in part by the U.S. Department of Energy under Contract DE-AT03-80ER53091.

E-5
Fourier Transform Mass Spectrometry of Silane. PETER HAALAND, Air Force Aero Propulsion Laboratory and ALFRED RAHBEE, Air Force Geophysics Laboratory - The Formation of silicon hydride cations from both electron impact and ion-molecule reactions of silane has been studied at 10^{-5} torr using Fourier Transform Mass Spectrometry (FTMS). The molecular cation has been analyzed using high mass resolution to distinguish it from other isotopically dilute species whose nominal masses are also 32 a.m.u. Results of kinetic branching studies are used to illustrate the selectivity of ion-molecule chemistry in silane systems. The FTMS technique, whose results avoid important pitfalls associated with quadrupole mass spectrometry, has also been applied to the study of polysilicon hydride cation reactions with silane and the formation of silicon-bearing negative ions by dissociative electron attachment to silane.

E-6 The Association of Ammonia with Halide Ions in The Gas Phase, R. G. KEESEE, D. H. EVANS, and A. W. CASTLEMAN, JR., Dept. of Chemistry, Pennsylvania State Univ.--The enthalpy changes, $\Delta H°$, and entropy changes, $\Delta S°$, for the gas-phase association of ammonia to Cl^-, Br^-, and I^- have been measured using high pressure mass spectrometry. The $-\Delta H°$ were determined to be 8.2, 7.7, and 7.4 kcal/mole (0.36, 0.33, and 0.32 eV) and the $-\Delta S°$ were 15.4, 19.1, and 20.9 cal/K-mole, respectively, for $^{35}Cl^-$, $^{81}Br^-$, and I^-. The $-\Delta H°$ values are considerably smaller than those for the association of ammonia to alkali ions and also of water and sulfur dioxide to both halide and alkali ions. One explanation can be based on electrostatic considerations. The quadrupole moment of ammonia leads to a repulsive interaction (considerably greater than that of water) when the ion-dipole orientation is most favorable for a negative ion. Similarly, these opposing interactions may be responsible for the relatively little variation in the enthalpy change for ammonia asscciation between Cl^- and I^-.

E-7 Negative Ion Molecule Reactions of WF_6: Evidence for a Pressure Dependent Branching Ratio, A. A. VIGGIANO and J.F. PAULSON, AFGL -- Rate coefficients have been measured in a selected ion flow tube (SIFT) for reactions of several negative ions with WF_6. With the exception of SF_5^-, all the reactant ions studied having an electron detachment energy less than 3.36 eV reacted rapidly by charge exchange. SF_5^- transferred a fluoride ion producing WF_7^-. Ions with detachment energies greater than 3.36 eV associated rapidly with WF_6^-. Br^-, with a detachment energy of 3.36 eV, reacted with WF_6 both by ion-neutral association and by charge exchange. The branching ratio for these two channels was found to depend on temperature and pressure. All these data indicate that the electron affinity of WF_6 is nearly equal to that of Br.

E-8 FLOWING AFTERGLOW MEASUREMENTS OF NEGATIVE ION ASSOCIATION REACTIONS

H. Böhringer, D.W. Fahey, F.C. Fehsenfeld, and E.E. Ferguson, Aeronomy Laboratory, NOAA, Boulder, CO 80303

Thermochemical data for some negative cluster ions of importance in atmospheric ion chemistry have been determined from equilibrium constant measurements in a flowing afterglow apparatus. The ions studied have the structure $X^-\cdot M$ with $X^- = Cl^-$, NO_2^-, NO_3^-, and HSO_4^- and $M = H_2O$, SO_2, H_2O_2 and HCl. The bond strengths of these cluster ions were found to be in the range ΔH = 50 to 102 kJ/Mol. ΔH increases as a function of the ligand molecules in the following order $(H_2O) < (SO_2) \lesssim (H_2O_2) \lesssim (HCl)$. The temperature dependence of the three body association reactions $X^- + SO_2 + He \rightarrow X^-\cdot SO_2 + He$ with $X^- = Cl^-$, NO_2^- and NO_3^- were studied at temperatures from 150 to 375 K in a flowing afterglow apparatus. The measured rate constants are given by the expressions $k_1 = 3.9 \times 10^{-29}(300/T)^{2.1(\pm 0.4)} cm^6\ s^{-1}$, $k_2 = 3.9 \times 10^{-28}(300/T)^{2.65\ (\pm 0.2)} cm^6\ s^{-1}$, and $k_3 = 1.65 \times 10^{-28}(300/T)^{3.75(\pm 0.2)} cm^6\ s^{-1}$.

E

E-9 Hydrated-Ion Molecule Reactions: Temperature Dependence as a Function of Hydration Number, P. M. HIERL, A.F. AHRENS, A.A. VIGGIANO, M.J. HENCHMAN and J.F. PAULSON, Air Force Geophysics Laboratory, Hanscom AFB, MA 01731 -- Rate constants have been measured using the Selected Ion Flow Tube (SIFT) technique over the temperature range 200 - 500K for the selectively hydrated reactant $OH^-\cdot(H_2O)_{0,1,2}$ with hydrogen halides and methyl halides. The former are representative proton transfer reactions and the latter representative displacement reactions, each of which show different temperature dependences for unhydrated reactants: $dk/dT = 0$ and $dk/dT < 0$ respectively. For both categories, the temperature dependence of most reaction rate constants is not changed significantly by hydration of the reactant ion.

SESSION F

10:55, Wednesday, October 10, 1984

ARGON AND SF_6 ARCS

Chairperson: H.-P. Stormberg
Philips Research Labs

F

F-1 Free-burning Arcs in Argon, G.N. HADDAD, Div.of Appl.Phys., CSIRO, Sydney, Australia - As part of a systematic investigation of the gas tungsten arc welding process, measurements of the temperature profiles and arc voltages have been made for free-burning arcs in argon as a function of pressure, length and current. Temperatures are derived from measurements of the intensities of spectral lines and local thermodynamic equilibrium (LTE) is assumed in the analysis. Comparisons of temperatures and column voltages are made with a recently developed two-dimensional theory[1]. The agreement is satisfactory. Measurements of arc voltages show that it is preferable to use a shielded Coulomb potential in calculations of the electrical conductivity[2]. Experimental evidence for departures from LTE at pressures below about 1.5 atmospheres is presented. The limitations of both the experimental and theoretical results are discussed.

1. R.S. Devoto, Phys. Fluids 16, 616 (1973)
2. P. Kovitya and J.J. Lowke, In press (1984)

F-2 Impact of Anode Evaporation on the Anode Region of a High Intensity Argon Arc, K. ETEMADI and E. PFENDER, State U. of N.Y. at Buffalo and U. of Minnesota -- Temperatures in a free-burning, high intensity arc have been measured spectroscopically while the anode is kept either in a molten or solidified state. A comparison of the temperatures measured below the cathode for both cases shows that vapor is not penetrating into the cathode region and, therefore, evaporation of anode material does not influence the immidiate vicinity of the cathode. The distribution of the line emission coefficients of copper also revealed that there is no trace of copper vapor in the core of the arc up to 0.5mm from the anode. The temperature measurements 1 mm above the anode indicated an overall drop of the temperature in the anode region which, in turn, is associated with a drop in current density in this region (flattening of the current density profile). Increased electrical conductivity in the arc fringes due to ionization of the Cu vapor is consistent with this finding.

F-3 Composition and Thermodynamic Properties of non-LTE Argon Plasma*-A. SEDGHINASAB, and T.L. EDDY, Georgia Inst. of Technology-- Thermodynamic properties of argon plasma, based on the most accurate set of energy levels determined to date, have been calculated and graphically presented using Multithermal Equilibrium (MTE) analysis[1]. Properties are given for various pressures (0.1,1,10, and 100 atm) and various kinetic and excitation non-equilibrium (T_e/T_a =1,3,10 and T_e/T_{exa} =0.3,1,3,10) in the excitation temperature range of 5000 to 35000°K. The argon plasma is assumed to consist of electrons, atoms, and the first four ions. The energy levels of the argon atom and ions have been predicted using the Rydberg-Ritz equation. The degeneracies of the predicted levels were obtained using the isoelectronic series of each species for quantum numbers of up to n=70. Griem's method of lowering of the ionization potential and the corresponding cut-off of the energy level summation has been used. Heavy particle interactions at high densities have been accounted for by utilizing the Debye-Hückel pressure correction criterion.

*Work supported by NSF Grant CPE-8311325.

[1]T.L. Eddy et al., IEEE Trans Plasma Sci., 1,31,1973.

F-4 Influence of Additives on Atmospheric Pressure RF Discharge in Argon, V.M. GOLDFARB, Avco Everett Research Laboratory -- Vapors of inorganic compounds and molecular gases introduced in the inductively coupled RF discharge used in processing of materials and in spectrochemical analysis influences plasma properties. Equilibrium composition and transport properties of an argon plasma with 0.01%-2% mol. of various additives have been calculated for 3kK-9kK temperature range. Effects of the additives on plasma temperature, radius, and spectral line intensities for ~1kW, 27MHz discharge were predicted and compared with results of optical measurements. Change in thermal and electrical conductivity result in up to $^{+200}_{-400}$K variation of a 7600K pure argon plasma temperature. Fiber thermal probe measurements of the heat transfer and gas temperature are also taken. Influence of diffusion and of the deviation from equilibrium on plasma composition and radiation is discussed.

F

F-5 Transient 2-D Simulations of Forced Convection-Stabilized Arcs in N_2 and SF_6,* R. R. MITCHELL, D. T. TUMA, and J. F. OSTERLE, Carnegie-Mellon U. --Arcs of interest in gas-blast circuit-breaker design have been simulated by solving the LTE conservation equations for mass, axial momentum, and energy in two dimensions (r,z) and time. The axial pressure distribution, which is assumed to be that of the cold gas alone, causes entrainment of cold gas into the arc due to the requirement of mass conservation. This entrainment is the major cooling mechanism in the cases considered thus far. Radiation from the arc central region, which is modeled by net emission coefficients, is assumed to be absorbed in the arc boundary layer. Use of an adaptive finite element mesh enables resolution of steep radial temperature profiles found experimentally in the arc laminar region. Good agreement has been obtained with detailed measurements on decaying arcs in laboratory-scale model breakers[1]. In contrast to previous theoretical work[2], which assumed a temperature profile at current zero and postulated very large turbulent cooling, the present calculations follow the entire experimental transient and indicate that convection and laminar thermal conduction suffice to cool the decaying arc.

*Work supported by NSF Grant CPE-8111625.

[1] E. Schade and K. Ragaller, IEEE Trans. Plasma Science PS-10, 141(1982).

[2] K. Ragaller, W. Egli, and K. P. Brand, IEEE Trans. Plasma Science PS-10, 154(1982).

SESSION G

13:30, Wednesday, October 10, 1984

POSTERS. MOSTLY DISCHARGES

GA: SWARMS

GB: ARCS

GC: LASERS

GD: LOW PRESSURE DISCHARGES

GE: BREAKDOWN

Chairperson: Harald Tischer
JILA

GA-1 Electron Energy and $N_2(X)$ Vibrational Distributions in Stationary Discharges, J.LOUREIRO and C.M.FERREIRA, Centro de Electrodinâmica, U.Tec. Lisboa -- Self-consistent electron energy distribution functions (EDF's) and collison rate coefficients, and $N_2(X,v)$ vibrational distributions were calculated for stationary nitrogen discharges by solving the Boltzmann equation coupled to a system of vibrational master equations including e-V, V-V, and V-T processes. Solutions were obtained for $3 \times 10^{-16} < E/N < 3 \times 10^{-15}$ Vcm^2 and $n_e/N < 10^{-5}$. The characteristic vibrational temperature, θ, increases with n_e/N and is in the range of several thousand degrees Kelvin under typical, moderate pressure and current discharge conditions. As shown in previous self-consistent time-evolution analyses[1] the tail of the EDF is strongly enhanced by superelastic e-V collisions resulting in a large increase in the electron excitation and ionization rates as θ increases, especially at the lower E/N values. These results are used in a kinetic model that satisfactorily explains recent measurements[2] of the $B^3\Pi_g$ and $A^3\Sigma_u^+$ vibrational populations in a glow discharge.

[1]M. Capitelli et al., Chem. Phys. 56,29(1981).
[2]G. Cernogora et al., J. Phys. B (at press).

GA-2 Strongly Coupled Non-Neutral Ion Plasma*, J. J. Bollinger, D. J. Wineland, and J. D. Prestage, Time and Frequency Div., NBS -- The density, n_o, and temperature, T, of small clouds of several hundred $^9Be^+$ ions stored in a Penning trap have been measured.[1] Such a system can be described as a non-neutral plasma. Radiation pressure from a laser was used to cool the ions. A second laser was used to probe the ion plasma and measure densities $n_o \sim 2 \times 10^7$ ions/cm^3 and temperatures $T < 100$ mK. These measurements determine a Coulomb coupling constant $\Gamma \equiv e^2(4\pi n_o/3)^{1/3}/k_B T$ as large as ten. Theoretical calculations predict that for $\Gamma \geq 2$, the plasma is to exhibit liquid behavior and at $\Gamma \sim 170$ a liquid-solid phase transition is expected to take place.[2] In the future, crystallization in a non-neutral ion plasma appears accessible.

*Work supported by the Office of Naval Research and Air Force Office of Scientific Research.

[1]J. J. Bollinger and D. J. Wineland, Phys. Rev. Lett. 53, 348 (1984).

[2]S. Ichimaru, Rev. Mod. Phys. 54, 1017 (1982).

GA-3 A 2 1/2 Term Spherical Harmonic Solution to the Boltzmann Equation. A. V. PHELPS,* JILA, NBS and Univ. of Colorado and L. C. PITCHFORD, GTE Labs.--The two-term spherical harmonic expansion technique for solving the electron Boltzmann equation has been extended to approximate the effects of the third term in the expansion. The approximations used to relate the $f_2(\varepsilon)$ terms to the $f_1(\varepsilon)$ terms are based on results obtained using Long's unpublished one-dimension-in-velocity approximation[1] and appear as modifications of the momentum transfer cross section. Since these effects are important when the inelastic cross sections are not small compared to the elastic cross section, we have tested the formulation in N_2. Calculated electron energy distributions are in very good agreement with our calculations[1] using the multi-term expansion at high energies for $40 < E/n < 100$ Td, where the two-term expansion results are significantly in error. Calculated drift velocities are too large by about 10%.

*AVP was partially supported by ARO.

1. L. C. Pitchford and A. V. Phelps, Phys. Rev. A 25, 540 (1982).

GA-4 A new determination of cross sections in methane and silane by using an exact method of solution ot the Boltzmann equation, P. SEGUR, J.P. BALAGUER, Centre de Physique Atomique, LA 277, TOULOUSE. -- We use a modified form of the S_N method to solve the Boltzmann equation. We are then able to take into account the strong anisotropy of the distribution function which is known to occur in methane and silane. For a given set of cross-sections, the swarm parameters calculated with this method are very different from these published by previous authors (obtained with the standard two term Legendre expansion of the distribution function). The cross sections which we deduce by comparing experimental and calculated values for drift velocity and transversal diffusion coefficient are very different from these of POLLOCK or DUNCAN and WALKER. With these two new sets of cross sections we make some calculations in mixtures of methane and silane, methane and argon, silane and argon. We note that our results for swarm parameters (at low E/N) are in good agreement with experimental values when they are available.

GA-5
Space And Time Dependent Boltzmann Calculation In The Forward/Backward Scattering Approximation

J.P. BOEUF *, P. SEGUR **, E. MARODE *,
* Ecole Supérieure d'Electricité (CNRS) Gif/Yvette,
** Centre de Physique Atomique (CNRS), Toulouse, FRANCE

The spatio-temporal evolution of an electron swarm under a uniform field has been simulated for a forward/backward scattering model, using a Mac Cormak numerical scheme. Using model cross-sections, the effect of attachment and ionization on the spatial variations of the swarm density and velocity distribution function and on the higher order transport coefficients has been analysed. It is shown that the non uniform spatial distribution of energy within the swarm can induce, for the electron number density, a large deviation from the Gaussian shape. This deviation is due mainly to the fact that ionization is more important in the front of the swarm while attachment prevails in the back of the swarm.

GA-6 The Einstein Relation for Electrons in High Density Argon. T. F. O'MALLEY, GE. - A prediction has been made [1] that the Einstein Relation must be modified for electrons in dense gases. While patiently awaiting a definitive measurement of De/mu, some empirical support has been found for the prediction by roughly extrapolating the Milloy-Crompton [2] data in dense Argon to E/N=0. This was done by first deriving a fairly general 2 term expansion of De/mu as a quadratic function of E/N. Significantly the second coefficient also depends indirectly on E/N, decreasing for small values because of the varying slope of the cross section. As a result, where a straight forward (but incorrect) quadratic expansion of De/mu extrapolates with deadly accuracy to the accepted value of kT=25meV, thus apparently disproving the prediction, the present curve bends upward for decreasing E/N and extrapolates to a higher value, much closer to the predicted 32 meV. Direct measurements are still much needed, but I believe this result forshadows their direction.

1. T. F. O'Malley, Phys. Lett. 95A, 32 (1983).
2. H. B. Milloy & R. W. Crompton, Aust. J. Phys. 30, 51 (1977).

GB-1 Collective Arc Spot Motion in a Magnetic Field, H.P. MERCURE, R.J. RAJOTTE, M.G. DROUET, IREQ, Varennes, Canada--Experimental results of a study on the collective behavior of low-pressure cathode arc spots in a uniform magnetic field are presented. The arc is struck between a flat anode and a conical cathode in He (5 cm spacing, 5 cm dia.). The spot tracks are found to drift systematically away from the usual retrograde direction. The influence of the external magnetic field, the total arc current, the cone-tip angle and ambient pressure is documented. The data illustrate the salient features of the peculiar arc spot motion. In particular, above a critical magnetic field value of about 1 kGauss, the drift angle shows a saturation akin to that of retrograde velocity with increasing field. The drift angle increases with the cone-tip angle up to about 60°. Finally, this drift disappears at pressures above 50 Torr (He) for a 10-kA arc in a .7-kGauss axial field (copper electrodes, 90° cone). A brief discussion of these results emphasizes the implications of this arc spot behavior in actual plasma devices.

GB-2 Effect of Wall Reflections on the High-Pressure Sodium Arc*, J.T. DAKIN and T.H. RAUTENBERG JR, General Electric Corporate Research and Development -- Effects of diffuse wall reflections on the electrical behavior and radiation output of a high-pressure, wall-stabilized Na-Hg-Xe arc are calculated and measured. Electric field and output spectrum are studied for a 60 Hz, 4 amp arc in a 7.2 mm diameter channel. The operating gas mixture is approximately 80 torr Na, 340 torr Hg and 210 torr Xe. Experimental variations in wall reflectivity are introduced by placing translucent, polycrystalline alumina shrouds around a single-crystal alumina arc tube. The arc energy balance model assumes local thermodynamic equilibrium, and one-dimensional cylindrical symmetry. The model incorporates a comprehensive treatment of radiation transport in the range 400-2400nm. The calculated spectrum includes 28 Na lines, 20 of which are treated as optically thick, and a number of molecular and continuum effects.

GB-3 Erosion of Silicon Carbide Arc Electrodes. V. Goldfarb, AVCO Everett Research Lab.--High-temperature ceramics could be used as electrodes in MHD generators and in arc devices. The 1-5 A arc spots transversing Silicon Carbide (SiC+Si) surfaces in air and alkali-seeded combustion gas have been studied. In air anode and cathode spots and erosion rates (from 10 to 25 μg/C) are similar. Electrode traces are 100-400 μm wide and 40-120 μm deep, current density is 2.10^4 A/cm^2. Surface temperature (2600 K) is lower tnan SiC decomposition temperature (3000°C). Heat flow to electrodes (23 W/A) is removed by thermal conduction; less than 2% of energy is spent for material removal which is predominantly oxidative process. SiO_2 deposit around the spot reduces arc mobility; this is responsible for high erosion rate. The phenomena is similar to the one observed[1] for steel arc anode. Under simulated MHD channel environment mobility of arc spots increases with gas conductivity. Cathode spots are more mobile and cathode erosion rate (~1μg/C) is 2-3 times lower than that of the anode. Velocity of arc roots should exceed ~1 m/sec to provide reduction of erosion rate needed to achieve 1000 hours lifetime of the MHD electrodes.

[1]V.Goldfarb et al. Phys. and Chem. Mater. Treatment 6, No.5, 1972.

GB-4 Theoretical Approach to the Interaction of Arc and Gas Flow, ZHONG-JIE,LI, 7th Designing Instit., Ministry of Machine Building, Xian, P.R. China.--An approximate solution of governing equations for arcs burning in a supersonic nozzle has been developed. Momentum and energy conservation compared with Hermann's results were discussed. The difference between the arc kinetic energy area and the enthalpy flux area was formulated. Also the published results of enthalpy flux shape factor have corrected in this paper. The effects of the gas pressure ratio, gas flow rate and velocity upon the arc thermal boundary have studied through this law. Calculations for published data shows that results are in good agreement of experiment. This approximation is useful for the further investigation on arc-induced shack and arc clogging.

1. H.L. Walmsley et al., IEEE Tr. plasma Sci., PS-8 1980, 39-49
2. W. Hermann et al., J.Phys., D.,7, 1974, 607.

GB-5 Physically Based Arc-Circuit Interaction, ZHONG-JIE, LI, 7th Designing Institute, Ministry of Machine Building, Xian, P.R. China--An integral arc model is extended to study the interaction of the gas blast arc with the test circuit in this paper. The deformation in the waveshapes of arc current and voltage around the current zero has been formulated to first approximation by using a simple model of arc voltage based on the arc core energy conservation. By supplementing with the time scale for the radiation, the time rates of arc processes[1] were amended. Both the contributions of various arc processes and the influence of circuit parameters to the arc-circuit interaction have been estimated by this theory. Analysis generated a new method of calculating test circuit parameters which improves the accurate simulation of arc-circuit interaction. The new method agrees with the published experimental results.[2]

1. S.K. Chan et al, J.Phys., D.9, 1976, 1085-99.
2. P. Heroin et al., CIGRE, No.13-12, 1097.

GB-6 The Influence of Arc Tube Diameter on the Properties of a High Pressure Sodium Discharge, P.L. DENBIGH, B.F. JONES and D.A.J. MOTTRAM, THORN EMI LIGHTING LTD., UK. --The high pressure sodium lamp is an example of a wall-stabilized arc in approximate local thermodynamic equilibrium. The diameter of the vessel containing the discharge has considerable influence on its properties, in particular, on its efficiency as an emitter of visible radiation. We have devised an experiment to assess this effect based on a specially designed arc tube whose diameter varies from 4mm to 7mm along its length. Our theoretical model suggests that the luminous efficiency of the discharge increases with diameter. This prediction has been confirmed by the experimental results which show increases in luminous efficiency of between 2% and 5% for each mm increase in diameter. This increase is due to the changing balance between the processes of thermal conduction and radiation transport in the discharge.

GB-7 Spectroscopic Temperature Measurements for SF_6 Double-Nozzle Arcs W.TIEMANN, Siemens R & D Center FRG

-- Radial temperature distributions of high-current SF_6 double-nozzle arcs have been measured spectroscopically at 8 equally spaced points along a 10 ms duration sine-half-wave. A good representation of the measured radial profiles around peak-current is $T(r) = T_0 - a_n r^n$ with $T_0 = 21\,000$ K and $n = 10$. This empirical distribution is the basis of a theorectical model developed to calculate from integral conservation laws the arc-cross-section at $z = 0$ as a function of current. From temperature measurements at different z-positions the variation E(z) of the electrical field-strength within the gap of the system has been determined. Theoretically interesting spectroscopic net-emission-coefficients were evaluated for the stagnation point.

GC-1 Surface-Wave Phenomena in Microwave Excited Rare-Gas Halide Lasers, R. W. Waynant, W. M. Bollen, and C. P. Christensen, Naval Research Laboratory, Washington, D.C. 20375.

Microwave excitation of rare gas halide lasers has appeal because of the potential for long pulsewidth, long lifetime operation with no electrode contamination of the laser gas. A 1.5 MW, 1-5 μs pulsewidth X-band microwave magnetron source has been used to excite laser discharges contained in a dielectric tube inside a waveguide section. A major limiting factor in good laser performance has been the rapid collapse of the discharge to the tube walls. Experiments to investigate this phenomena show that plasma surface waves are excited resulting in the electric fields, and, therefore, the electron collisions responsible for light emission, are confined to the inside tube surface. The surface waves are seen to deflect microwave energy in directions not otherwise accessible to electromagnetic waves. The experimental results as well as basic theory will be presented.

GC-2 XeCl Quantum Yields and Formation Rates from Xe^{*+}, Cl_2, FCl and HCl D. C. LORENTS, R. L. SHARPLESS, and D. L. HUESTIS, Chemical Physics Laboratory, SRI International--Using UV photons from the SSRL synchrotron the reactions of Xe^* in selected states with Cl_2, FCl and HCl have been measured. The yield of $XeCl^*$ as a function of Xe^* electronic state was obtained relative to the yield of $Xe^*(7^3S)$ and Cl_2. In the case of FCl both XeF^* and $XeCl^*$ are formed with XeCl as the favored product. $XeCl^*$ formation and quenching rates determined for each of the states reacting with the donor will be presented. $XeCl^*$ is also observed from the reaction ClF^* and Xe when ClF is photo-excited in the 120-137 nm range. The photo absorption cross section of ClF, measured in range 115-300 nm, will be presented.

*Work supported by DARPA under ONR Contract No. N00014-84-C-0256.

GC-3 Triggering of air breakdown with an excimer and a pulsed CO_2 lasers. S. YOSHIDA, J. SASAKI, Y. ARAI, K. TATEISHI, M.P. LEI, T. UCHIYAMA, Keio U., Japan
A KrF laser of 50 mJ and a pulsed CO_2 laser of 1 J are simultaneously focused in atmospheric air under the influence of non-uniform electric field. The purpose of the present work is to study the effect of the simultaneous presence of ir and uv laser pulses on DC breakdown voltage with long distance breakdown on mind. The electric field is produced by a pin to plane electrode system with the spacing of 30 mm where 80% of the self-breakdown voltage is continuously applied. When both pulses are spatially and temporally overlapped, the breakdown probability is enhanced by a factor of 2 over that obtained by the CO_2 laser pulse alone. No breakdown is observed when only the KrF laser is focused. These results are consistent with our preliminary experiments that show the probability of optical gas breakdown by a CO_2 laser pulse is enhanced if the gas is uv preionized. Through these experiments, we confirm the concept that the seed electrons produced by uv emission are increased in number by the simultaneous irradiation of ir laser.

GC-4 Theoretical Investigation of Nuclear-Excited Kr2* Excimer Fluorescence, Alan Chung and Mark Prelas, University of Missouri-Columbia --- We first developed a computer code to benchmark the e-beam excited Kr2* fluorescence data by Eckstrom et. al. [1]. The success in modeling the e-beam data lend us confidence in modifying the code to study nuclear-excited Kr2* system, which is excited by:

Uranium + neutron --> fission fragments

The power deposition is about .1 to 1000 W/cm3, with an electron temperature of .1 to .4 eV. The fluorescence efficiency is found to be very high (>=40% for pressure > 760 T). Hence, the nuclear-excited Kr2* system should be a very efficient photolytic driver.

1. D. J. Eckstrom et. al., Development of Rare Gas Excimer Photolytic Drivers, SRI Report MP 81-22.

GC-5 Sensitivity Analysis of Electron-Beam Excited Xe_2^* Fluorescence*. ALAN CHUNG and MARK PRELAS, University of Missouri-Columbia--Sensitivity analysis is a powerful mathematical technique that identifies the major reactions, the effects of errors in rate constants, and temperature effects in a plasma chemistry model[1]. This paper discusses the successful implementation of the state transition matrix method in the study of electron-beam excited Xe_2^* system. Major reactions in this 37-reaction model have been identified. In addition, sensitivity analysis can easily reduce the system complexity.

1. J.J.Hwang, et.al., J Chem. Phys., 71, 1794(1979).

*Work supported by National Science Foundation.

GC-6 Electron Beam Excited CW Ionic and Atomic Lasers, J. MEYER, J. ROCCA, B. PIHLSTROM and G. COLLINS, Colorado State University -- Various singly ionized and atomic laser systems have been investigated using energetic direct current electron beams to pump the active medium. Cw laser oscillation was observed on 43 ionic transitions in seven metal vapors and one rare gas at wavelengths between 440 and 1800 nm. Two atomic systems were investigated yielding 8 transitions in the near-infrared. In most cases, the population of the upper laser levels occurred through selective thermal energy charge transfer reactions between rare gas ions and ground state atoms. The combined efficient ionization of rare gas atoms by beam electrons and subsequent transfer of the energy stored by the ions to ground state metal atoms can form upper laser levels in a selective fashion and lead to an increase in power and efficiency over conventional devices. The possibility of obtaining cw electron beam operation at efficiencies $>10^{-3}$ in the 220-260 nm will be discussed.

GC-7 Stimulated Emission from Laser Produced Magnesium Plasmas

P. D. Kleiber, A. M. Lyyra, S. P. Heneghan and W. C. Stwalley
Iowa Laser Facility, University of Iowa,

We have observed stimulated emission on the transitions 4^3S_1 - $3^3P^0_J$ (J = 2,1) near 518 nm following pulsed laser excitation of Mg vapor near the 3^1S_0 - $3^1P^0_1$ resonance transition at 285 nm. The laser efficiently photoionizes the Mg vapor creating a large electron density; electron impact collisions are presumed to mediate the process, rapidly transferring population from the laser pumped $3^1P^0_1$ level to the triplet manifold. Details of the experimental observations are presented. A qualitative model involving laser pumping of an accidental double resonance, 3^1S_0 - $3^1P^0_1$ and 3^3P^0 - 5^3D_J, to deplete the lower state population is also discussed.

GC-8 Production of Sputtered Vapor in a Pulsed Copper Hollow Cathode*. W. WINIARCZYK+ and L. KRAUSE, U. of Windsor, Canada--Spectral emission from a pulsed Cu hollow cathode was investigated in relation to discharge current and buffer gas pressure to gain information on the density of the sputtered Cu vapor and on the persistence time of the metastable and ground-state atoms. The cathode was excited with 250μs current pulses up to 1 A/cm^2, using He, Ne and Ar as buffer gases. The intensities of the several emitted CuI lines were found to depend strongly on the simmer current. In atmospheres of Ne or Ar, the intensities of the resonance lines exhibited characteristic maxima during the initial 30μs of the current pulses. The density of the sputtered Cu atoms was determined by absorption measurements using a second Cu hollow cathode as a light source. Absorption measurements carried out outside the cathode cavity, indicate that substantial quantities of Cu vapor are being ejected from the cavity.

* Work supported by the Natural Sciences and Engineering Research Council of Canada.

+ On leave from Jagiellonian University, Kraków, Poland.

GC-9 Interaction of CO_2 Laser Radiation With a Shock-Heated Hydrogen Plasma. N.W. JALUFKA and Barbara J. KLOC, NASA, Langley Research Center.--The interaction of a short pulse (1 Joule, 80 nsec FWHM) CO_2 laser beam with a dense ($n_e \sim 10^{17} cm^{-3}$), low temperature ($T_e \sim 1$ eV) hydrogen plasma has been investigated. The plasma was produced in an electromagnetic shock tube and lasted for several microseconds. Spectroscopic techniques were used to obtain time resolved electron density and electron temperature measurements. Absorption of the laser beam by inverse Bremsstrahlung was observed for several microseconds after the arrival of the plasma in the interaction area. Partial absorption was observed for many microseconds in the decaying plasma. The electron temperature was observed to increase by amounts up to 0.25 T_e after absorption of the laser beam. Calculations of plasma heating by inverse Bremsstrahlung indicate that only a small percentage of the absorbed laser energy goes into heating the electrons. The bulk of the absorbed laser energy goes into expansion of the plasma.

GD-1 Excitation Processes in Microwave Argon/Helium Discharges, J.MAREC,S.SAADA;E.BLOYET,E.DERVISEVIC,C.LAPORTE,P.LEPRINCE,M.POUEY, Lab.Phys.Gaz et Plasmas,Orsay,France--Capillary Ar/He discharges were produced by surface wave technics at 2.45 GHz,total pressure 1mb He percentage up to 70%.Electron density near the gap was about 10^{13} cm^{-3}.We found that teh electric field E is increasing with He percentage whereas n_e is decreasing.As n_e and E are everywhere known in the discharge,we are able to relate the relative intensities of ArI ArII and HeI lines to these both parameters.Semi-empirical laws were established,$I_{ArI} \propto n_o n_e E^3$ (n_o=neutral density),$I_{ArII} \propto n_e^3 E^{5.4}$ and $I_{HeI} \propto n_o n_e^2 E^7$ .First law and dependance on n_e for Ar lines are the same as in pure argon gas.Dependance on n_e of ArII and HeI lines show that upper levels are populated via a 3 steps process for ArII (fundamental ion,unsaturated metastable ion)and via a 2 steps process for HeI(2^3S metastable).Dependance on E can be only explained in the case of ArI,however the difference on E exponent for ArII(4.5 in pure argon) means that an additional ionisation process of argon has to be taken into account.Under our conditions,the dominant process would be the Penning ionisation.

GD-2 Influence of Excitation Frequency on Microwave Discharge characteristics,J.MAREC,C.LAPORTE,E.BLOYET,E.DERVISEVIC,A.GRANIER,P.LEPRINCE,S.SAADA,Lab.Phys.Gaz et Plasmas,Orsay,France--Discharges produced in argon at low pressure p(0.5 to 5mb)by surface waves at 210 MHz and 2.45GHz are compared.Electron density n_e of these plasma columns decreases axially from the excitation gap and everywhere in the plasma n_e and the electric field E can be known.Discharge maintaining needs that wave power lost in plasma(attenuation α)balances power needed for electron-ion pair maintaining(mean power for 1 pair Θ).Energy balance equation is $2\alpha P_{in} = \Theta n_e S$($P_{in}$=input power,S=section)and to be solved α and Θ have to be determined.α is known from dispersion equation and depends on ω,n_e,ν(p,diameter d)teh collision frequency.Assuming that losses due to (in)elastic collisions are balanced by Θ and neglecting the volume recombination,we calculate Θ .It depends only on p and d.Thus,the operating point of the discharge is the intersection of $\alpha(n_e)$ and $\Theta S n_e / 2P_{in}$ under given conditions(ω,P_{in},p,d).Maintaining of the discharge needs an effective electric field E_{eff}.It is constant along the column like ν and Θ.Plasma emission(ArI,ArII lines)depends on $n_e$and E_{eff},thus ω via n_e.Lines intensities can be increased by n_e,thus ω or(and)E_{eff},i.e.,decreasing p or d.

GD-3 Electron Density and Electron Temperature Measurement in a Low-Pressure Sodium Discharge using Laser Absorption, H.J. CORNELISSEN and H.J.H. MERKS-EPPINGBROEK, Philips Research Laboratories, Eindhoven -- In a low-pressure sodium-neon discharge the radial Na ground-state density profile is strongly depleted at the axis of the tube due to the ambipolar diffusion of electrons and ions to the wall being much faster than the neutral back-diffusion. The radial Na ground-state profile is measured with dye laser absorption at the D1-line. From the continuity equation an expression is deduced relating the Na-profile with the electron density profile. The electron density and electron temperature then result from the measured conductivity of the plasma. For a discharge current from 0.6 to 1.0 A the electron temperature drops from 12000 K to 9500 K, which agrees within 500 K with Langmuir probe measurements. Electron densities range from 2.5 10^{18} to 4.0 10^{18} m^{-3}, which is a factor 1.8 higher than the probe measurements.

GD-4 Optical Pumping in a Low-Pressure Mercury Discharge, P. van de WEIJER and R.M.M. CREMERS, Philips Research Labs, Eindhoven, the Netherlands -- A mercury discharge (diameter 19 mm, P_{HG}=12 Pa, $i \lesssim 10$mA) has been irradiated with a 10 ns dye laser pulse tuned resonant to a mercury transition. We observed one or more of the following phenomena for 16 mercury lines (between 365 and 589 nm):
- fluorescence (direct, two-step or collision induced).
- optogalvanic effect, if one or more of the levels involved in the transition participate significantly in the ionization mechanism(s) of the discharge.
- amplified stimulated emission if a population inversion is created. This inversion can be created by the pupming process directly or by collisional excitation transfer of the upper state of the transition.
- photoionization, if the laser populates an autoionizing level. This can be achieved by a one or two photon process.

GD-5 Three Regimes of Capacitive RF Discharge, V.A. GODYAK, Moscow State Univ., Moscow, USSR-- Experimental and theoretical studies were performed in capacitive rf discharges in helium at pressure 0.1-10 torr, frequencies 1-40MHz and plasma densities $10^8 - 10^{11}$ cm^{-3}. It was shown that magnitude of the ratio ω_e/ω (where ω_e and ω are plasma and generator frequencies, respectively) determines each of three regimes of rf discharges observed. These regimes are governed by different role of sheaths at rf electrodes. Under relatively small values of ω_e/ω one can reach α-regime where effects of sheath are neglible and current-volt characteristic is negative. As ω_e/ω grows the α-regime gradually transforms to β-regime where nonlinear effects in sheaths and ion acceleration to rf electrodes are essential and current-volt characteristic is linear. At high ω_e/ω rf discharge sharply turns into γ-regime where multiplying of secondary electrons in the sheath drastically changes ionization and energy balances in rf discharge. In this regime the plasma density $n \sim p^2$ (where p is gas pressure) and does not depend on ω while in α and β regimes $n \sim \omega^2$. The rf disdischarge map presented in this work permits determination of a set of discharge parameters needed for reali - zation of desireable discharge regime.

GD-6 Electron Oscillation Velocity in Collisionless Radio-Frequency Discharge Plasmas, O.A. POPOV* and V.A. GODYAK+, Moscow State Univ., Moscow, USSR-- Experimental study of capacitive radio-frequency (rf) discharges was made in mercury vapor at pressures 10^{-4}-10^{-2} torr on frequency 40.8 MHz and rf voltage on electrodes below 200 volts. It was found that electron oscillation velocity in rf plasma, $\upsilon_\sim$, obtained from experimental data of discharge current density and plasma density, did not actually vary as rf voltage and rf power change magnitudes of $\upsilon_\sim$ were much less than those of electron thermal velocity in rf plasmas. At pressures $p \lesssim 10^{-3}$ torr $\upsilon_\sim$ stopped its growth with pressure and had a constant value of $\sim 3 \times 10^6 cm^{-1}$. This behavior of electron oscillation velocity and its values differs substantially from those obtained from plasma electron energy balance which considers only electron-neutral collisions. Experimental dependencies of $\upsilon_\sim$ are explained by the effects of the non-collisional dissipative mechanism occurring on the oscillating potential barrier formed in sheaths at rf electrodes.

*Present address: Eaton Corp., Beverly MA 01915.
+Present address: 856 47th St., Brooklyn NY 11220.

GD-7 Time Averaged Measurements of the Sheath Structure in a Parallel Plate RF Discharge at 13.56 MHz, C. A. DEJOSEPH, JR. and P. BLETZINGER, AF Wright Aeronautical Laboratories -- The plasma in a parallel plate RF discharge has a distinct structure along the discharge axis which depends on gas type, pressure and RF frequency. Time averaged, spectrally resolved measurements of the intensity as a function of axial position in N_2, Ar and CF_4 or mixtures of these gases show increased emission symmetric to the midpoint of the discharge, in addition to the electrode sheaths. With increase of pressure, the layers move closer to the electrodes; decreasing the RF frequency moves them towards the midpoint. Additional DC bias on one electrode changes the position; the exact nature of this change depends on bias amplitude and polarity. Adding an attaching gas (CF_4) diminishes the intensity of the layers. Our interpretation of the observed structures will be compared with previous descriptions.

GD-8 Spectroscopic Detection of Gas Phase SiH_x Species. Joda C. Wormhoudt and Alan C. Stanton, Aerodyne Research, Inc.*--Techniques for detection of SiH_x species are important as diagnostic tools in the study of chemical vapor deposition processes. In our experiments aimed at development of such techniques, SiH_x species are produced from silane by thermal decomposition or by dissociation in a microwave discharge. The SiH and SiH_2 radicals are detected by infrared tunable diode laser absorption near 2000 cm^{-1} or by visible resonance fluorescence. The former technique may be adapted to quantitative measurements, while the latter method is useful for spatially resolved measurements of relative concentrations. Results of the high resolution IR measurements of SiH and SiH_2, including measured line positions and estimates of absorption line strengths, are presented. Comparisons are made with fluorescence detection, and a discussion of applications of the techniques to measurements in CVD reactors is presented.

*Supported by AFOSR Contract F49620-84-C-0036.

GD-9 Large Volume Plasmas Sustained by Surface Waves at Radio and Microwave Frequencies, M. CHAKER, M. MOISAN, and G. SAUVE, Physics, U. of Montreal--Up to now, the production of plasma columns through the propagation of electromagnetic surface waves had been reported essentially in the microwave range (200MHz-10GHz). It will be shown that such plasmas can be achieved at much lower frequencies, at least down to 27MHz. The possibility of operating this plasma both in the RF and microwave frequency range is unique as compared to the other HF produced plasma we know. It allows to optimize the plasma parameters for given applications. We will also discuss methods for producing large plasma column diameters and, as an example, characteristics of a 124mm diameter, 3.7 metre long surface wave produced plasma column, will be presented.

GD-10 A He-Ne Laser using a Surface Wave Produced Plasma, C. MOUTOULAS, L. BERTRAND, J.-L. LACHAMBRE, and M. MOISAN, Physics, U. of Montréal--A simple He-Ne laser has been constructed that uses an electromagnetic surface wave produced plasma as the active medium. It has been shown[1] that such plasmas have radial distributions of excited atom density that differ completely from those of a DC positive column plasma. Furthermore, it has been predicted[2] that the electron energy distribution changes as the wave frequency is varied across the RF domain up to the microwave range ($>$ 300 MHz). The surface wave produced plasma offers this unique possibility of spanning the pumping frequency. Laser output power and gain studies are presented with particular emphasis on the wave frequency dependence. Optimization of gaseous lasers is a possible application.

[1] M. Moisan et al, Rev. Physique Appliquée 17, 707 (1982).

[2] C.M. Ferreira and J. Loureiro, J. Phys. D: Appl. Phys., to appear (1984).

GD-11 An Improved Model of the Low Pressure Hg-Rare Gas Positive Column Discharge, R. LAGUSHENKO and J. MAYA, GTE Lighting Products, Danvers, MA -- This model takes into account effects of non maxwellian electron energy distribution, associative ionization, volume recombination and e-impact transitions between $Hg(6^3P)$ and $Hg(6^1P)$ states. The model allows one to calculate all discharge parameters of triple mixtures such as Hg+Ar+Ne and Hg+He+Ar. The electron energy distribution is obtained from an approximate analytical solution to the Boltzman equation[1]. This expression takes into account depletion of the tail of the distribution due to inelastic collisions. Power input into the positive column and UV output calculations are in agreement with experiments within a few percent and 5-10%, respectively, for discharge tube dimensions of r=6-38mm, P_{Hg}=1-26μ and I=0.1-0.5A. The inclusion of previously neglected processes improves the agreement between calculations and experiments by anywhere from 24% to about a factor of 2.

[1]R. Lagushenko and J. Maya, J. of App. Phys. 55, 3293 (1984).

GD-12 Theoretical Investigation of a Radial Opening Switch,* M. vonDADELSZEN, W.M. MOENY, Tetra Corporation, P.J. ROACHE, Ecodynamics, Inc.--The Electric Field Code, ELF, has been used to model the electric field, conductivity, and electron number density distributions within a UV-sustained glow discharge radial opening switch. The effects due to electrode slits, flashboard spark distribution, masking of the UV source, and the angular dependency of the screen transmissivity are included. Comparisons are then made between positioning the flashboard behind the inner and outer electrodes for various concentrations of UV ionization seedant, the objective being to obtain uniform electric field within the radial discharge.

* Work supported by the Naval Sea Systems Command

GD-13 Effects of Turbulence on the Characteristics of a Glow Discharge as Derived from Continuity and Energy Considerations - O. BIBLARZ, W. R. OKER, and R. J. WALLACE, Naval Postgraduate School, Monterey, CA -- While it is known that turbulence affects the stability of glow discharges, the mechanisms operative in delaying transition to the arc-mode are not fully understood. This is perhaps not surprising since both glow discharge and turbulence phenomena are in themselves difficult to describe. A significant part of the problem lies in the very long characteristic times of turbulence phenomena when compared to the glow discharge instability times. We have been studying the influence of turbulence on diffusion and heat conduction within the equations that describe a glow discharge instability. The equations of ambipolar diffusion and overall energy are modelled[1] in an unsteady, cylindrical coordinate system in an IBM 3033. Typically, perturbations of the electric field disturb an otherwise stable configuration. The time evolution of the perturbation is followed until turbulence is fully operative. The resulting stability conditions as a function of turbulence and perturbation strength are then studied.

[1]W. R. Oker, MSAE thesis, NPS, to be published.

GE-1 Electron-Density Growth in Rapidly-Varying Fields,* G. N. Hays, Sandia National Laboratories, L. C. Pitchford, GTE Laboratories, Inc., J. T. Verdeyen, University of Illinois, J. B. Gerardo, Sandia National Laboratories--Measurements have been performed of the temporal growth of the electron density following the sudden application of a high-power, S-band microwave pulse (6 nsec, 200 W peak) in partially ionized nitrogen. Under these conditions and at 0.1 Torr of nitrogen, we find at least 100 nsec are required before the growth becomes exponential. Results will be presented as a function of E/N and comparisons will be made with numerical solutions to the time-dependent Boltzmann equation. These experiments and calculations show the transient electron response to the applied field and the subsequent approach to collisional equilibrium with the field.

*Work supported by the U. S. Department of Energy under contract number DE-AC04-76DP00789.

GE-2 Air Corona Discharge Chemical Kinetics,* L. E. KLINE and I. E. KANTER, Westinghouse R&D -- We have theoretically studied the initial chemical processing steps which occur in pulseless, negative, dc corona discharges in flowing air. A rate equation model is used because these discharges consist of a very small ionization zone near the pin with most of the pin-plane gap filled by a drift zone where both the electric field and the electron density are relatively uniform. The primary activated species are $N_2(A), O$ and $O_2(a^1\Delta)$. The predicted activated species density due to one discharge is 100 ppm per ms · mA cm^2 assuming E/n=60 Td. In pure, dry air the final product due to these activated species is primarily O_3. The NO_x production is about 0.5 ppm per mA. In moist air there is an additional production of about 1.5 ppm per mA of HO_x species. The predicted ozone formation reactions will be "intercepted" when impurities are present in the air. Impurities present at densities below about 0.1% will react primarly with the activated species rather than with electrons. Hence the predicted activated species density provides an estimate of the potential chemical processing performance of the discharge.

* Supported, in part, by US Army Contract No. DAAA 09-82-C-5396.

GE-3 Surface Flashover Discharges as Intense Photon Sources in the Extreme Ultraviolet,* J. R. WOODWORTH and P. F. MCKAY, Sandia National Laboratories--We are investigating surface flashover discharges as UV photon sources for preionizing anodes in light-ion-fusion accelerators. In these experiments the flashover source was formed by discharging a capacitor bank across a spark gap which consisted of two copper electrodes epoxied to an insulator and facing each other across a ~ 0.5 cm gap. The flashover source was constructed in a stripline configuration to minimize overall system inductance.

When the flashover source was driven by a 2.9 μf, 45 kV-capacitor bank, the peak current through the discharge was ~ 250 kiloamperes. When driven at these levels, a single spark radiated a peak intensity of over 50 megawatts of 20- to 70-eV photons and had a total output energy per pulse of 40 Joules. Scaling, effects of substrate material and applications will be discussed.

*This work was supported by the U. S. Department of Energy under contract number DEAC04-76-DP00789.

GE-4 A Model of Flashboard Breakdown With Empirical Scaling Laws,* C.M. YOUNG, J.M. ELIZONDO, W.M. MOENY, J.G. SMALL, Tetra Corporation--Tetra is using multiple surface-spark arrays for pre-ionizing self-sustained and for UV-sustained high pressure glow discharges. A three-stage model of single row multiple spark arrays has been developed based on experimental data. Stage 1 involves initial charging and conditioning of the board. During Stage 2, primary arcs are formed in the first few gaps but extinguish in tens of picoseconds. In Stage 3, the arcs are sustained until complete breakdown of the row is achieved. Empirical scaling laws have been determined which relate key parameters to the minimum row breakdown voltage as a function of the number of gaps in a row. This model is also extended to multiple row flashboards and enables a-priori prediction of flashboard impedance.

* Work supported by the Naval Sea Systems Command

SESSION HA

15:30, Wednesday, October 10, 1984

SILANE DISCHARGES

Chairperson: Vince Donnelly
AT&T Bell Labs

HA-1 Negative Glow-Diffusion Model Of The RF Plasma Reactor, ALAN GARSCADDEN and W. B. BATESON, AIR FORCE WRIGHT AERONAUTICAL LABS, OHIO 45433.

A theory of the rf discharge has been developed treating the electron energy distribution in two main parts: a fast beam resulting from ion bombardment of the electrodes and a slower distribution of secondaries and ultimate electrons that is in equilibrium with the plasma field. The fast group is modulated in energy by the applied rf about the self-bias energy. The profiles of these electrons are obtained in two dimensions treating the boundary as a diffusion source term and the inelastic collisions as loss terms. The division of voltage is determined by requiring that at a given time, the sum of the displacement current and convective current are constant. The conductivity of silane and silane-argon mixtures are determined from Boltzmann calculations and from drift tube measurements. The particle balance is determined by the secondary electron coefficient and high field ion mobility as well as the ionization, recombination and attachment rates of the plasma region. On this model the electronegative discharges should have lower bias sheaths and less influence of the fast group.

HA-2 Measurement of Electron Density in d.c. and r.f. Silane Discharges Using Microwave Techniques,* C.B. FLEDDERMANN, L.J. OVERZET and J.T. VERDEYEN, University of Illinois at Urbana-Champaign--The electron density in d.c. and r.f. silane/helium discharges has been measured as a function of pressure, discharge current, r.f. power and percent silane. For the d.c. measurements, a microwave resonant cavity was used to measure the shift in plasma, while the r.f. measurements were performed using a microwave interferometer technique to measure the phase shift induced by the plasma. For both the d.c. and r.f. cases, there is a sizable decrease in electron density when relatively small concentrations of silane are added to the discharge. The hollow cathode system was also used to measure the decay of the electron density in the afterglow when the hollow cathode is pulsed. It appears from these measurements that the dominant electron loss mechanism is attachment of electrons by the product radicals from the dissociation of SiH_4 in the discharge.

*Work supported by the Air Force Aero Propulsion Laboratory under contract #F33615-83-K-2335.

HA-3 Sheath Models for DC Silane Discharges, H. CHATHAM and A. GALLAGHER, JILA, Univ. of Colo. & NBS.-- A comparison of recent dc cathode sheath models[1-3] is presented. One of the models considered[2] is extended to a self-consistent form which includes the motion of electrons and ions in the cathode fall field. This derived model is applied to a calculation of the current densities of silicon-containing ions in a silane discharge cathode sheath. The rate equations for the ion-molecule reactions of these ions with silane are solved numerically using estimated ion mobilities. The results of this calculation are compared with mass spectrometric measurements of silicon-containing ion current densities at the cathode of dc silane discharges.

[1]J. P. Boeuf and E. Marode, J. Phys. D, Appl. Phys. 15, 2169 (1982).
[2]W. H. Long, Jr., Tech. Report AFAPL-TR-2038 (1979).
[3]H. C. Chen and A. V. Phelps, private communication.

HA-4 Theory of the Plasma Edge: Recycling ↔ Sheaths. J. H. Whealton, R. J. Raridon, W. L. Stirling, M. A. Bell, S. L. Milora and C. C. Tsai, *ORNL -- We consider the models for a plasma edge consisting of (a) Vlasov equations for plasma positive ions, in the plasma sheaths near a metal boundary, (b) Vlasov equations for electrons and/or neutrals thus ejected from such surfaces and (c) Vlasov equations for subsequent ionization and dissociation of volume-produced particles. These Vlasov equations are solved simultaneously with Poisson's equation in as many dimensions as desired with boundaries of arbitrary shape and connectivity. These calculations are applied to plasma edge pumps and ion deposition situations to determine pumping efficiency as a function of boundary shape and uniformity of ion deposition on irregular surfaces. This model is highly nonlinear and heretofore unsolvable for problems of this variety.

---

*Operated by Martin Marietta Energy Systems, Inc. under contract No. DE-AC05-840R21400 for the U. S. Department of Energy, Office of Fusion Energy.

HA-5 Infrared Measurements of Disilane Production From A D.C. Discharge in Silane*, ROBERT CHENEY, RANDALL SCHADT, and RICHARD ANDERSON, U. of Missouri- Rolla, Rolla, Missouri and C. A. DEJOSEPH, JR., AF Wright Aeronautical Laboratories -- Gallagher, et al.[1] have reported disilane production in a silane discharge by sampling the discharge products with a mass spectrometer. A similar experiment was repeated using a Fourier spectrometer instead of a mass spectrometer. The silane d.c. discharge products were sent to a 20m path length White cell and the absorption spectra of silane and disilane were examined between 824 and 912cm^{-1} under different experimental conditions. Silane pressure (1% in argon) and discharge current affected the disilane production.

1. A. Gallagher and J. Scott, SERI Report XB-2-02085 (1982)

*This research was performed at Wright Patterson Air Force Base under the SCEEE faculty and graduate student fellowship program.

HA-6 Dissociation Rates of Silane in an R.F. Discharge by Tunable Diode Laser Absorption, C.A. DEJOSEPH,JR. and D.R. POND, AF Wright Aeronautical Labs -- Effective dissociation rates have been measured for silane diluted in argon at low pressure(0.2-0.3 torr) in a low power(1-2 watt) R.F. discharge at 13.6 MHz. The discharge tube consists of three parallel, wire-mesh electrodes with the center electrode driven. Gas flow is through the electrode mesh. The effective dissociation rate is determined by monitoring the decrease in the i.r. absorption of an isolated silane line as a function of gas residence time in the discharge. Absorption is measured just downstream from the discharge. The data show an initially high rate which drops to near zero for long residence times. Both the relative concentration at which dissociation ceases and the initial rate depend on R.F. power.

HA-7 Glow Discharge Electron Beam Processing of Microelectronic Materials, J. J. ROCCA, C.A. MOORE, L. R. THOMPSON, and G. J. COLLINS, Colorado State University -- Large area electron beams generated in direct current glow discharges have been used to perform several microelectronic fabrication processes. A thin planar sheet of kilovolt electrons traveling a few millimeters above a substrate has been used to deposit thin films. In an ambient of SiH_4 and N_2O the electron beam dissociates these gases to form SiO_2 films; using SiH_4 and NH_3 in the same configuration yielded films of silicon nitride at substrate temperatures between 50 and 450°C. The deposition conditions and film properties will be discussed. A 7.5 cm diameter cylindrical electron beam of multikilowatt power has been used to uniformly anneal ion implants in single crystal silicon. Diffusion of dopants induced by this transient heating (<1 min.) was found to be negligible. This source was also used to form titanium disilicide from two structures. For Ti deposited on Si structures, the sheet resistivity increased by a factor of 2.5 before reaching its ultimate minimum value. This is shown to be caused by diffusion of oxygen into the titanium followed by cleaning of the silicide by the advancing silicon atoms.

SESSION HB

15:30, Wednesday, October 10, 1984

METAL HALIDE AND MERCURY ARCS

Chairperson: Harald Witting
General Electric R&D

HB-1 Convection and Additive Segregation in High-Pressure Lamp Arcs: Early Results from a Space Shuttle Experiment. A.H. BELLOWS, A.E. FEUERSANGER, G.L. ROGOFF, GTE Laboratories Inc.; H.L. ROTHWELL, GTE Lighting Products--Convection can significantly affect electrical and radiative properties of high-pressure arc discharges, especially those containing minor additives. To determine the effects of natural convection on metal halide lamps (metal additives in high-pressure mercury) and to provide gravity-free data for comparison with computer models, an experimental study of Na-Sc-Hg arcs (175 W ac and dc) was carried out on the NASA Space Shuttle. Primarily, the arcs were photographed through spectral filters to obtain separate images with Na, Sc and Hg emission. Also white-light images were made, and electrical, thermal, and luminosity data were recorded digitally. For comparison, the same measurements were made in the laboratory with vertical arc operation. In this talk the experiment will be described, examples of data will be shown to illustrate the observed electrical and axial additive segregation effects--due to cataphoresis as well as convection--and planned procedures for extracting temperature and density distributions from the film will be outlined.

HB-2 **Measurement of Cadmium Vapor Pressure in the Metal Halide Arc** - R. P. Gilliard and T. D. Russell, General Electric Company, Cleveland, OH - -Spectral diagnostics of operating arcs are used to determine the core densities of cadmium as an additive in high pressure mercury and metal halide (NaI, ScI_3, ThI_4) arcs. Based on the cold spot temperatures of the arc tube (700°C to 800°C), the total charge of cadmium would be expected to be vaporized, which the data substantiate when only mercury and cadmium are present; however, the presence of the metal halides suppresses the cadmium vapor pressure significantly. Absorbance measurements in closed cells containing various amounts of cadmium and metal halides point to a chemical interaction between cadmium and the metal halides which affects the cadmium vapor pressure.

HB-3 A Multithermal Equilibrium (MTE) Arc Plasma Heat Transfer Model, T.L. Eddy and D.W. Pruitt, Georgia Tech and AEDC.-- Experimental measurements on arcs and other thermal plasmas have shown that the energy distributions in various energy modes can be expressed by the temperature of that mode. Typical temperatures of importance are the electron and gas translational, the upper level population, and the ionization temperatures. Preliminary analysis using the associated MTE model shows that the conservation equations for plasma heat transfer in a "thermal" or an arc plasma can be presented as a series of non-local transport terms (conduction, diffusion, radiation, convection, etc.) and a series of local "source" terms. The local terms include the up/down collisional excitation and ionization processes, summed over all levels. The local collisional terms can be expressed by two to eight thermodynamic "source" properties (depending on the MTE model required) which are functions of the local MTE temperatures. The thermodynamic source property values can be determined experimentally or calculated on a one time basis. The resulting solution of the conservation equations by traditional methods is simplier, should be more accurate, and utilizes intermediate parameters of convenience for R&D work.

HB-4 Analytical Expressions for the Populations and Ionization Frequencies of Excited Atoms in Non-equilibrium Hydrogen Plasma, J.A. KUNC, U. of Southern California--An approximate analytical solution of the master equations (in the form given by Bates et. al.[1]) in a steady-state, non-equilibrium hydrogen plasma is presented. A Maxwellian distribution is assumed for electrons; the reabsorption of radiation is accounted for through Holstein's escape factors. The expressions for the populations of excited atoms give results that are in good agreement with the numerical results of Bates et. al.[1] in the range of plasma conditions $8{,}000°K \leq T_e \leq 64{,}000°K$ and $10^{10} cm^{-3} \leq n_e \leq 10^{16} cm^{-3}$. The analytical expressions for the populations of excited atoms and the analytical relationships for the ionization cross sections[2] lead to simple expressions for the frequencies of ionization of excited atoms.

[1]D.R. Bates, A.E. Kingston and R.W.P. McWhirter, Proc. Roy. Soc. A267, 297 (1962).

[2]J.A. Kunc, J. Phys. B13, 587 (1980).

HB-5 Determination of Particle Numbers in High Pressure Lamps, R. SCHÄFER*, Philips GmbH Forschungslaboratorium Aachen / Germany - The set-up for the determination of mercury pressures from the absorption of the frequency doubled 514.5 nm Ar^+ laser line described recently[1] has been modified to measure the absorption on the central ray through the lamp. It is shown that the total particle number per unit length can be calculated from the absorption data without exact knowledge of the temperature profile. The method has been applied to measure the variation of the particle number during warm-up and cool-down phase of a 400 W mercury lamp as well as for the measurement of axial particle number profiles during the stationary state. The results show that the particle number is lower in the arc column than in the electrode regions.

[1]H.P. Stormberg and R. Schäfer, Bull. Am. Phys. Soc. 29, 156 (1984)

*present address: Philips Lighting Division, Eindhoven, The Netherlands

HB-6 Determination of Temperature Profiles from Optically Thick Lines, H.-P. STORMBERG, Philips GmbH Forschungslaboratorium Aachen / Germany - A method for the evaluation of temperature profiles of high pressure discharges is proposed, which is based on a numerical solution of the radiative transfer equation. The quantities that have to be provided for the numerical evaluation are readily obtainable, because only the absolute side-on intensity of the respective line has to be measured as a function of the lateral coordinate. The method can also be applied if only a part of the line is measured. Temperature profiles have been determined from optically thick mercury lines, for which the broadening constants are known.[1] Comparison with temperatures derived from optically thin lines shows good agreement for high pressure mercury discharges. As a further advantage of using optically thick lines of transitions with low excited states the temperature profile can be determined for larger radii than from optically thin lines. This is demonstrated using the 254 nm mercury resonance line.

[1]H.-P. Stormberg and R. Schäfer, J. Appl. Phys. 54, 4338 (1983)

HB-7 Volumetric Instability in a High Power Mercury Discharge,* A. MANDL and M.W. McGEOCH, Avco Everett Research Laboratory.--The pulsed discharge I/V characteristics of mercury vapor have been measured. An e-beam preionized discharge with Neon or Helium buffer has been operated at temperatures up to 875°K in a longitudinal magnetic field. Typical current densities ranged from 1 Acm^{-2} to 10 Acm^{-2} at fields up to 2.5 kV cm^{-1}. For a wide range of discharge conditions the specific energy loading in Hg/He mixtures was limited to ~10 $J\ell^{-1}$ $Amag^{-1}$ by the sudden collapse of the discharge impedance. A detailed model of the mercury discharge has been developed which includes seven atomic Hg levels and eight molecular Hg levels whose populations are driven by the computed electron excitation rates (both inelastic and superelastic) and neutral collisions. The model gives a very close description of the experimental data and indicates that there is a volumetric arc caused by a combination of two-and three-step ionization of Hg.

*Work supported by U.S. Army BMD, Huntsville

SESSION I

19:30, Wednesday, October 10, 1984

WORKSHOP ON RF DISCHARGES

Chairperson: J. Verdeyen
University of Illinois

I

I-1 Things we don't understand about Plasma Etching, BRIAN CHAPMAN and COLLEAGUES, Tegal Corporation, Novato, CA--Those of us involved in the plasma etching of semiconductor materials are painfully aware of the substantial gap between the understanding of plasma technology and its everyday implementation in the fabrication of integrated circuits. In the majority of cases, our understanding simply lags behind the implementation. This occurs in both the chemistry of the discharge process and in aspects of reactor design. In other cases, practical process appears to contradict our 'understanding' of process, or at least to produce surprising results. This contribution to the workshop would discuss some of these contradictory or surprising results, as well as others where our understanding is immature or nonexistent.

I-2 Plasma Potentials of 13.56 MHz rf Argon Glow Discharges in a Planar System. J.W. Coburn, IBM Research, San Jose, CA. -- The plasma potential of 13.56 MHz low pressure argon glow discharges has been measured for various modes of applying the rf power in a geometrically asymmetric planar system. The plasma potential is determined from the energy distribution of positive ions incident on the grounded electrode. The voltages on the excitation electrode (target electrode) are carefully measured and the capacitive sheath approximation is used to relate these measured voltages to the measured plasma potential. This approximation is successful in most of the situations encountered in this low pressure (20 millitorr) relatively low power density regime. The effects of superimposing dc voltages on the excitation electrode are discussed.

I-3 Dynamics of Radio Frequency Glow Discharges, RICHARD A. GOTTSCHO and MARY L. MANDICH, AT&T Bell Laboratories -- The distinguishing feature of RF discharges which sets them apart from DC glows is, of course, the application of a time-varying field. How the plasma "responds" to this field can influence both homogeneous and heterogeneous chemistry. In particular, the ion energy distribution, gas-phase composition, and surface reaction rates can change substantially as the applied frequency is varied from below to above the ion plasma frequency, ω_i. In order to understand this plasma response and the concomitant changes in chemistry, we have looked at the concentrations of ions and radicals and the magnitude of the local field as they vary in time. This is done by firing a pulsed laser synchronously with the applied potential and then monitoring the laser-induced fluorescence from ions and radicals. Spatial and temporal resolution are typically 10^{-4} cm^{-3} and 10 ns, respectively. I will describe the results of these diagnostic experiments with particular emphasis on changes in sheath properties, ion transport to electrode surfaces, and ion impact phenomena as the operating frequency is varied from below ω_i to above ω_i.

I-4 Theoretical Modelling of Planar RF Discharges,* D. W. Ernie, Univ. of Minnesota -- A model which has been developed to describe the voltage and current characteristics of an asymetrical planar rf plasma reactor will be discussed. This discharge configuration is modelled by an equivalent electrical circuit consisting of an ideal rf source, a blocking capacitor, and the two plasma sheaths at the discharge electrodes. The sheaths are represented by a parallel configuration of capacitive and current controlling elements. The sheath current is approximated by the static plasma probe current-voltage characteristic. A model which has been derived for the time dependent sheath capacitance will be presented. Numerical solutions of this circuit model for the sheath potentials, the plasma potentials, and the sheath currents, as a function of discharge parameters, will be given and compared to available experimental data. The implications of these results for the design of plasma processing systems will be discussed.

*Work supported by Air Force Wright Aeronautical Laboratories and I.B.M.

I

I-5 Energy Partitioning and Excitation Rates in RF Parallel Plate Discharges.* M.J. KUSHNER, Math. Sciences Northwest --The electron energy distribution function (EEDF) in RF parallel plate discharges is comprised of an e-beam component, resulting from electrons accelerated through the sheaths, and a thermal group, in which the majority of electrons reside. The EEDF is a function of both time and position between the electrodes, a consequence of the time and spatially varying applied electric field. This is especially true in and near the sheaths. The response of the sheath to the EDF also influences the ion energy distribution function (IEDF) incident onto the electrodes, the form of which is most important with respect to plasma processing. The result is that electron impact excitation rates also have a complex behavior which additionally depends on parameters such as gas pressure, electrode separation, discharge symmetry, and RF frequency. Using Monte-Carlo simulations, the EEDF, IEDF, and excitation rates will be examined as a function of these parameters. Differing sheath models will be used to examine effects of sheath properties on excitation rates.

*Work supported by Math. Sciences Northwest IR and D

SESSION JA

08:15, Thursday, October 11, 1984

ELECTRON TRANSPORT

Chairperson: Barbara Whitten
Lawrence Livermore Lab

JA-1 Electron Swarm Properties of SF_6-$CC\ell_2F_2$ Mixtures, M.F. FRECHETTE and J.P. NOVAK, IREQ, Varennes, Québec, Canada--Two-term approximation of the Boltzmann equation has been used to calculate transport coefficients of SF_6 - $CC\ell_2F_2$ mixtures. Concurrent measurements of the apparent effective ionization coefficients $\bar{\alpha}$ have been performed by the help of Townsend steady-state method. Good agreement has been found between calculated and experimentally determined values in the range of reduced fields $120 \leq E/p \leq 180$ V cm^{-1} Torr^{-1}. Limit fields E/p^* defined by the condition $\bar{\alpha}\,(E/p^*) = 0$ were evaluated from calculated and experimental values and compared to uniform breakdown measurements.[1] All data exhibit positive synergism with a maximum critical field of about 127 V cm^{-1} Torr^{-1} at 75% $CC\ell F_2$ content. In comparison with the values obtained from uniform field breakdown measurements, present experimental values of E/p^* are in good agreement while the calculated values are approximatively 3% lower.

[1] I.C. Somerville, D.J. Tedford, and A. Thurogood, 6th Int. Conf. Gas Discharges, London, 1980, p. 271.

JA-2 Density Gradient Expanded Energy Distribution Functions*, B. M. Penetrante and J. N. Bardsley, U. of Pittsburgh -- We have developed a Monte Carlo technique for calculating each of the terms of the density gradient expanded energy distribution functions. The gradient-dependent (GD) term in this expansion is the basis for the calculation of the longitudinal diffusion coefficient in the Boltzmann formulation. For electrons in the ramp model gas and methane, the agreement between the multiterm spherical harmonic Boltzmann solutions[1] and the Monte Carlo solutions is excellent for both the homogeneous and the GD energy distributions. However, a disturbing discrepancy in the GD energy distribution persists for the case of nitrogen.

*Work supported by the Office of Naval Research.
[1] L. C. Pitchford, private communication.

JA-3 Model Calculations of Electron Transport in Non-Uniform Fields - T.J. Moratz[1] and L.C. Pitchford[2], Sandia National Labs, Albuquerque, NM - Monte Carlo simulations to determine electron transport and rate coefficients in lineraly varying fields have been performed for three model cases and as a function of the field gradient. By beginning the simulation with an equilibrium electron energy distribution, the nonlocal effects due to the field gradient can be isolated. Results of the spatially dependent electron transport and rate coefficients have been obtained for three cases; a constant collision frequency model, Reid's model atom and N_2. Comparison of these spatially dependent results with the local field values allows us to quantify conditions for which the local field approximation is valid. At low E/N in the Reid model atom, departures from local field values of the transport coefficients are seen for gradients above 400Td/cm at 3 Torr. In N_2 at moderate to high E/N, the coefficients which reflect the high energy tail of the electron distribution are the slowest to reach their local field values.

1. Present address, Univ. of Pittsburgh, PA.
2. Present address, GTE Labs, Waltham, MA.

This work supported by the U.S. Dept. of Energy.

JA-4 Hydrodynamic Models of Electron Transport in Rapidly Varying Fields - L.C. Pitchford*, Sandia National Labs, and J. Ingold, General Electric Co., - Electron transport and rate coefficients in rapidly varying fields are functions of both E(t)/n and the product nt. To date, a kinetic (Boltzmann or Monte Carlo) description is necessary to describe the time-dependence of the transport and rate coefficients. In an attempt to develop a simple description of the time-dependent transport coefficients, we examine here the time-dependent drift velocity calculated from two different approximate methods. One method involves the solution of the first three moments of the Boltzmann equation, while the other method assumes that the first-order corrections to the equilibrium value are functions of $d(E(t)/n)/d(nt)$[1]. We find that for times longer than the momentum relaxation time, the first method yields values in fair agreement with the Boltzmann calculations, but the second method has so far not proven useful.

1. N.L. Aleksandrov et al, Sov. J. Plasma Phys. 6 618 (1980).

*Present address, GTE Labs, Waltham, MA.

The work of LCP was supported by U.S. Dept. of Energy and Wright Patterson Air Force Base.

JA-5 Equation of Evolution for Electrons in a Weakly Ionized Gas and Influenced by Space-Time Varying Electric Fiels,* E.E. Kunhardt, Polytechnic Institute of NY -- An equation of evolution for electrons in a weakly ionized gas, taking into account the space-time varying electric field that may be present due to either external sources or space-charge, is presented. This equation, obtained through a multi-time scale perturbation procedure, constitutes a one moment description of the electron gas. This description is valid for times longer than the momentum transfer and energy exchange collision times. Formal expressions for the phase-space distribution function and the coefficients appearing in the evolution equation are also presented. For the constant field case, the analysis yields the density gradient expansion for the distribution function.[1]

*Work supported by the Office of Naval Research.

[1]K. Kumar, H.R. Skullerud, and R.E. Robson, Aust. J. Phys. 3, 343 (1980).

SESSION JB

08:15, Thursday, October 11, 1984

THERMAL ARC SPRAYS

Chairperson: Paul A. Siemers
General Electric R&D

JB-1 Plasma Spraying, E. PFENDER, Department of Mechanical Engineering, University of Minn., Minneapolis, Minn. 55455 -- The principle of D.C. plasma torches which are primarily used for plasma spraying will be discussed including the gas heating process within the torch and the subsequent formation of a plasma jet. Examples of measured and calculated temperature and velocity distributions in plasma jets will be shown in conjunction with a discussion of their parameter dependence.

Because of the importance of plasma transport properties on particle heat and momentum tranfer in the plasma jet, a brief discussion of relevant plasma transport properties will be included in this presentation.

Finally, some comments will be made about the plasma state during soft vacuum plasma spraying.

JB-2
Plasma-particle interactions in thermal plasma spraying, M.BOULOS, Department of Chemical Engineering, Université de Sherbrooke, Sherbrooke, Québec, Canada, J1K 2R1
Particle injection in the plasma jet represents one of the critical steps in plasma spraying that can substantially influences the trajectory and the temperature history of the particle. A review will be made of particle injection techniques and their effects on the effeciency of the thermal treatment of the particles. Comparison will be made between calculated and measured particle trajectories in a d.c. plasma jet. The problem of plasma-particle interactions under dense loading and reduced pressure conditions will be discussed.

JB-3 Properties of Plasma-Sprayed Coatings, P. FAUCHAIS, U.E.R. des Sciences, Université de Limoges, 87060 Limoges Cedex, France -- The quality of plasma-sprayed coatings depends to a large degree on the particle deposition process (particle deformation on impact) and on the solidification of the particles arriving at the substrate. Characteristic properties of metallic and oxide coatings (microstructure, porosity, adherence, hardness) will be discussed in conjunction with their primary parameter dependence.

In the last part of this presentation some of the advantages and disadvantages of plasma spraying in soft vacuum will be briefly discussed.

SESSION K

10:00, Thursday, October 11, 1984

GLOW DIAGNOSTICS

Chairperson: Louis Palumbo
Schaefer Associates

K-1 Determination of the Effective Radiative Lifetimes of the 6 $^3P_1$ Atomic Mercury level in Low-Pressure Mercury Discharges, P. van de WEIJER and R.M.M. CREMERS, Philips Research Labs., Eindhoven, The Netherlands -- Experiments are described in which low-pressure mercury, mercury-argon and mercury-krypton discharges were irradiated with a dye laser pulse at 365.5 nm, thus exciting mercury atoms from the metastable 6 $^3P_2$ level to the 6 $^3D_2$ level. The 6 $^3D_2$ level decays radiatively to the 6 P levels. By recording the times dependence of the overpopulation in the 6 $^3P_1$ and the 6 $^1P_1$ level at the fluorescence signals at 254 nm and 185 nm, respectively, the effective radiative lifetime of these levels were determined. The effective radiative lifetime of the 6 $^3P_1$ level was measured in the k_oR regime 0.1-500.
The 6 $^1P_1$ lifetime was determined for the following discharge conditions: tube diameter 10-36 mm, mercury density 7.10^{18}-2.10^{21} m^{-3}, and noble gas pressure 0, 130, 400 Pa.

K-2 Isotope Effects in Atomic Resonance Radiation Transport,* M. GROSSMAN, R. LAGUSHENKO and J. MAYA, GTE Lighting Products, Danvers, MA --Intensity and response time of atomic resonance radiation transport through an atomic vapor mixture is greatly affected by radiation trapping phenomenon. We have extended Holstein's treatment of resonance radiation transport to include hyperfine mixing and line broadening due to rare gases (RG) and metal atoms, energy transfer between isotopes (in a multiple isotope system) and overlap of the hyperfine structure of the different isotopes. We carried out calculations for a variety of isotopic compositions in Hg+RG and Cs+RG mixtures. Our calculations indicate a reduction of up to 50% in resonance trapping time due to altered isotopic composition of an atomic vapor under certain conditions. We have experimentally verified some of these predictions in a weakly ionized Hg-Ar plasma. By enriching Hg in ^{196}Hg up to 2-4% we have measured an increase in 253.7nm emission efficiency of $\sim$5% indicating a reduction of 6-8% in resonance trapping time. In the case of Cs vapor, addition of ^{137}Cs at a concentration of 0-50% to natural ^{133}Cs is calculated to reduce the response time of an atomic resonance filter by as much a factor of 2.

*Work supported in part by DOE.

K-3 Dissociation and Product Formation Kinetics of NF_3 Etchant Gas Discharges,* K. GREENBERG[1] and J. T. VERDEYEN, University of Illinois at Urbana-Champaign -- This work has dealt with an investigation of some of the fundamental properties of the NF_3 plasma. The percentage dissociation of the parent gas by the discharge was inferred by monitoring changes of the mass spectrum ion signals when the discharge was initiated. These measurements have shown an extremely large dissociation of the NF_3, at least two orders of magnitude larger than that of pure CF_4 under similar discharge conditions (same current, pressure, etc.). By observing the optical emission from a pulsed discharge it was also possible to observe the time evolution of various species in the plasma. These transient studies have led to a simple mathematical model which can describe the dissociation of the parent gas, the production of atomic fluorine and, consequently, the etching of silicon by the discharge.

*Work supported by the Joint Services Electronics Program (U.S. Army, U.S. Navy, U.S. Air Force).

[1]Present address: Sandia National Laboratories, Albuquerque, New Mexico.

K-4 Neutral Particle Density Transients in Gaseous Discharges,* A. Metze, D. W. Ernie, H. J. Oskam, and L. M. Chanin, Univ. of Minnesota -- A model is presented which describes the neutral density transients in gaseous discharges. It is shown that the duration of the initial density transient is governed by the speed of sound in the gas in which the discharge is produced. The development of the gas-flow velocity pattern in the discharge tube is a consequence of the interplay between three competing volume forces: (a) the driving volume force, which is generated by the interaction of the charged particles with the neutral particles, (b) the viscosity force and (c) the neutral pressure gradient force. The influence of the geometry of the discharge tube on the neutral particle density transients is also discussed. The initial neutral particle density transient is believed to be the origin of acoustic resonances observed in rf excited gaseous discharges.

*Work supported by NSF under Grants No. CPE-8122086 and No. CPE-8105468.

K-5 Optogalvanic Spectroscopic Measurement of Singlet Helium Rydberg Series. B. N. GANGULY and ALAN GARSCADDEN - AFWAL/POOC-3, WPAFB OH 45433. Atomic helium transitions from the metastable helium $2s\,^1S$ to high Rydberg levels $np\,^1P$, up to n = 46 have been measured in a low pressure low current d.c. discharge using optogalvanic spectroscopy. A frequency-doubled pulsed dye laser, pulse length 7 nsec, was used and the actual current perturbation or the voltage change of the discharge was measured accurately. The linewidth of the probing laser was 0.3 cm^{-1} permitting the linewidth of the singlet Rydberg series to be measured. The measurements were made just outside the cathode fall, in the negative glow and positive column region. The Stark broadening was found to be minimum in the negative glow region and maximum in the positive column. The linewidth variation of more than a factor of two was observed for the $29p\,^1P$ transition. The series advance was observed to be proportional to the Stark broadening. These transitions permit the estimation of relatively low electric fields.

K-6 Electric Field Measurements in Glow Discharges Using Optogalvanic Detection of Rydberg atoms.* J.E. LAWLER, D.K. DOUGHTY and S. SALIH, Dept. of Physics, U. of Wisconsin-Madison--Spatially resolved electric field measurements in the cathode fall region are performed using linear Stark effects in Rydberg atoms. The large linear Stark effects of Rydberg atoms are straightforward to calculate. A wide range of electric fields can be observed by proper choice of principle quantum number. The Rydberg atoms are produced by laser excitation from metastable levels. The fragile Rydberg atoms are rapidly collisionally ionized, and are detected using optogalvanic effects. Single step excitation using a frequency doubled dye laser is used in He. Two step excitation using intersecting dye laser beams is used in Ne. The two step method provides pinpoint measurements of discharge fields. The pinpoint field measurements are integrated along a well defined path from anode to cathode and found to agree with the discharge voltage to ~1%. The field measurements provide a map of the cathode fall region.

*Supported by the AFOSR and ARO grant 81-0208

K-7 Energy Distribution of Ions Arriving at the Electrodes of a RF Discharge,* A. Metze, D. W. Ernie, and H. J. Oskam, Univ. of Minnesota -- A simplified one-dimensional model has been developed to analyze the influence of rf modulation on the energy distribution of the ion surface flux in gas discharges. To first order, the effect of rf modulation can be modeled by superimposing a periodic rf potential onto a highly negative biased planar probe. Calculations based on this model will be presented and discussed. These calculations show that the width of the ion energy distribution becomes narrower and the minimum value of the distribution becomes larger for increasing rf frequency. For non-sinusoidal, periodic rf modulation, the ion energy distribution is asymmetrical. These results will be used to give a qualitative explanation of the ion energy distribution measured at the electrodes of rf discharges. Limitations of the model and implications of the model, for the design of plasma processing systems, will be discussed.

*Work supported by Air Force Wright Aeronautical Laboratories and I.B.M.

SESSION L

11:30, Thursday, October 11, 1984

POSTERS. MOSTLY ATOMIC AND MOLECULAR

LA: ATOMIC AND MOLECULAR PROPERTIES

LB: PHOTON ABSORPTION AND EMISSION

LC: ELECTRON COLLISIONS

LD: ATOMIC AND MOLECULAR COLLISIONS

Chairperson: Pablo Vicharelli
National Center for Atmospheric Research

LA-1 Atomic Transition Probabilities in Refractory Metals,* S. SALIH, D.W. DUQUETTE,+ and J.E. LAWLER,+ Dept. of Physics, U. of Wisconsin-Madison--Accurate transition probabilities for a large number of spectral lines in the first and second spectra of 3d, 4d and 5d metals are being measured. Radiative lifetimes of hundreds of levels in TaI, WI, MoI, NbI, HfI, ReI, RhI, RuI, NbII, CoII++, and other atoms and ions are measured using time-resolved laser-induced fluorescence on an atom or ion beam. The atom or ion beam is produced by a versatile hollow cathode discharge source. Branching ratios of levels in WI, NbI, HfI, and ReI are measured from calibrated spectra recorded on the Kitt Peak one-meter Fourier Transform Spectrometer. The transition probability measurements are used in solar and stellar elemental abundance determination. Some of the elements mentioned above are commonly used as electrodes in discharge devices. Accurate transition probabilities are also useful in studying concentrations and the effects of sputtered electrode material on laboratory discharges.
*Supported by NSF Grant AST83-17713.
+Guest Observer, Kitt Peak National Observatory, operated by AURA, Inc., under contract with the NSF.
++In collaboration with Ward Whaling, Caltech.

LA-2 Kinetic Modeling in Neon-like Ions;* B. L. Whitten & A. U. Hazi, Lawrence Livermore National Laboratory

Neon-like ions of intermediate Z ($26 \leq Z \leq 43$) are of interest because they are potential candidates for soft x-ray lasers. The kinetics of neon-like ions are complex, but the acquisition of large atomic data bases makes possible the development of kinetic models. Recent experiments on laser-generated plasmas allow us to test the accuracy of our models. We present a model which calculates the 3-3 and 3-2 transitions of neon-like selenium. The ground state, n=3, and n=4 excited states are included explicitly; the n=5 through n=10 states are each lumped into one generic level. The model includes collisional and radiative transitions among these levels, and solves steady state rate equations for the populations. We use this model to investigate the effect of various processes on the 3-2 and 3-3 spectra. Comparisons with experiment are also presented.
*Work performed under the auspices of the U.S. Department of Energy by Lawrence Livermore National Laboratory under contract #W-7405-Eng-48.

AD-A159 928 ANNUAL GASEOUS ELECTRONICS CONFERENCE (37TH) HELD AT BOULDER COLORADO ON 9-12 OCTOBER 1984 PROGRAM AND ABSTRACTS(U) COLORADO UNIV AT BOULDER 12 OCT 84 2/2

UNCLASSIFIED N00014-84-F-0137 F/G 9/5 NL

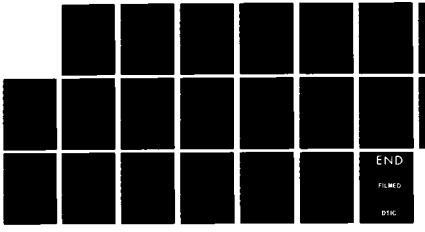

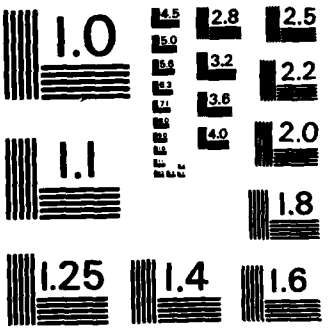

MICROCOPY RESOLUTION TEST CHART
NATIONAL BUREAU OF STANDARDS - 1963 - A

LA-3 Photon-Echo Experiments on Coherence Multipole Decays M. R. WOODWORTH and I. D. ABELLA, U. Of Chicago-- Observations of the multipole moments (e.g., the population, orientation, and alignment) of spatially degenerate atomic states have proven very useful in atomic physics [1]. It has been suggested that the multipole moments of the superposition of spatially degenerate states can also be measured, using a two-pulse spontaneous photon echo [2]. Though the photon echo signal is proportional to the dipole moment of the superposition, it can be modulated by higher order moments created by the first pulse and mixed into the dipole term by the second. Decays of the higher order moments should be sensitive to anisotropies of the interaction potential. Experiments are in progress to measure higher order multipole decays in photon-echo experiments using r.f. glow discharges of Krypton and Neon [3].

1. A. Omont, Prog. Quantum Electronics 5, 69 (1977)
2. T. Baer, Phys. Rev. A 18, 2570 (1978)
   D. S. Bakaev, I. V. Evseev, and V. M. Ermachenko, Opt. Spectrosc. (USSR) 49, 119 (1980)
3. M. R. Woodworth, Opt. Lett. 8, 307 (1983)

LA-4 **Emission and Absorption Characteristics of Long-Pulsed, Electron-Beam Excited, Pure Helium Plasmas** - L. W. Downes, S. D. Marcum and W. E. Wells, Miami University.--In many past experiments emission spectra from short-pulsed (3-10 ns), electron-beam excited, high-pressure helium plasmas (200-3500 Torr) have been observed. We have studied the emission and absorption characteristics of similar plasmas excited by an electron beam with variable pulse length (120-900 ns). Time resolved spectroscopy shows that the characteristics of such plasmas, while agreeing with earlier studies at short pulse lengths, vary considerably as the pulse length is increased. Of particular interest are previously unreported molecular type emissions in the region of 431 nm. Those emissions have very slow rise-times (>100 ns) and become the dominant emissions from the plasma at late times during the discharge and throughout the afterglow period. At 1000 Torr the decay lifetime of the 431 nm emission is roughly 2 μs. In addition, absorption measurements indicate that a broad-band absorption (350-550 nm) is associated with the helium species emitting at 431 nm. The characteristics of the states responsible for this behavior will be presented and discussed.

LA-5 **Emission and Absorption Characteristics of a Thermally Generated Heat Pipe Sodium Plasma**- V. Petricevic, L.W. Downes, D. G. Hild, S. D. Marcum, M. Mihailidi, D. A. Stetser, and W. E. Wells, Miami University, Oxford, OH 45056 — The plasma was studied between 5 Torr and 500 Torr of sodium and between 600 K and 1500 K (along the axis of the heat pipe through the hot region and the transistion regions). At lower temperatures the emission is dominated by a very wide band self-reversed sodium D atomic emission (590 nm). At the higher temperatures the atomic emission is not present and only diffuse radiations from the dimer triplet states are observed. The triplet emissions observed are 400-450 nm, 550-580 nm, 850-880 nm. No singlet dimer emission has been detected. Significant absorption is noted throughout the region of observation (350-900nm) except for two windows of near zero absorption. These windows correspond to the diffuse triplet emission in the violet and infrared. These observations may have significance for laser operation because of the excimer nature of the diffuse triplet bands.

LA-6 Electronic Structure of the Lithium Molecular Anion, Li_2^-* H. H. MICHELS and R. H. HOBBS, UTRC, East Hartford, CT, 06108, and L. A. WRIGHT, MRC, Albuquerque, NM, 87106--Calculations have been performed on the electronic structure and potential energy curves for the Li_2^- anion using CI wavefunctions optimized for the ground and excited molecular states. The ground $^2\Sigma_u^+$ state of Li_2^- lies below the X $^1\Sigma_g^+$ state of Li_2 and can be treated using standard variational methods. The excited states of Li_2^- are, in general, resonant states and are unstable with respect to autoionization. These states, however, are of interest in low-energy e + Li_2 dissociative attachment and vibrational excitation processes. Our calculated electronic affinity for Li_2 is 0.42 eV, in good agreement with previous theoretical studies. In contrast with the H_2 system, we find a rich spectrum of low-lying resonant states for Li_2^-.

*Work supported in part by AFOSR under Contract F49620-83-C-0094 and by AFWL under Contract F29620-82-C-0077.

LB-1 Virtual State Resonance Effect on the Photodetachment Threshold Behavior of Li^- Leaving ^2P Li*, Y. K. BAE and J. R. PETERSON, Chemical Physics Laboratory -- Absolute cross sections of Li^- photodetachment near the threshold of Li (2^2P) + εs channel have been measured. Multichannel scattering theory has been applied to develop proper parametric forms for analyzing total cross sections near excitation thresholds that are energetically close to poles of the scattering matrix. The behavior of Li^- photodetachment near the Li (2^2P) threshold can be accurately fitted using the form derived to describe the effect of a virtual state resonance on a Wigner cusp. From the fitting parameters, the position of the virtual state, the phase shift of Li (2^2S) + εp channel at the threshold of Li (2^2P) + εs channel, and the electron affinity of Li have been determined to be 55 ± 10 meV, 1.4 ± 0.1 radian, and 617.3 ± 0.7 meV respectively.

*Work supported by AFOSR under the Contract No. F49620-82-K-0030.

LB-2 Effects of Femtosecond Laser Pulses on Atomic Collision Processes.* J.F. SCIPIONE and PAUL L. DE VRIES, Miami University -- A computational procedure for the time evolution of a quantum mechanical wave function has been developed. The procedure utilizes the fast Fourier transform to calculate the spatial derivatives and a second order difference approximation for the temporal derivatives that are required for the propagation of the wavefunction. The algorithm has been applied to a model calculation of an atomic collision occuring in the presence of ultrashort, intense bursts of radiation which mimic the effects of actual femtosecond lasers. The effects of the laser radiation, including the intensity and duration of the pulse, will be discussed.

*Supported by the Petroleum Research Fund and by the Faculty Research Committee of Miami U.

LB-3 Prompt and Delayed Photolysis of Cs_2,* F. DAVANLOO and C. B. COLLINS, Univ. of Texas at Dallas; A. S. INAMDAR† and N. Y. MEHENDALE, Univ. of Poona; A. S. NAQVI, King Saud Univ. of Riyadh--In this work a time-delayed, double resonance technique was used for the study of the state selective photolysis of Cs_2 with particular attention being placed on the production of the fine structure components of the 5^2D and 6^2P states of Cs. Not only were the prompt sources from dissociation and predissociation of excited states of Cs_2 confirmed, but new kinetic channels for delayed photolysis were found. Over the visible wavelength range two delayed processes for the production of Cs (5^2D) and Cs(6^2P) atoms were characterized. Most recent observations have confirmed that these delayed sources produce a single fine structure component of the products. They are tentatively identified as proceeding through a precursive state belonging to the 5dX manifold of Cs_2, where X is most probably Π or Δ.

*Supported by NSF Grant PHY 8214273.

†Present address: Physics Dept., Univ. of Alberta

LB-4 Optical Escape Factors for Some NII Lines: Implications on the Opacity of Lightning, P. A. Vicharelli, National Center for Atmospheric Research* --Optical escape factors for lines of the 4630.5 and 5679.6 Å NII multiplets have been calculated for a cylindrical geometry using the theoretical formalism of Irons.[1] Results are presented as functions of temperature T and a reduced radius $\rho = (N^+/N_e)R$, where N^+ and N_e are the nitrogen ion and electron densities, respectively, and R is the discharge radius. It was found that for $T \lesssim 15{,}000$K the discharge is optically thin even for large (~1 m) values of ρ. However, for $T \gtrsim 25{,}000$K the optical escape factors may be considerably less than unity. These results are important in the quantitative characterization of the opacity of lightning, which has been assumed to be either optically thick[2] or optically thin[3] in the past. On the basis of these calculations we propose that the core of the lightning channel is only partially optically thin (74 ±6%) with a radius of the order of 0.005 m.

*NCAR is sponsored by the National Science Foundation.

[1]F.E. Iron, J. Q. S. R. T. 22, 1 (1979).
[2]Yu.N. Zhivlyuk & S.L. Mandel'shtam, Soviet Phys. JETP 13, 338 (1961).
[3]M.A. Uman & R.E. Orville, J.Geophys.Res.70, 5491(1965).

LC-1 Electron-Excited Hydrogen and Helium Collisions,* E. J. MANSKY and M. R. FLANNERY, Georgia Institute of Technology--The Multichannel Eikonal Treatment (MET) is modified so as to facilitate highly accurate description of various asymptotic long range dipole couplings important in electron excited atom collisions. MET is applied to excitation in e-H(2s), e-H(2p), e-He($2^{1,3}$S) and e-He($2^{1,3}$P) collisions at intermediate energies. Integral and differential cross sections together with various coherence and alignment parameters for the radiative decay of the n=2 and 3 collisionally-excited P and D states of H and He are determined from MET with 10 channels associated with n = 1, 2, and 3 sublevels. Comparison is made with various recent measurements.

*Research supported by AFOSR under Grant AFOSR-84-0233.

LC-2 Ab initio study of low-energy electrons interacting with HCN molecules.* A. JAIN and D. W. NORCROSS,† JILA, Univ. of Colo. and NBS.--Our earlier study of low-energy electron scattering with HCN molecules[1] is further improved by treating exchange exactly (in a separable exchange approximation[2]) in Σ, Π and Δ symmetries: the 3.8 eV Π resonance is shifted towards lower energy (2.56 eV, the experimental position is around 2.26 eV[3]), while in Σ and the Δ symmetries the difference is within 15%. We also study possible negative ion states of HCN by calculating potential energy curves with respect to C-H and C-N stretches. For example, there is evidence of an avoiding crossing between a $1\Sigma^+$ and a $2\Sigma^+$ state (C-H stretch) of HCN^-.

*Supported by the U. S. Department of Energy (OBES).

†Staff Member, Quantum Physics Division, NBS.

[1]A. Jain and D. W. Norcross, Bull. Am. Phys. Soc. 29, 803 (1984).

[2]T. N. Rescigno and A. E. Orel, Phys. Rev. A 24, 1267 (1981).

[3]P. D. Burrow, personal communication.

LC-3 Ro-vibrational excitation of $HC\ell$ by Electrons,* N. T. PADIAL and D. W. NORCROSS,† JILA, Univ. of Colorado and NBS -- Ab initio calculations have been made in the multipole-extracted adiabatic-nuclei approximation. These employed a new parameter-free model[1] of the correlation-polarization interaction and an exact treatment of exchange. Both effects are extremely important. The results for the cross sections $v - v' = 0 - 1$ and $0 - 2$ are in excellent agreement with measurements in shape, but suggest that a renormalization of the measured cross sections[2] by a factor of 0.6 is required. They are consistent with the model of a single electronic state of $HC\ell^-$ coupled to a continuum severely distorted by the dipole potential, yielding both a broad resonance at 2.5 eV at equilibrium and an attractive bound state of $HC\ell^-$ that merges smoothly with the neutral curve at about 2.6 Bohr.

*Supported by the U. S. Department of Energy (OBES).
†Staff Member, Quantum Physics Division, NBS.
[1]N. T. Padial and D. W. Norcross, Phys. Rev. A 29, 1742 (1984).
[2]K. Rohr and F. Linder, J. Phys. B 9, 2521 (1976).

LC-4 Production of Excited Nitrogen Atoms and Ions by Electron Impact on Nitrogen Molecules,* DAVID L.A. RALL, FRANCIS A. SHARPTON,† CHUN C. LIN, AND L.W. ANDERSON, U. of Wisconsin-Madison--Emission lines of the N atoms and N^+ ions are produced by electron-beam dissociative excitation of N_2 molecules. The $ns \rightarrow 3p$ (n=5 to 9), $np \rightarrow 3s$ (n=3 to 7), $nd \rightarrow 3p$ (n=4 to 8), $nf \rightarrow 3d$ (n= 4,5) transitions of N and the $3p \rightarrow 3s$, $3d \rightarrow 3p$, $4s \rightarrow 3p$, $4p \rightarrow 3d$, $4f \rightarrow 3d$ transitions of N^+ have been observed and optical emission cross sections at various incident electron energies have been measured. The energy dependence of the cross sections of the N emission lines is similar to that of the N^+ lines at high incident electron energies, but the low-energy behaviors are quite different. These features are explained by the mechanisms involved in the production of the excited N atoms and N^+ ions. Absolute optical emission cross sections for the N and N^+ lines are presented.

*Supported by Air Force Office of Scientific Research.
†Present address: Northwest Nazarene College, Nampa, ID.

LC-5 Cross Sections for Electron Impact Ionization and Dissociative Ionization of the Free Radicals: CF_3, SiF_3, and SiF_2. Robert C. Wetzel, Frank A. Baiocchi, and Robert S. Freund, AT&T Bell Laboratories. Absolute ionization cross sections have been measured for the free radicals CF_3, SiF_3, and SiF_2. A crossed beam method is used, in which a beam of fast (several keV) free radicals is prepared by charge transfer neutralization of a mass selected ion beam and is then crossed by a beam of electrons with energy varied from 0 to 200 eV. The dominant ionization process is found to be dissociative ionization with loss of one F atom. The resulting cross sections and cross section ratios for 70 eV electrons are:

$CF_3 \rightarrow CF_2^+$	$\sigma = 0.7 \pm 0.2\text{Å}^2$	$CF^+/CF_2^+ = 0.86 \pm 0.05$ $CF_3^+/CF_2^+ = 0.46 \pm 0.03$
$SiF_3 \rightarrow SiF_2^+$	$\sigma = 1.0 \pm 0.3\text{Å}^2$	$SiF^+/SiF_2^+ = 0.68 \pm 0.09$ $SiF_3^+/SiF_2^+ = 0.49 \pm 0.07$
$SiF_2 \rightarrow SiF^+$	$\sigma = 1.4 \pm 0.4\text{A}^2$	$SiF_2^+/SiF^+ = 0.90 \pm 0.11$

LC-6 Electron Impact Excitation of the $n \geq 3$ States of He* - D. F. REGISTER+, S. TRAJMAR, Jet Propulsion Laboratory, California Inst. of Techn., Pasadena, CA 91109 and D. C. CARTWRIGHT and G. CSANAK, Los Alamos National Laboratory, Los Alamos, NM 87545. -- Differential electron impact excitation cross sections (DCS) have been measured for the 3^3S, 3^1S, 3^3P and $(3^1P+3^1D+3^3D)$ levels of He at 30, 50 and 100 eV impact energies. The cross sections have been normalized to the absolute scale by utilizing the He 2^1P differential excitation cross sections which in turn were obtained by normalization with respect to the elastic differential cross sections. From the DCS, integral and momentum cross sections were obtained. In addition, some measurements were carried out on the n = 4 and 5 manifolds. Calculations based on first order many-body theory have been carried out utilizing accurate target wave functions. The theoretical results will be compared to the experimental data and to previous calculations.

*This work was supported partially by NASA and partially by DOE.

+Present address: Phillips Petroleum Co., Bartlesville, OK 74003

LC-7 **Dissociative Attachment in Ammonia**, P.D. BURROW and K.L. STRICKLETT, University of Nebraska*--We have examined the total negative ion production from dissociative attachment of electrons to NH_3 and ND_3, and have found a vibrational progression not observed previously in the 5.65 eV peak[1]. The vibrational spacing and Franck-Condon envelope are similar to those of the lowest Rydberg state of the neutral, in which the ν_2 out of plane bending mode is excited[2]. We therefore assign the negative ion state to $(1a_1)^2(2a_1)^2(1e)^4(3a_1)^1(3sa_1)^2\ ^2A_1(C_{3v})$, and suggest that fragment ions are produced through the negative ion analog of the predissociation process in $NH_3^*(3sa_1)$[3].

*Supported by NSF grant CPE-8012421.

1. T.E Sharp and J.T. Dowell, J. Chem. Phys. 50, 3024, (1969)
2. P. Avouris, A.R. Rossi, and A.C. Albrect, J. Chem. Phys. 74, 5516, (1981)
3. R. Runau, S.D. Peyerimhoff, and R.J. Buenker, J. Mol. Spectrosc. 68, 253, (1977)

LC-8 Electron Temperature Dependence of the Recombination of Electrons with O_4^+ Ions*, J. L. DULANEY, M. A. BIONDI and R. JOHNSEN, Univ. of Pittsburgh -- A microwave afterglow-mass spectrometer apparatus employing microwave electron heating has been used to investigate the dependence on electron temperature T_e of electron recombination with the $O_2^+ \cdot O_2$ dimer ions (O_4^+). At $T_e = T_+ = T_n \simeq 140$ K, we find $\alpha[O_4^+] = (6.0 \pm 0.2) \times 10^{-6}$ cm^3/s. From 140 K < T_e < 4000 K, $\alpha[O_4^+]$ varies more rapidly than $T_e^{-\frac{1}{2}}$, which is a stronger dependence on T_e than that found for other dimer ions (e.g., $CO^+ \cdot CO$ and $N_2^+ \cdot N_2$). We are currently improving the calibration of the T_e scale by means of ambipolar diffusion frequency measurements as a function of microwave heating power. This will permit a more quantitative statement concerning the T_e dependence of $\alpha[O_4^+]$.

*Work supported, in part, by Air Force Cambridge/DNA under Contract No. F19628-81-K-0002.

LC-9 Laboratory Studies of Electron Beam Growth in N_2, P. IP, and W.A.M. BLUMBERG, AFGL, Hanscom AFB, MA 01731, B.D. GREEN, W.J. MARINELLI, and G.E. CALEDONIA, Physical Sciences, Inc., Research Park, Andover, MA 01810 -- The spatial distribution of electrons scattered out of a collimated electron beam incident on a low pressure N_2 target has been investigated using the AFGL LABCEDE facility. Spatial distributions were obtained for beams of 2-6 kV electrons propagating through target thicknesses of 0.05 to 3.5 Torr-cm. The spatial growth of the electron beam was observed with a calibrated, two dimensional scanning photometer which monitored the spatial dependence of 391.4nm First Negative Band fluorescence from N_2^+ excited by energetic electrons. Abel inversion techniques were used to obtain radial distributions of electrons as a function of target thickness, beam voltage, and current. The present results will be compared with prior measurements reported for higher electron energies and for greater target thickness, as well as theoretical calculations.

Supported by the Air Force Office of Scientific Research and the Defense Nuclear Agency.

LC-10 A Limit for the Quenching of $H_2(c^3\Pi_u)$ Metastables,* H. TISCHER and A.V. PHELPS, JILA, U. of Colo. & NBS.--$H_2(c^3\Pi_u)$ metastables are produced in a pulsed discharge and monitored by absorption of a cw dye laser.[1] The current pulses are $\leq 5\times10^4$ A/m^2, 300 nsec duration and falltimes of 150 nsec. From the decay of the discharge current and the emission from states of the n=3 manifold, the decay of the metastable excitation is estimated to be 150 nsec. For H_2-densities above 4.5×10^{21} m^{-3} we find that the decay of the metastable absorption signal follows the current and emission signal. This observation yields a lower limit for the quenching rate coefficient of the metastables of 1.5×10^{-15} m^3 s^{-1}. Additional measurements of the steady-state absorption at low currents plus the pulsed measurements give a nearly linear dependence on the discharge current density in the range from 30 A/m^2 to 10^5 A/m^2. Therefore, quenching of the metastables by electrons can be ruled out as the dominant destruction mechanism.

*Work supported in part by Air Force Wright Aeronautical Laboratories.

[1]D. S. Bethune, J. R. Lankard and P. P. Sorokin, J. Chem. Phys. 69, 2076 (1978).

LD-1 **A New Method for the Rapid and Accurate Solution of the Schrodinger Equation.*** PAUL L. DE VRIES, Miami U. -- The Magnus approximation, a common method of propagating quantum mechanical wavefunctions describing scattering events, has been reexamined. Rather than making the usual formal series expansion of the Magnus solution, a computational procedure has been introduced to determine the functional form of certain propagation parameters. These parameters then yield propagators that, like the Magnus approximation, preserve the Wronskian, but are more accurate and rapidly convergent. This is particularly true when a Legendre fit to the true potential is employed; results for a model phase shift calculation indicate that, with the same modest effort, the new method is as much as five orders of magnitude more accurate than the first order Magnus method.

*Supported by the Petroleum Research Fund.

LD-2 Analytical and Numerical Solutions of the Time Dependent Debye-Smoluchowski Equation,* M. R. FLANNERY and E. J. MANSKY, Georgia Institute of Technology--The macroscopic Debye-Smoluchowski Equation (DSE) with a radiation boundary condition has been derived[1] from a basic microscopic theory of association/dissociation processes, A+B → AB, between A and B in a thermal gas bath. There are at present no exact analytical solutions of DSE for general interactions V(R) between A and B for all separations R and time t. We formulate here exact analytical solutions for the conditional probability density and reaction rates (a) at long and short times for all R and (b) at all times for large R and compare the results with direct numerical solutions. We also propose highly accurate working expressions for the rates of transport influenced reactions at all times.

*Research supported by AFOSR under Grant AFOSR-84-0233.

[1]M. R. Flannery, Phys. Rev. A (1985).

LD-3 Time-Resolved Study of Ion-Molecule Reactions in Oxygen at High Gas Densities,* J.DE URQUIJO, C. CISNEROS and I. ALVAREZ, Instituto de Física, UNAM, México -- Ion mobilities of O^-, O_2^-, O_3^- and O_2^+, and rate coefficients for the reactions leading to the formation of O_2^- and O_3^- have been measured using a pulsed Townsend apparatus. The oxygen density was 1.3 to 16.8×10^{24} m^{-3} and the reduced field strength E/N was 7.6 to 11.5×10^{-20} V m^2. Fitting to the ion transients was done from an improvement to the earlier analysis of Burch and Geballe[1]. Resulting values for the two- and three-body rate constants and for the ion mobilities have been found in good agreement with previous values reported by other workers who used lower gas densities. Also, values of the ionization and attachment coefficients could be derived from this study.

*Work supported in part by CONACyT, México, Grant PCCBBNAL 020668.

[1]Burch D.S. and Geballe R., Phys. Rev. 106 188 (1957)

LD-4 Reactions of Zr^+ and ZrO^+ Ions with O_2*, S. DHEANDHANOO, R. JOHNSEN, and M. A. BIONDI, Univ. of Pittsburgh -- The oxidation reactions of ions of zirconium and zirconium oxide with oxygen molecules have been studied using a Selected Ion Drift Apparatus (SIDA). A heated Penning-type discharge in a mixture of neon and $ZrBr_4$ is used to produce Zr^+ ions. The reaction $Zr^+ + O_2 \rightarrow ZrO^+ + O$ is found to be fast, $k = (1 \pm 0.1) \times 10^{-9}$ cm^3/sec at $\bar{E}_{ion} = 0.04$ eV, and shows no variation with ion energy over the range 0.04 eV < E_{ion} < 0.2 eV. The second oxidation step, $ZrO^+ + O_2 \rightarrow ZrO_2^+ + O$ proceeds with a considerably smaller rate coefficient; $k = (8 \pm 0.2) \times 10^{-12}$ cm^3/sec at $\bar{E}_{ion} = 0.04$ eV, decreasing to 2×10^{-12} cm^3/sec at $\bar{E}_{ion} = 0.3$ eV.

*Work supported, in part, by Air Force Cambridge/DNA under Contract No. F19628-81-K-0002.

LD-5 Ion-Molecule Association Reactions Involving Cyano-Compounds.* C. V. SPELLER and M. MEOT-NER (MAUTNER), NBS-Gaithersburg, MD 20899 - The gas-phase equilibria for several ion-molecule association reactions involving cyano-compounds, as for example, $HCNH^+ + H_2O \rightleftarrows HCNH^+ \cdot H_2O$, was determined using the NBS pulsed high-pressure mass spectrometer. A linear correlation is found between the bond dissociation energy ΔH_D° of the ion dimer and the difference ΔPA between the proton affinities of the proton donor and the proton acceptor (HCN and H_2O, resp., in the case of reaction above). The correlation $-\Delta H_D^\circ(\text{kcal-mol}^{-1}) = \Delta H_D^\circ(0) - b\Delta PA$ for $-NH^+ \ldots NCR$ bonds yields the parameters $(\Delta H_D^\circ(0), b) = (35.3, 0.34)$ and $(27.2, 0.31)$ in amineH^+-nitrile and nitrileH^+-nitrile systems, resp.; for $RCNH^+ \ldots O$- bonds, $(\Delta H_D^\circ, b) = (28.5, 0.32)$ in nitrileH^+-water systems; and for $-OH^+ \ldots N$- bonds, $(\Delta H_D^\circ(0), b) = (29.6, 0.33)$ in oxonium ions-HCN systems. The correlations are in accord with trends predicted by ab initio calculations of Desmeules and Allen[1].

*Submitted by A. Parr.

[1]P. J. Desmeules and L. C. Allen, J. Chem. Phys. 72, 4731 (1980).

LD-6 Mass Spectrometric Study of $C_{2m}H_{2m}^+ \cdot (N_2)_n$ Clusters.* C. V. SPELLER,** NBS-Gaithersburg, MD 20899 - Experimental results concerning ion-molecule clustering reactions in α-particle irradiated gas mixtures (trace C_2H_2 in N_2) will be presented. The measurements were performed using the LPGP-U. Paris-Sud high-pressure mass spectrometer. Polymeric acetylene ions $C_{2m}H_{2m}^+$ (m=1 to 10) are formed starting with $C_2H_2^+$. Free energies ΔG° for the clustering reaction $C_{2m}H_{2m}^+ \cdot (N_2)_{n-1} + N_2 \rightleftarrows C_{2m}H_{2m}^+ \cdot (N_2)_n$ were determined, for n=2 and 3, from the measured equilibrium constants at 129°K and total pressures ranging from 10 to 50 torr. For m=2 $\Delta G^\circ_{n-1,n}$ (kcal-mol^{-1}) = -0.9 for n=3 and 4; for m=3 the $\Delta G^\circ_{n-1,n}$ values are found to be $\sim$ -0.9 (n=2), -0.9 (n=3), -0.7 (n=4), -0.7 (n=5) and -0.6 (n=6). The study of ion-molecule reactions in N_2-C_2H_2 mixtures at low temperatures and high pressures is of interest for modelling the ionospheric chemistry of the atmosphere of Titan.

*Submitted by Albert Parr.

*Partially supported by INAG-CNRS (ATP Planetologie).

**Experimental work conducted while the author was at the Universite de Paris-Sud.

LD-7 Structure and Stability of $NH_4^+(NH_3)_m(HCN)_n$ Clusters.* C. V. SPELLER, NBS-Gaithersburg, MD 20899, C. A. DEAKYNE, College of the Holy Cross, Worchester, MA and M. MEOT-NER (MAUTNER), NBS, Gaithersburg, MD 20899 - The gas-phase equilibria for the ion-molecule reaction $NH_4^+\cdot(HCN)_{n-1} + HCN \rightleftarrows NH_4^+\cdot(HCN)_n$ were determined using the NBS pulsed high-pressure mass spectrometer. Enthalpy, entropy and free energy changes ($\Delta H°$, $\Delta S°$ and $\Delta G°$, resp.) were calculated from the temperature dependence of the corresponding equilibrium constants (van't Hoff plots), for total pressures in the torr range and for temperatures ranging from 220 to 550°K. The ($-\Delta H°$, kcal-mol^{-1}; $-\Delta S°$, cal-mol^{-1}-K^{-1}; $-\Delta G°_{298}$, kcal-mol^{-1}) for n=1 to 6 are found to be (20.5; 20.2; 14.5), (17.4; 23.4; 10.4), (13.7; 21.5; 7.3), (11.1; 22.1; 4.5)), (8.5; 21.0; 2.3) and (7.4; 19.9; 1.5), resp. Thermodynamic values were also derived for the mixed ion clusters $NH_4^+(NH_3)_m(HCN)_n$. Ab initio calculations have been performed in order to investigate the structure and stability of the studied ion clusters.

*Submitted by Albert Parr.

LD-8 * Modeling of Ion Molecule Reactions at High Pressures, C. D. EBERHARD and C. B. COLLINS, U. of Texas at Dallas and J. STEVEFELT, GREMI, U. of Orléans, France-- Recent modeling of ion molecule reactions[1] has suggested that the dynamics of the complex formed from the initial encounter between the reactants may control the overall rate at which the products appear. At atmospheric pressures both coherent and incoherent collisional processes of excitation and deexcitation of the complex contribute substantially to the yield of products. A phenomenology is predicted that largely agrees with observations of termolecular rate coefficients for ion molecule reactions in the 10(-28) to 10(-30) cm^6sec^{-1} range.[2,3] Primary variables are the dependence of the energy transfer function upon parameters describing collisions with the complex and the approximate geometric shape of the complex.

*Supported in part by NSF Grants ECS8314633 and INT 8116436 and in part by CNRS.

1. C. B. Collins, F. W. Lee, W. M. Tepfenhart and J. Stevefelt, J. Chem. Phys. 78, 6079 (1983).
2. F. W. Lee, C. B. Collins, and R. A. Waller, J. Chem. Phys. 65, 1605 (1976).
3. J. M. Pouvesle, A. Bouchoule and J. Stevefelt, J. Chem. Phys. 77, 817 (1982).

LD-9 Study of Two-Body and Three-Body Channels for the Reaction of Metastable Helium Atoms with Nitrogen, J.M. POUVESLE and J. STEVEFELT, GREMI, U. of Orléans, France, and C.B. COLLINS, Z. CHEN , V. GYLYS, and H. JAHANI, U. of Texas at Dallas -- This work concerns the kinetics of atmospheric pressure plasmas. Results have been obtained that exploit the large dynamic range and high data rates available from time resolved spectroscopic studies of preionized stripline discharges. Most recent attention has been focused upon the reactions of $He(2^3S)$ with N_2 in an effort to resolve conflicts in the anomalously rapid termolecular channels of reaction that were previously reported [1,2]. This work reports the characterization of late time periods in the decay of ionization produced in 1-4 atmospheres of helium containing up to 1400 mTorr of N_2. A new value was found for the termolecular reaction of (2^3S) with N_2 of $1.5 \times 10^{-31} cm^6 sec^{-1}$ that is in good agreement with a model of collisionally induced capture. An indirect channel of reaction was also found that seems to explain the higher rates reported earlier.

[1]F. W. Lee and C.B. Collins, J.Chem.Phys., 65, 5189,1976
[2]G. Myers and A.J. Cunningham, J.Chem.Phys.,67, 3352,1977

LD-10 Cross Section for Electronic Energy Transfer Between Mercury Isotopes,* R. LAGUSHENKO, M. W. GROSSMAN and J. MAYA, GTE Lighting Products, Danvers, MA --Previous estimates of the cross section (σ) for the process $^iHg(6^3P_1)+{}^jHg(6^1S_0) \rightarrow {}^iHg(6^1S_0)+{}^jHg(6^3P_1)$, where i and j are any one of the six stable Hg isotopes, are no better than a factor of ten[1]. We have recently measured the hyperfine structure of the 253.7nm Hg resonance line in low pressure Hg-Ar discharge for natural Hg as well as Hg enriched in ^{196}Hg by 2-4%, as a function of temperature. Using our previously developed resonance radiation transport model in a low pressure Hg+Ar plasma we calculated the exact shape of the hyperfine structure and found a high degree of sensitivity to the value of (σ). By varying (σ) we were able to obtain a best fit to the measured hyperfine structure as a function of temperature. This fit determined the value of (σ). We believe the accuracy of this determination is about 30%.

*Work supported in part by DOE.

[1]T. Holstein, D. Alpert and A. O. McCoubrey, Phys. Rev. 85, 1985 (1952).

LD-11 An OODR Study of Collision Induced Energy Transfer between Unperturbed Electronic States, D.H. KATAYAMA, AFGL, Hanscom AFB, MA. 01731 -- A two laser, optical-optical double resonance (OODR) technique has been used as a direct probe of the electronic energy transfer process between rovibronic levels of the A and X states of $^{14}N_2^+$. For the first time collisional selection or propensity rules are obtained for a homonuclear molecule which has no perturbations or "gates" between the states involved. The electronic transfer rate between the A(v = 4) and X(v = 8) rotational manifolds is shown to be comparable to that for rotational energy transfer (RET) and in spite of the competition between these two mechanisms it is demonstrated that there is a propensity towards $\Delta J \approx 0$ rather than ΔE (energy gap) ≈ 0. In addition, the selection rule s $\leftrightarrow$ a is shown to apply for this process. Other pairs of vibronic levels show similar propensity rules and demonstrate that these are truly electronic energy transfer processes rather than a form of RET as occurs when the rotational levels are known to be perturbed in the isolated molecule.

LD-12 Symmetric Charge-Transfer Cross Sections in Rare Gas (Rg^+-Rg) Systems,* E. J. MANSKY and M. R. FLANNERY, Georgia Institute of Technology--Symmetric resonance charge-transfer, elastic, diffusion and viscosity cross sections for the ion-atom collisions: $Rg^+ + Rg$, Rg = He, Ne, Ar, Kr, Xe are determined via a full quantal phase-shift analysis using the pseudopotential of Sinha, et al. [1] for He_2^+; and the spin-orbit ab-initio potentials of Cohen and Schneider [2] for Ne_2^+, Wadt [3] for Ar_2^+, Kr_2^+, and Xe_2^+; and Michels, et al. [4] for Ne_2^+, Ar_2^+, Kr_2^+, and Xe_2^+ at lab energies ranging from 0.001 eV to 1 keV. The long-range ion-atom polarization attraction is explicitly acknowledged in the full interaction and in a JWKB correction to the numerical asymptotic phase shift. Differential cross sections are also obtained. Comparison is made with existing experimental and theoretical data.

*Research supported by AFOSR under Grant AFOSR-84-0233.

[1] S. Sinha, S.L. Lin, and J.N. Bardsley, J. Phys. B 12 (1979) 1613.
[2] J.S. Cohen and B. Schneider, J. Chem. Phys. 61 (1974) 3230.
[3] W.R. Wadt, J. Chem. Phys. 68 (1978) 402.
[4] H.H. Michels, R.H. Hobbs, and L.A. Wright, J. Chem. Phys. 69 (1978) 5151.

LD-13 Association/Dissociation in Dense Gases and Adsorption/Desorption on Surfaces,* M. R. FLANNERY, Georgia Institute of Technology--A new comprehensive theory[1] is described for the time evolution towards equilibrium of association and dissociation in a dense gas. Expressions are formulated and are illustrated for the net probabilities of association to stable vibrational levels and dissociation to the continuum from an arbitrary bound vibrational level via collision with the thermal gas bath. A general variational principle emerges: The rate which corresponds to the overall direction of the process always adjusts itself to a minimum and the time evolution towards equilibrium is hindered. Analogy is established with Kirchhoff's Laws and Tellegen's Theorem for electrical networks, and with the Principle of Least Dissipation basic to thermodynamics, heat conduction, and fluid mechanics. The theory can also be modified to provide the first basic microscopic account of Associative Desorption of atoms from and Dissociative Chemisorption of molecules to surfaces.

*Research supported by AFOSR under Grant AFOSR-80-0055.

[1]M. R. Flannery, Phys. Rev. A, (1985).

SESSION MA

08:00, Friday, October 12, 1984

SPARK DEVELOPMENT

Chairperson: W. Byszewski
GTE Labs

MA-1 The Probability of Electrical Breakdown: Evidence for a Transition Between the Townsend and Streamer Mechanisms - R. V. HODGES, R. N. VARNEY, and J. F. RILEY, Lockheed Palo Alto Research Laboratory - The probability that an electron initiates breakdown has been investigated by measurements of spark delay times in a uniform field gap provided with a small photocurrent of free electrons. In N_2, H_2, and Ar the dependence of the breakdown probability on overvoltage agreed with calculations based on the Townsend mechanism. In SF_6 and CCl_2F_2 a transition was observed with increasing pressure from a dependence that agreed with the Townsend theory to a more gradual rise with voltage. This transition has been ascribed to a decrease in the secondary ionization coefficient with increasing pressure, which resulted in an average electron avalanche size at the static breakdown voltage that approached the critical value for streamer formation. A unified breakdown probability theory, for which the Townsend and streamer mechanisms are limiting cases, has been developed to account for the data over the full pressure range. The implications of these results for measurement of the static breakdown voltage and the secondary ionization coefficient will be discussed.

MA-2 2-D Numerical Simulation of Streamers in Atmospheric N_2*, S.K. Dhali† and P.F. Williams††, Texas Tech --We have continued the numerical simulation of two-dimensional, space-charge dominated transport in nitrogen. We have obtained results for applied voltages of both polarities ranging from 1.0 to 1.8 times the uniform field breakdown voltage; for preionization densities of 0, 10^6, and 10^8 cm^{-3}, and for several different initial conditions. We find 1) that propagation velocities generally increase with applied voltage; 2) that cathode-directed streamers propagate slower, leave behind higher ionization densities, and produce steeper density and field gradients than do anode-directed streamers; 3) that the dielectric relaxation time plays an important role in streamer propagation; and 4) that within broad limits, streamer propagation is only weakly dependent on the shape of the streamer tip. The dependence of the streamer velocity on ionization density ahead of the streamer is not simple and will be discussed.

*Work supported by AFOSR

†Present Address: Southern Illinois University
††Present Address: University of Nebraska

MA-3 Streak Photographic Studies of Trigatron Triggered Breakdown*, M.R. Wages, P.F. Williams,† G. Schaefer, K.H. Schoenbach, Texas Tech--In a trigatron spark gap breakdown is triggered by applying a voltage pulse to a trigger electrode which is generally placed in the center of one main gap electrode but is insulated from it. The top of the trigger pin is approximately in the plane of the main electrode surface, and triggering is always associated with the appearance of a spark between the trigger and main electrodes. We have used optical streak photography to investigate the physical mechanisms responsible for trigatron triggering. Under some conditons we see a luminious front propagate across the gap, starting from the region of the trigger pin, and roughly coincident with the appearance of the trigger spark. The velocity of the front is ~10^8 cm/sec, and we associate it with a streamer. Under other conditions breakdown seems to result from the appearance of a diffuse glow followed by a transition to a constricted spark channel. The breakdown mechanism is strongly influenced by the position of the trigger pin.

*Work Sponsored by AFOSR.
†Present Address: University of Nebraska.

MA-4 Kinetic Investigation of Streamer Development*, E.E. Kunhardt, Polytechnic Inst. of NY, and Y. Tzeng, Auburn University-- Results are presented from simulations of the evolution of an electron avalanche in a uniform electric field and its transition into streamers. A Monte Carlo technic has been used to describe the dynamics of the electrons in phase-space taking into account collective effects due to the space-charge electric field. This field is obtained form Poisson's Eq. assuming cylindrical symmetry. The role that the space-charge field, the electron velocity distribution, and photoionization play in the formation of streamers have been elucidated. The properties of streamers shortly after formation have been determined. The results presented are for nitrogen at applied electric field-to-gas density ratios (E/N) of 3×10^{-15} V-cm^2 and 1×10^{-14} V-cm^2 and for background neutral densities of 1×10^{10} cm^{-3} and 2.45×10^{19} cm^{-3}.

*Work supported by the Office of Naval Research.

MA

MA-5 Interferometric Measurements of Laser Preionization Triggered Spark Columns.* W.D. KIMURA, M.J. KUSHNER, E.A. CRAWFORD, and S.R. BYRON, Mathematical Sciences Northwest -- Short pulse (<5 nsec) laser interferograms of a 40 kV, ≈ 17 kA, 100 nsec spark column are measured at wavelengths from 350-610 nm. Spark breakdown is initiated using a KrF laser (248 nm) to volume preionize the gas mixture. Laser triggering creates reproducible axisymmetric columns, and permits accurate temporal and spatial measurements. Gas mixtures tested include $SF_6/N_2/He$, H_2, CH_4/H_2, and $Xe/CH_4/H_2$ at 1-3 atm abs. Measured electron and heavy particle density profiles reveal a high electron density (≈ 10^{19} cm^{-3}) inner core with a thin outer shell of high density shocked gas. Predictions from a computer code (SPRAD), being developed at MSNW to model the spark column formation, agree well with the experimental data.

*Work supported by NSWC Contract No. N60921-83-C-A057.

MA-6 A First Principles Model for Laser Triggered Spark Columns.* M.J. KUSHNER, and R.D. MILROY, Mathematical Sciences Northwest --A computer model (SPRAD) for a laser triggered spark column has been developed which, from first principles, describes the hydrodynamic and radiative expansion of a narrow (≈50 μm) laser produced plasma column into a wide (≈1 mm) arc capable of conducting 10 kA. The expansion of the arc is primarily a result of convective transport of the hot ionized core in a radial expansion wave. Non-convective expansion of the arc at the inner edge of the shock proceeds by an electron avalanche initiated by electrons produced by photoionization and by thermal ionization resulting from adiabatic heating of the neutral gas. The high neutral density shock wave at the front of the expansion limits the growth of the plasma column by confining the hot region in a shell of cold gas with a low E/N. In gas mixtures containing mostly hydrogen, the inner core of the spark column is fully ionized and the electron temperature can exceed 15 eV. In noble gas and hydrogen mixtures, the electron temperature is only a few eV.

*Work supported by ONR Contract No. N00014-83-C-0417 and NSWC Contract No. N60921-83-C-A057.

MA-7 A Thermodynamic Model for Laser Triggered Spark Gaps.* M. J. KUSHNER, Mathematical Sciences Northwest --Experiments and kinetic modeling have shown that the growth mechanism for arcs in laser triggered spark gaps is dominantly convective expansion of the hot plasma column, augmented by photo- and thermal ionization in the shock front at the edge of the column. With this insight, a thermodynamic scaling model for laser triggered spark gaps has been developed for mixtures of argon and hydrogen. The model self consistently calculates the diameter, and plasma temperature of the arc for a specified current, gas mix and initial pressure. To obtain these parameters, densities for local thermodynamic equilibrium are computed for a range of temperatures. With these results, the electrical conductivity, internal energy, and photon absorption coefficients and emissivities are calculated. An energy balance is then iteratively obtained between joule heating, internal energy, and radiation. A unique solution results by relating the final arc diameter to the plasma temperature through the sound speed of the sonic expansion. Results will be discussed for arc columns carrying 1-10 kA.

*Work supported by ONR Contract No. N00014-83-C-0417.

SESSION MB

08:00, Friday, October 12, 1984

IONIZATION PROCESSES

Chairperson: L.W. Anderson
University of Wisconsin

MB-1 Ionizing Collisions of Laser-Excited Neon Atoms §
W. BUßERT, T. BREGEL, M.-W. RUF and H. HOTOP, Fachbereich Physik der Universität, 6750 Kaiserslautern, FRG

With a crossed beams arrangement[1] we have studied the ionization of Ar and Kr atoms in collisions with laser-excited short-lived Ne($2p^5$ 3p) atoms for relative velocities in the range 500-1200 m/s. Low background electron spectrometry was used to selectively detect the product electrons and to determine the relative ionization cross sections for the Ne(3p J=1,2,3) multiplet states. The cross sections strongly depend on the state and, in some cases, on the collision energy. Strong polarization effects have been observed in the electron spectra, especially for Ne(3p $^3D_3$). Model calculations of the cross sections, based on potential energy curves constructed from known Na(3s,3p)+Ar(Kr) potentials provide a detailed understanding of the experimental results.

§ Work supported by the Deutsche Forschungsgemeinschaft (Sonderforschungsbereich 91)

[1] W. Bußert, J. Ganz, H. Hotop, M.-W. Ruf, A. Siegel, H. Waibel, P. Botschwina and J. Lorenzen, Chem. Phys. Lett. 95, 277 (1983)

MB-2 Photodissociation Dynamics and Energetics of Small Gas Phase Cluster Ions,* M.F. JARROLD, A.J. ILLIES and M.T. BOWERS, Dept. of Chemistry, U. of California, Santa Barbara, Ca 93106 -- A crossed ion beam/laser beam apparatus has been constructed that allows determination of photodissociation properties of mass selected ion beams.[1] The photo products are subjected to mass and energy analysis using an electrostatic analyser. Product branching ratios and accurate kinetic energy distributions are obtained. In favorable cases product internal state distributions are also obtained. Variation of the laser polarization allows determination of the nature of the dissociating transition, information on the lifetime of the photoexcited state, and the photofragment dissociation dynamics in the center of mass frame. Data has been obtained on approximately 15 clusters. Sample results will be given, including those for $(Mn)_2^+$, $(SO_2)_2^+$ and KrO_2^+.

*This work is supported by AFOSR under Grant 82-0035 and NSF under Grant CHE80-20464.

[1] M.F. Jarrold, A.J. Illies and M.T. Bowers, J. Chem. Phys. 79,6086 (1983).

MB-3 Electron and Metastable Spatial Distributions for Positive Columns with Ionization from a Metastable State, F.J. ROMEIRAS and C.M. FERREIRA, Centro de Electrodinâmica, U.Tec. Lisboa -- The spatial distributions of electrons and metastables, n_e and n_M, for a positive column with direct and two-step ionization are governed by two coupled continuity equations, $-D_e\nabla^2 n_e = n_e(\nu_i + C_{Mi}\, n_M)$, $-D_M\nabla^2 n_M = n_e(\nu_M - C_M n_M)$, whose solutions depend only on two parameters: $P \equiv C_M n_M(0)/\nu_M$, $Q \equiv \nu_M C_{Mi}/\nu_i C_M$. At low currents $P \to 0$ while at high currents the concentration of metastables saturates and $P \to 1$. Solutions were obtained for a wide range of values of Q and $0 \leq P < 1$, for cylindrical and planar geometries and for vanishing densities at the boundary. For $P = 0$ n_e, n_M take the usual Bessel (cosine) shape. As P increases n_e is slightly modified but returns to the Bessel(cosine) shape as $P \to 1$; meanwhile n_M becomes progressively flatter. The average densities $\bar{n}_e$, $\bar{n}_M$ can be charaterized by appropriately defined diffusion lengths Λ_e, Λ_M. $\Lambda_e \to R/2.4(L/\pi)$ as $P \to 0$ and $P \to 1$; $\Lambda_M \to R/2.4\,(L/\pi)$ as $P \to 0$ and diverges as $P \to 1$. These results together with Boltzmann calculations provide similarity laws of E/N vs. NR for I/R = const and of n_M/N vs. I/R for NR = const; an application to argon is discussed.

MB-4 Photoionization of Kr and Kr_2 at 193 nm and 248 nm, D.B. GEOHEGAN, A.W. McCOWN and J.G. EDEN, University of Illinois at Urbana-Champaign -- A microwave absorption technique was used in conjunction with two excimer lasers to obtain photoionization cross sections of atomic and molecular krypton at several excimer laser wavelengths. The electron density arising from the resonantly-enhanced three-photon ionization of $Kr(^1S_o)$ at 193 nm was observed to display a quadratic dependence on laser intensity which yielded an effective two-photon cross section of $1.4 \cdot 10^{-32}$ $cm^4 - W^{-1}$. In a separate experiment, the single-photon photoionization cross sections of electronically excited atomic and molecular krypton were measured at 248 nm. Following the formation of the excited states produced by a 193 nm laser pulse, the increase of electron density due to the arrival of a 248 nm laser pulse was measured at two different time delays. The molecular and atomic cross sections were found to be $1.4 \cdot 10^{-18}$ cm^2 and $5.7 \cdot 10^{-19}$ cm^2, respectively.

MB-5 Laser Ionization of Lithium Vapor,* J. K. RICE and G. C. TISONE, Sandia National Laboratories—A promising method of efficiently producing a lithium plasma suitable for application to ion-beam fusion is based on laser saturation of the lithium resonance transition at 670.8 nm. We have developed a numerical model of this process, including a space- and time-dependent description of laser absorption and collisional-kinetic processes. The time dependence of the ionization process and the time dependence of the fluorescence from the ^2S and ^2D have been measured in a column of Li vapor. Measurements have been made at Li densities up to $10^{16}/cm^3$ and laser intensities up to 10^8 W/cm^2. The results of these measurements will be compared with model predictions.

*This work was supported by the U. S. Department of Energy under contract number DEAC04-76-DP00789.

MB-6 **Effect of Electronic Alignment Upon the Process $2Na^*(^2P_{3/2}) \rightarrow Na_2^+ + e^-$.** **G. P. RECK, E. W. ROTHE, R. THEYUNNI AND C. C. TUNG, Wayne State University.*—** **A thermal beam of Na atoms is excited to $3^2P_{3/2}(F=3)$ and aligned using a single-mode linearly-polarized Ar^+ ion pumped dye laser. Reaction between two excited atoms to produce Na_2^+ occurs at subthermal energies in a single atomic beam. The ion yield of Na_2^+ is measured as a function of the direction of polarization of the laser light relative to the atomic beam direction. Changes as large as a 50% decrease are observed upon 45° rotation of the polarization. These results are at odds with a previous measurement[1] of this polarization. Possible reasons for these discrepancies will be discussed and an interpretation in terms of the relevant potential curves (Σ, Δ) will be given.**

*** Supported by NSF CPE 81-66325**

[1] J. G. Kircz, R. Morgenstern, and G. Nienhuis, *Phys. Rev. Letters* 48, 610 (1982).

SESSION N

10:00, Friday, October 12, 1984

INVITED PAPERS

Chairperson: Ronald Waynant
Naval Research Lab

N

N-1 RF-Excited Waveguide Lasers, L. NEWMAN, United Technology Research Center

N-2 Progress in the Pursuit of an X-Ray Laser, W.L. Morgan, Lawrence Livermore National Lab

INDEX OF AUTHORS

37th Annual Gaseous Electronics Conference

October 9-12, 1984 University of Colorado, Boulder

Monday, October 8

19:30		Reception	UMC Glenn Miller Lounge

Tuesday, October 9

08:30	A:	Ion Transport	UMC Center Ballroom
09:50		Coffee Break	
10:15	B:	Electron Collisions	UMC Center Ballroom
13:15	CA:	Lasers	UMC Center Ballroom
13:15	CB:	Glows and Switching	UMC East Ballroom
15:15	D:	Workshop on Ion-Molecule Reactions	UMC Center Ballroom

Wednesday, October 10

08:15	E:	Ion-Molecule Reactions	UMC Center Ballroom
10:15		Coffee Break	
10:55	F:	Argon and SF_6 Arcs	UMC Center Ballroom
13:30	G:	Posters. Mostly Discharges	UMC West Ballroom
	GA:	Swarms	
	GB:	Arcs	
	GC:	Lasers	
	GD:	Low Pressure Discharges	
	GE:	Breakdown	
15:30	HA:	Silane Discharges	UMC Center Ballroom
15:30	HB:	Metal Halide and Mercury Arcs	UMC East Ballroom
19:30	I:	Workshop on RF Discharges	UMC Center Ballroom

Thursday, October 10

08:15	JA:	Electron Transport	UMC Center Ballroom
08:15	JB:	Thermal Arc Sprays	UMC East Ballroom
09:30		Coffee Break	
10:00	K:	Glow Diagnostics	UMC Center Ballroom
13:30	L:	Posters. Mostly Atomic and Molecular	UMC West Ballroom
	LA:	Atomic and Molecular Properties	
	LB:	Photon Absorption and Emission	
	LC:	Electron Collisions	
	LD:	Atomic and Molecular Collisions	
15:30		Lab Visits	JILA
20:00		Banquet	UMC Glenn Miller Ballroom

Friday, October 11

08:00	MA:	Spark Development	UMC Room 235
08:00	MB:	Ionization Processes	UMC Forum Room
09:40		Coffee Break	
11:30	N:	Invited Lectures	UMC Center Ballroom

END

FILMED

11-85

DTIC